ESD-TR-69-52

ESSIE

# REFRACTION-INDUCED TRACKING ERRORS AND CORRECTION METHODS FOR THE AIR FORCE WESTERN TEST RANGE



L. G. Rowlandson
J. R. Herlihy

December 1968

AEROSPACE INSTRUMENTATION PROGRAM OFFICE
ELECTRONIC SYSTEMS DIVISION
AIR FORCE SYSTEMS COMMAND
UNITED STATES AIR FORCE
L. G. Hanscom Field, Bedford, Massachusetts



(Prepared under Contract No. F19628-68-C-0209 by Syracuse University Research Corporation, Merrill Lane, University Heights, Syracuse, New York.)

## LEGAL NOTICE

When U. S. Government drawings, specifications or other data are used for any purpose other than a definitely related government procurement operation, the government thereby incurs no responsibility nor any obligation whatsoever; and the fact that the government may have formulated, furnished, or in any way supplied the said drawings, specifications, or other data is not to be regarded by implication or otherwise as in any manner licensing the holder or any other person or conveying any rights or permission to manufacture, use, or sell any patented invention that may in any way be related thereto.

## OTHER NOTICES

Do not return this copy. Retain or destroy.

ESD-TR-69-52


# REFRACTION-INDUCED TRACKING ERRORS AND CORRECTION METHODS FOR THE AIR FORCE WESTERN TEST RANGE

L. G. Rowlandson
J. R. Herlihy

December 1968

AEROSPACE INSTRUMENTATION PROGRAM OFFICE
ELECTRONIC SYSTEMS DIVISION
AIR FORCE SYSTEMS COMMAND
UNITED STATES AIR FORCE
L. G. Hanscom Field, Bedford, Massachusetts



(Prepared under Contract No. F19628-68-C-0209 by Syracuse University Research Corporation, Merrill Lane, University Heights, Syracuse, New York.)

# FOREWORD

This report is prepared for the

Aerospace Instrumentation Program Office
Electronics System Division
Air Force Systems Command of the United States Air Force
L. G. Hanscom Field
Bedford, Massachusetts

Air Force Program Monitor - Lt. C. Schafer, ESD/ESSIE

Project Number 6684, Task 6684.05

Covering research over the period

1968 February 1 to 1968 December 1

Prepared under Contract No. F19628-68-C-0209 by

Syracuse University Research Corporation
Merrill Lane, University Heights
Syracuse, New York

This report was reviewed and approved by

C. Schafer, Lieutenant, USAF
Program Manager for ESD/ESSIE/6684

The smooth and effective conduct of these operations was due to the extensive cooperation we had from Mr. A. D. Hoffmann and Scheduling and Flight Controllers of the Air Force Western Test Range. We also appreciate the support provided by PMR in the area of aircraft control, meteorological data gathering and radar position information.

We had many stimulating discussions with Mr. C. Gardner and Mr. Miller of WTNIM/AFWTR which enabled us to maintain an awareness of the AFWTR short and long term requirements and to appreciate the time elements involved.

Finally, we received enthusiastic support from our ESD Program Manager, Captain J. F. Shunk, Lieutenant K. Troup and Lieutenant C. Schafer in all areas of this investigation. This support was equally provided by Plans and Operations, Test Operations and Airborne Engineering of the L. G. Hanscom Field complex.

## ABSTRACT

The effect of refraction on radar and ballistic camera tracking accuracy is presented against a background of operational requirements and limitations. A method to compute refraction-induced errors using closed form expressions is presented together with a comparison of these errors against ray tracing results. For a hypothetical missile trajectory it is shown that the closed form solutions using an exponential model atmosphere are in good agreement with the ray tracing results using radiosonde data. The analysis also shows that the closed form expressions can be used to correct ballistic camera tracking errors. In this case a modified form of the exponential model is used to describe the optical refraction profile. Variations in refractivity in time and space are examined for their effect on tracking accuracy. The analysis shows that time variations of the refractivity profile near the radar can produce significant variations in the elevation angle error. Spatial variations far from the radar are restricted in their effect and because of earth curvature only variations near the radar are significant. For tracking below five degrees elevation angle the tracking errors can best be determined from ray tracing analysis with real-time, corrected, radiosonde data. However, the ability to track much below five degrees is shown to be impaired by multipath propagation effects. Recommendations are given for real-time evaluations of the ray tracing and closed form calculations of tracking errors. The advantages of the simplicity of application of the closed form equations for real-time corrections is stressed in the report.

TABLE OF CONTENTS

## LIST OF ILLUSTRATIONS

# INTRODUCTION

A refraction investigation was carried out at the Air Force Western Test Range to determine the tracking errors which would be produced by the troposphere. Refraction measurements were made using a Crain microwave refractometer[1,2] mounted, together with other instrumentation, in a USAF C131B Convair. This facility is described in detail together with the ground based analysis programs in the Appendix.

Additional refraction data were obtained from rawinsonde measurements launched from North Vandenberg, the Boathouse, San Nicolas Island, and Point Mugu. The Pacific Missile Range (PMR) provided radar tracking and meteorological support on many occasions when flights were conducted in their range.

The initial effort began in January 1967 through June 1967, at which time the contract was with the Mitre Corporation, Bedford, Massachusetts. During this period an analysis of the effects of refraction errors on bilateration and trilateration tracking errors was presented to AFWTR in April 1967.[3]

In June 1968, the refraction investigations were reinitiated at AFWTR under the direction of the Syracuse University Research Corporation. The aircraft and meteorological support facilities were again made available on this latter effort.

This report presents an analysis of the refraction conditions affecting the radar tracking systems which support the AFWTR firing program. These trackers are located at Tranquillan Peak, San Nicolas Island, and Point Mugu. The fourth station at Point Pillar (near San Francisco) is not included in the investigation described herein. It was intended to complete the program in the AFWTR sector at Vandenberg before initiating refraction studies at Point Pillar.

In an investigation of this kind, very large quantities of data are collected, not only from the aircraft measurements but also from the meteorological support facilities at AFWTR. This total compendium of data are carefully described and stored at Syracuse in the event that further detailed analysis is required. It is not intended that the report describe this total mass of data but rather selected situations are presented which illustrate the nature of the problem and from which some definite conclusions and recommendations can be made.

A concerted effort is made to relate this investigation to previous refraction studies carried out at PMR and AFWTR. In this way, the present investigation and analysis represents an extension of these former programs and takes advantage of the extensive ray tracing comparisons reported earlier by Gardner.[4]

Several methods are discussed which can be used to correct range and elevation angle tracking errors together with their relative advantages. From a description of the spatial and temporal variations of the radio refractivity the magnitudes of residual errors are calculated and their effect in the system is related to operational procedures.

Since ballistic tracking cameras experience tracking errors due to the dry term of refractivity, a brief discussion of these errors is presented. Consideration is given to the use of an exponential function to correct these tracking errors.

A method to correct velocity measurement errors is presented. This investigation was not intended to be the major effort during this contract period; therefore, the presentation is brief but demonstrates a correction method which could have considerable potential.

The most significant part of the presentation herein concerns the calculation of tracking errors from simple, closed, functions. This correction method requires that the vertical variation of refractivity be represented by an exponential model. In comparison with Gardner's analysis it is shown that this simple method can be used to correct tracking errors for a wide range of conditions.

Finally, recommendations are made for evaluating the error correction programs, initially using post-flight data to be followed by the application of selected correction techniques during live firings. Methods are also presented to acquire and apply appropriate meteorological data in the correction programs.

## SECTION I

## THE EFFECT OF TROPOSPHERIC REFRACTION ON ELECTROMAGNETIC PROPAGATION

Before discussing refraction-induced errors and correction techniques in detail, it is useful to review the nature of these errors and general methods for correction which presently exist.

The index of refraction in the troposphere is given by[5]

$$n = 1 + 10^{-6}\left[\frac{77.6}{T}\left(P + \frac{4810\ e}{T}\right)\right] \tag{1}$$

where P = the pressure of a volume of air (mb)
T = the temperature of the air (° K)
e = the water vapor pressure in the volume (mb)

The variable part of the index is called the refractivity and is designated

$$N_T = \frac{77.6}{T}\left(P + \frac{4810\ e}{T}\right) \tag{2}$$

where the dry term is

$$N_{DRY} = \frac{77.6\ P}{T} \tag{3}$$

$$N_{WET} = \frac{77.6}{T}\left(\frac{4810\ e}{T}\right) \tag{4}$$

The velocity of propagation of electromagnetic energy is given by

$$v = c/n \tag{5}$$

where c is the velocity of light or the velocity of electromagnetic propagation in a vacuum.

From propagation analysis it can be shown that at a point in space the reciprocal of the radius of curvature of an electromagnetic signal (ray theory) is a function of the gradient of the logarithm of refraction, n.[6] The most significant and sustained gradients (variation of n with distance) occur in the vertical direction and the curvature causes the signal to propagate towards the region of increasing index.

For radio frequencies the index of refractivity which affects the velocity and direction of propagation is given by the total $N_T$ term (Equation (2)). With the exception of water vapor resonance at 22 GHz and oxygen resonance at 60 GHz, the index is essentially frequency independent up to 72 GHz.[6,7]

In the visible optical region the refractivity is expressed by only the dry term (Equation (3)) and the effect of water vapor can be neglected.[6]

In both the radio and optical frequency range the magnitude of refractivity tends to decrease exponentially with height due to the overwhelming influence of the exponentially height-dependent pressure term.[8] However, at radio frequencies the variability of the water vapor pressure near the earth's surface (generally under 25,000 feet) can cause large variations from an average exponential behavior.

Direct measurements of refractivity can be made with microwave refractometers and pressure, temperature, and water vapor instruments. From these measurements a spatial pattern of the refractivity can be developed with the most sustained variations occuring in the vertical direction. In most cases the refractivity structure is defined in the vertical direction, and it is assumed that the measurements can be applied at other locations over the earth's surface thereby assuming a spherically symmetrical atmosphere.

Figure 1 defines the geometry associated with ray tracing analysis of the effect of the vertical variation of refractivity on angle and range errors. Using a ray theory approach the signal is transmitted to and/or received from a target at T. The apparent elevation angle of the object is $\theta_0$, whereas the true elevation angle is $\beta_0$. Due to the downward curvature of the ray an elevation angle error, $\epsilon$, is produced. In theory, if the refractivity of the medium was accurately known the magnitude of the elevation angle, $\epsilon$, could be determined by ray tracing analysis for given geometrical coordinates at each end of the ray. (Ray tracing methods will be discussed later.)

The true geometrical range to the target is $R_0$. The measured range to the target is along the electrical path, $R_e$. By measuring the time for a signal to travel between the end points of the ray (echo ranging) and assuming that the velocity of propagation is c (velocity in vacuum) two errors result. The first error results from the fact that the geometrical distance along $R_e$, calling this distance $R_g$, is longer than the distance along $R_0$. The target, therefore, appears to be farther away than it actually is. The second error results from the fact that the velocity of propagation is less than the velocity in vacuum by an amount $n^{-1}$ (Equation (5)) at every point along the ray. The delay produced by this reduced propagation velocity along the ray causes a retardation error in the range measurement which will be designated, $\Delta R$. The distance along $R_e$, measured by the round-trip travel time of a signal, is therefore too large due to velocity retardation. Ray tracing analysis has shown that the geometrical or first error, $R_g - R_0$, is a second order error compared to the retardation error, $\Delta R$.[7] Therefore, when range error is mentioned herein we are refering to the retardation error, $\Delta R$.

A4383

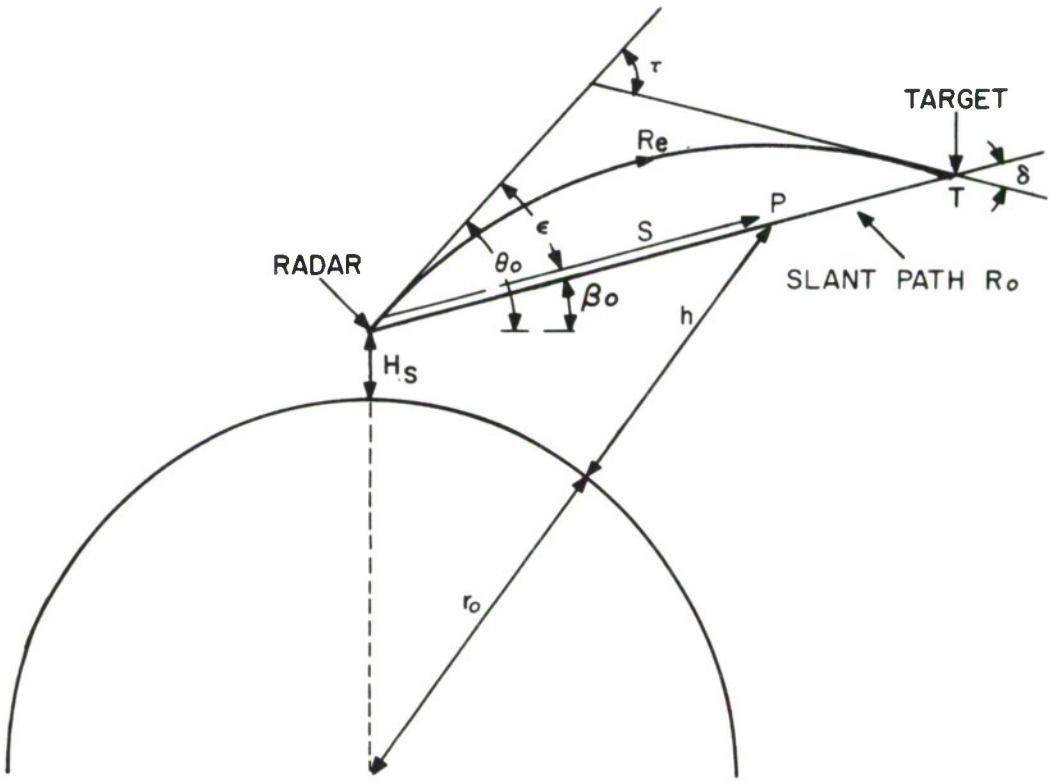


FIGURE 1. RAY GEOMETRY

## SECTION II

## THE DETERMINATION OF TRACKING ERRORS BY RAY-TRACING ANALYSIS

The determination of range and directional errors can be carried out with great accuracy using digital computer facilities. The usual method is to assume that a given refractivity profile (refractivity versus height) represents a spherically symmetrical condition over the earth's surface.[9] The troposphere is broken up into small enough height sections such that the index gradient, dn/dh, can be considered to be constant within any given section.[10] Since n will vary with height the magnitudes of these gradients will generally differ for each height section. From optical ray theory, the incremental bending of a ray can be calculated as it passes through a particular section.[6] Similarily the retardation produced in the section can be determined. By summing these effects it is possible to calculate the total bending, $\tau$, impressed on the ray over the path $R_e$ and to determine the retardation error, $\Delta R$. Once the path of the ray has been determined in this manner all other parameters are available from these calculations, such as the true range, $R_o$, the elevation angle error, $\epsilon$, and the doppler tracking error angle, $\delta$ (reference Figure 1). Discussions on the effect of this angle, $\delta$, on velocity measurement errors will be presented later.

A comparison of ray-tracing programs used within various ranges shows that in terms of mathematical precision there is essentially no disagreement.[11] The 7030 program designated Refchex used on this contract has been checked against Gardner's REFRAC and Bean and Thayer's program,[12] showing that there are no significant differences. Therefore, the accuracy available with present digital ray-tracing programs is not a limitation to the determination of tracking errors for a prescribed index profile.

There are, however, certain considerations which affect the usefulness of ray-tracing techniques for the real-time correction of tracking data.

(i) In the first place, can a refractivity profile be determined and used in the error correction program in a short enough period of time such that current conditions are represented?

(ii) Second, what errors are introduced by the assumption that this refractivity measurement is spatially invariant?

(iii) Third, if the tracking errors are calculated by ray tracing with this particular profile, how much calculation time and computer storage is required to cover the limits of tracking angles and ranges?

(iv) Fourth, can this error data be acquired from storage quickly enough to correct real-time tracking data?

## SECTION III

## THE SPATIAL AND TEMPORAL VARIATIONS OF THE REFRACTIVE INDEX

Aircraft measurements of the refractive index profiles were made from near sea level to about 15,000 feet and at intervals in distance out to 200 nautical miles from Vandenberg AFB and Point Mugu. Figure 2 shows a map of the area with the tracks generally flown along a westward outbound bearing. As shown, spirals were repeated on the inbound flights at the same coordinates as outbound to determine the changes which occurred in time.

A rawinsonde launch was scheduled to coincide with the first aircraft spiral on the outbound leg. Although the aircraft instrumentation was calibrated against psychometric measurements on the ground, prior to the flight the rawinsonde profile provided a check on the aircraft measurements in flight.

### 1. Aircraft and Rawinsonde Measurements

Figures 3a, b, and c show typical comparisons of aircraft and rawinsonde measurements. As the aircraft ascends it circles about a vertical axis which is generally three miles diameter at altitudes below 3,000 feet and about four miles diameter at 15,000 feet. For this reason, much of the fine structure shown on the aircraft profile can be attributed to horizontal variations. It is pertinent to later discussions to note on Figure 3a that the rawinsonde does not respond to an inversion which was measured by the aircraft. The aircraft was about 10 miles seaward from the rawinsonde launch site.

In this connection, a difficulty is presented by the fact that the winds tend to be westwardly in which case rawinsondes launched from the coastal sites are blown inland. Figure 4 shows representative trajectories of rawinsondes launched from North Vandenberg and the Boathouse. Figure 5 shows a plot of wind direction versus altitude from eight rawinsonde launches, four from North Vandenberg and four from the Boathouse. In this instance, the wind has shifted to the northwest over the period 29-31 May 1967. In general, meteorological measurements provided by AFWTR and PMR over the test periods show the wind prevailing from west to northwest.[13] It was not possible for the aircraft to track the rawinsonde since visibility near the launch areas was usually obstructed by fog and/or haze.

Due to the drift on most rawinsonde launches their measurements are not in the undisturbed maritime air mass which is west of the Tranquillan Peak and Point Mugu tracking stations. Comparisons with aircraft measurements have not shown any significant local differences except in situations when a strong maritime inversion is present. Due to the inland drift of the rawinsondes, the intensity of these inversions can frequently be underestimated.

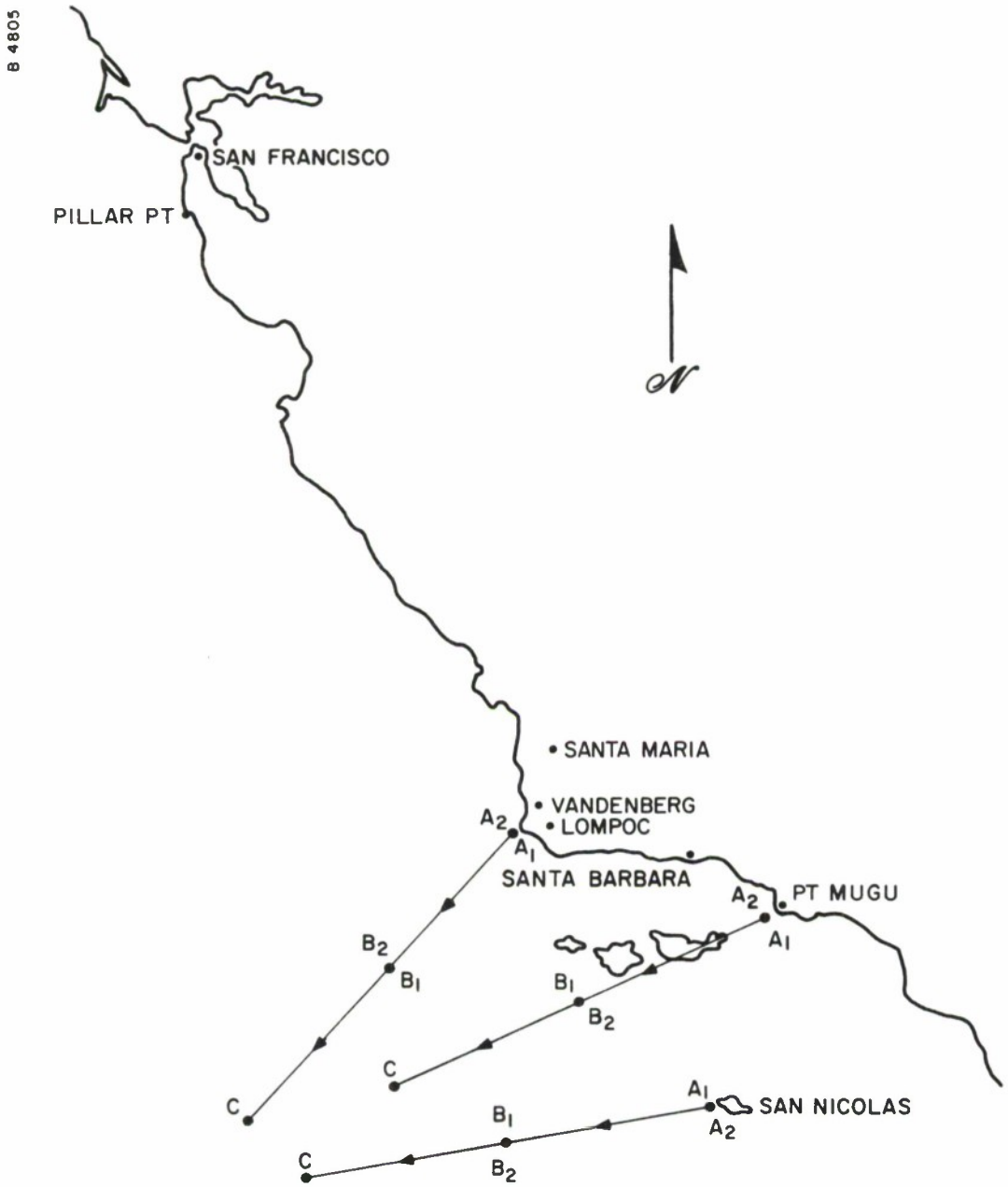


FIGURE 2. FLIGHT TEST AREA

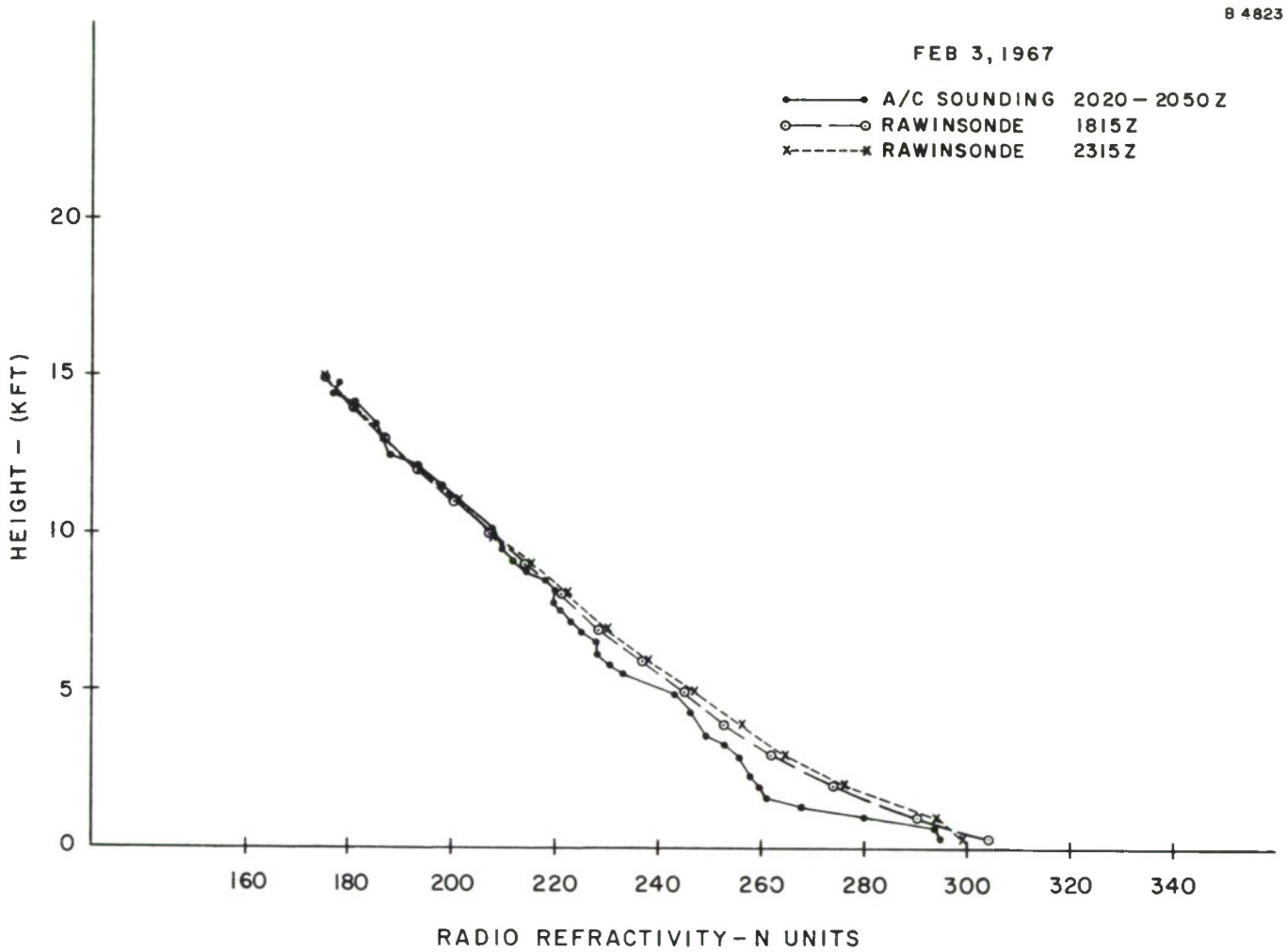


FIGURE 3a. A COMPARISON OF AIRCRAFT AND RAWINSONDE REFRACTIVITY PROFILES

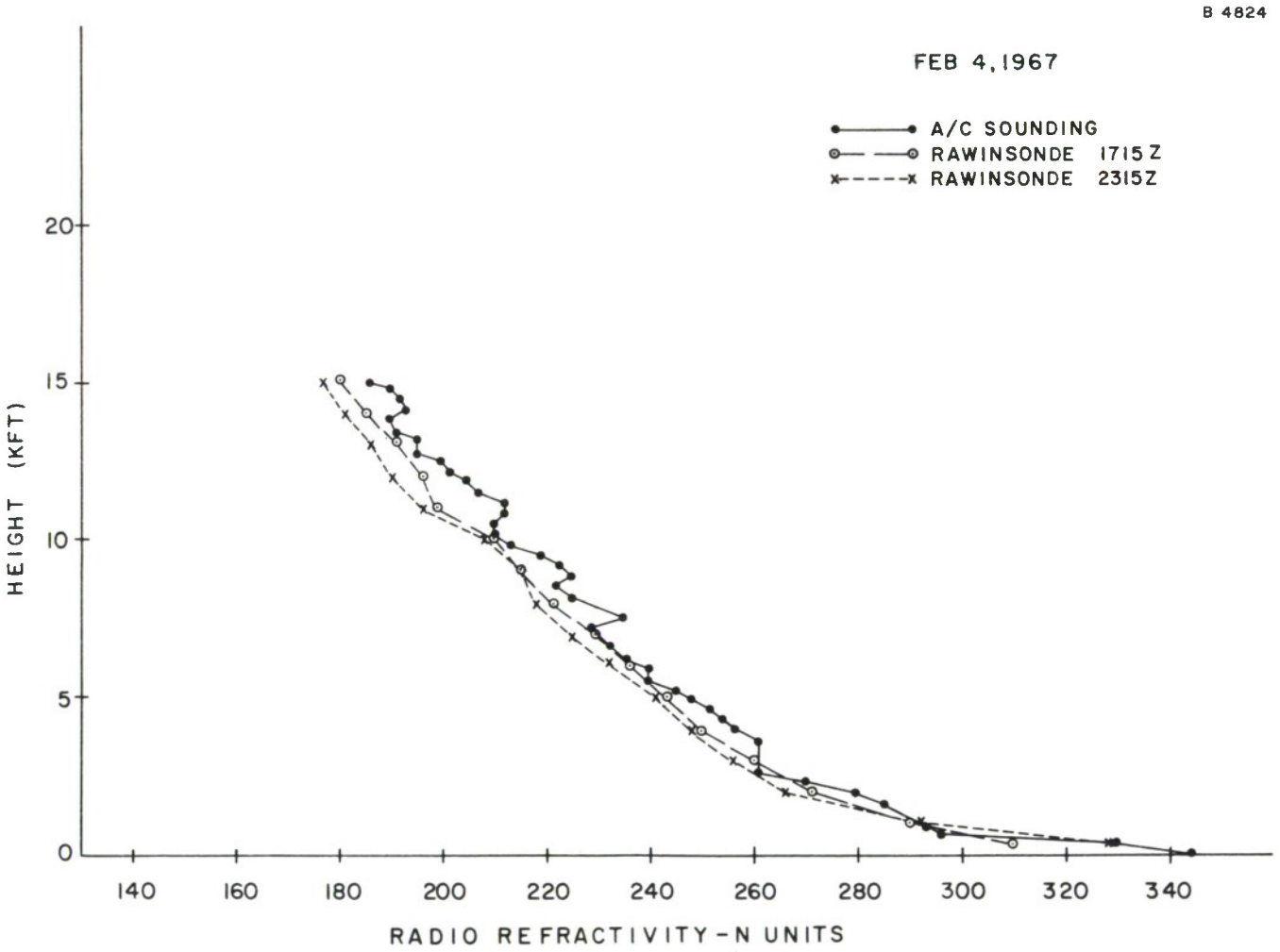


FIGURE 3b. A COMPARISON OF AIRCRAFT AND RAWINSONDE REFRACTIVITY PROFILES

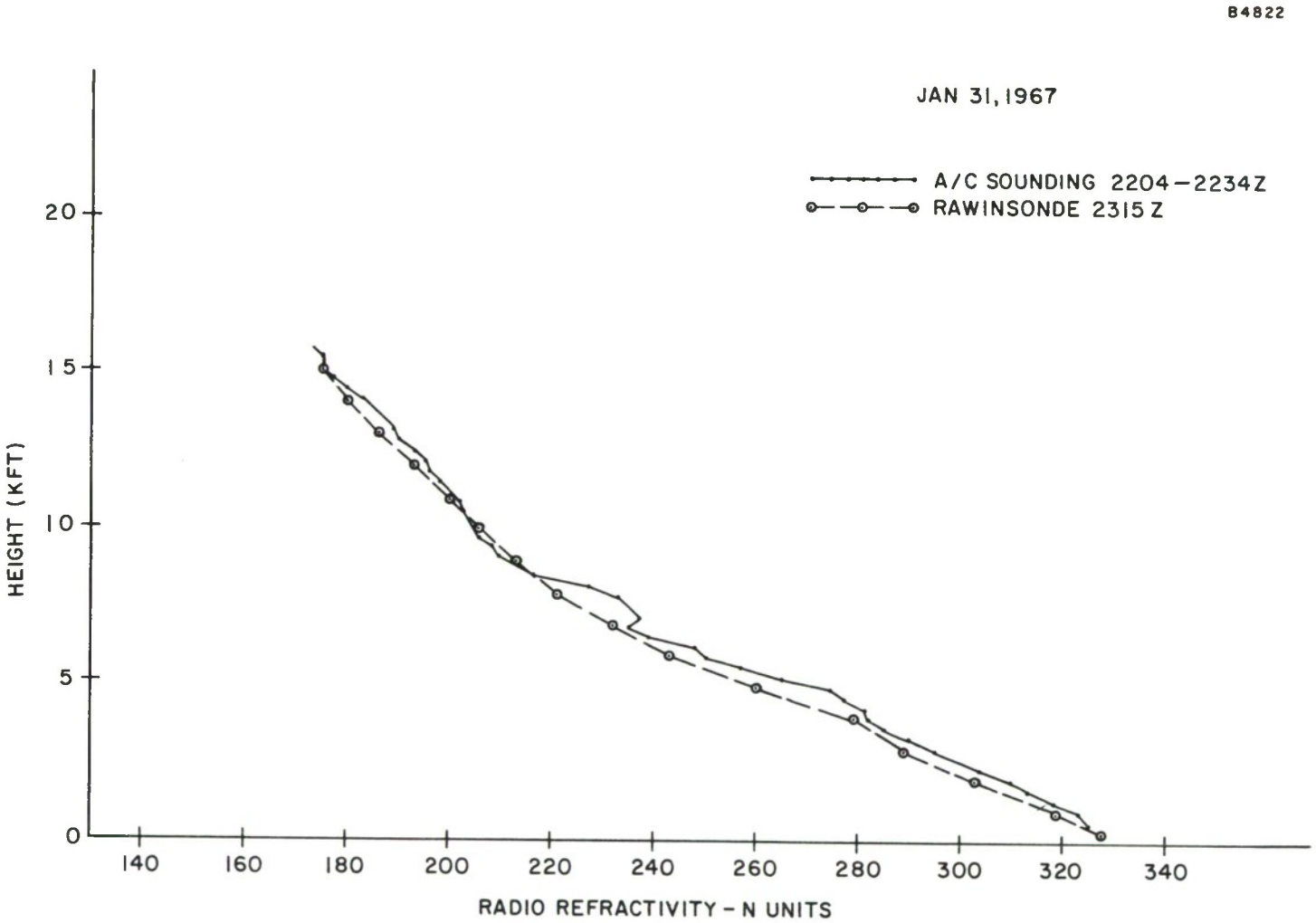


FIGURE 3c. A COMPARISON OF AIRCRAFT AND RADIOSONDE REFRACTIVITY PROFILES

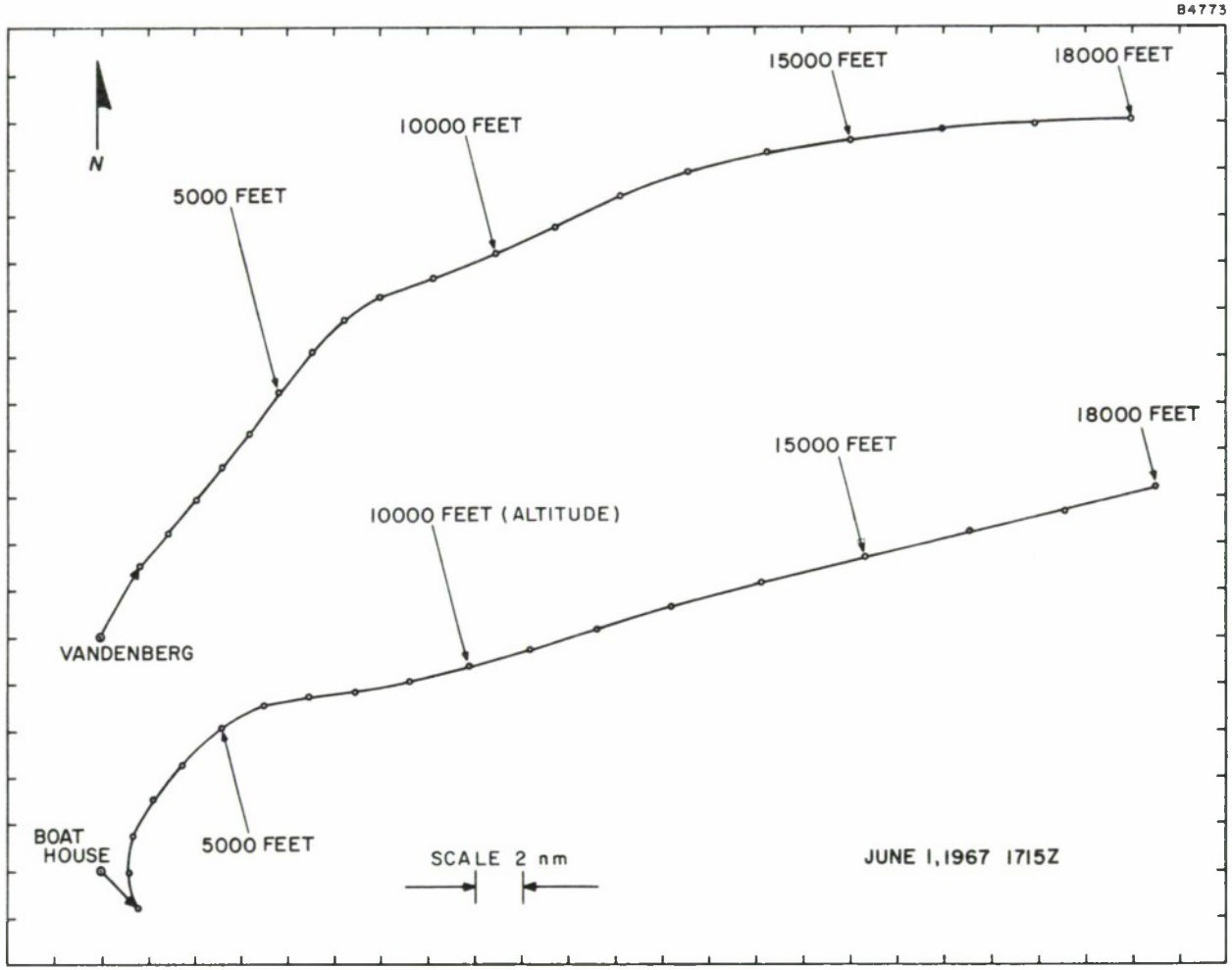


VANDENBERG AND BOATHOUSE RADIOSONDE TRACKS

FIGURE 4. VANDENBERG AND BOATHOUSE RADIOSONDE TRACKS

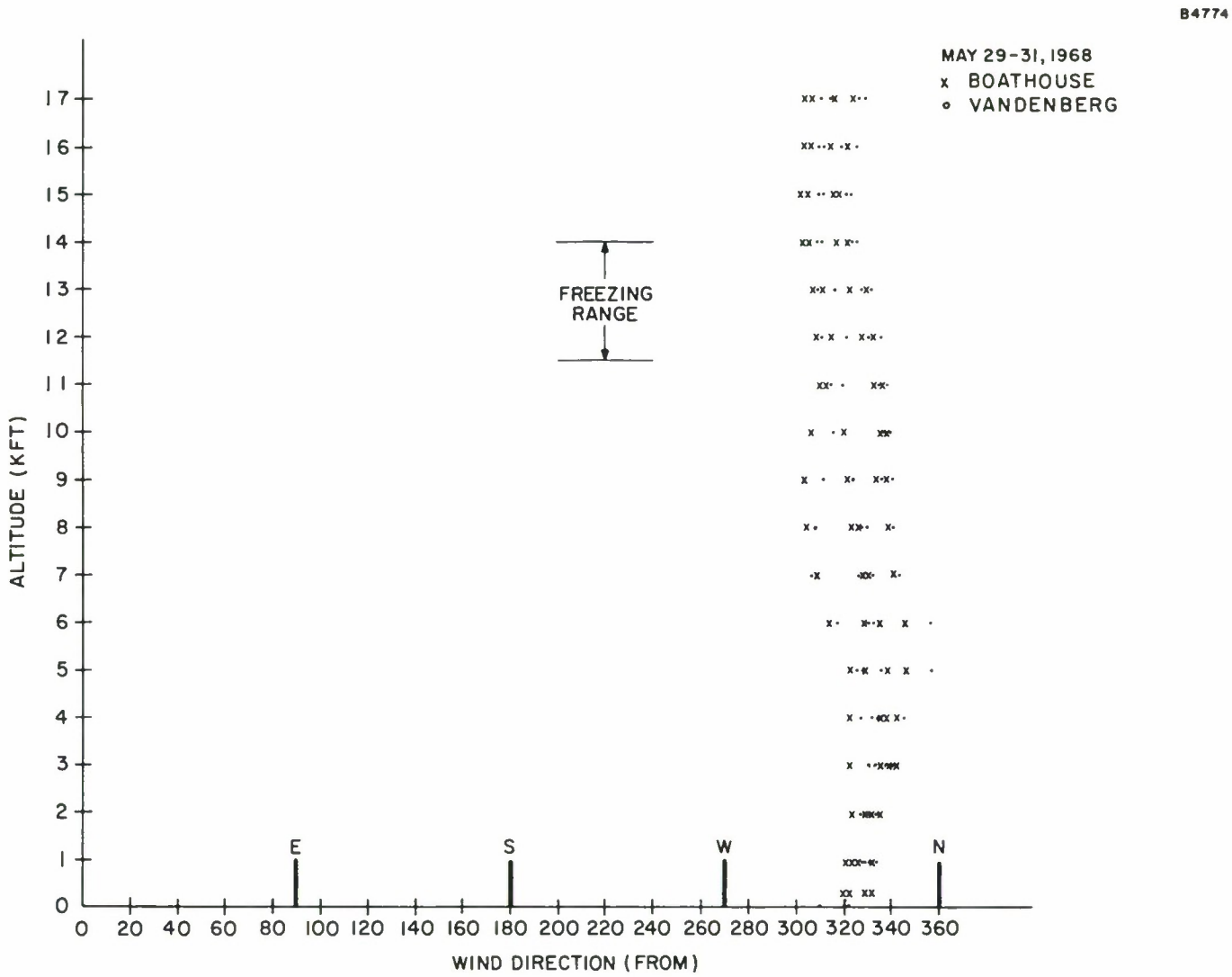


FIGURE 5. BOATHOUSE AND VANDENBERG RADIOSONDES

San Nicolas Island launches were expected to represent fairly undisturbed maritime conditions. It was initially anticipated that these launches could provide a meaningful description of refractivity for use by all the tracking stations in the AFWTR and PMR areas.

Figures 6, 7, and 8 show a comparison of profiles for simultaneous launches. In general there is not good agreement until heights near twenty thousand feet have been reached. In Figure 7, even in the presence of a strong inversion (vertical stability) at San Nicolas and Point Mugu and a weak inversion at Vandenberg, there are significant variations occurred above the inversion layer.

Aircraft measurements of the inversion characteristics and observations of cloud structure indicate there are large spatial variations in water vapor and visible water, respectively. At heights below ten thousand feet there are large differences in the magnitudes of water vapor pressure between stations. Therefore, evidence indicates that the San Nicolas rawinsonde cannot be used to determine a profile for general application to all the tracking stations.

## 2. Aircraft Measurements of the Radio Refractivity in the Seaward Direction

From aircraft measurements, it was possible to get in indication of the spatial and temporal variations of radio refractivity along the seaward extension of the range from Vandenberg. Figures 9 and 10 show refractivity profiles obtained along a flight path bearing two hundred and sixty degrees from Vandenberg. Profiles $A_1$, $B_1$, and $C_1$ represent vertical spirals outbound and $B_2$, $A_2$ co-located spirals inbound. Soundings made during the climb from the bottom of one spiral to the top of the next vertical spiral are designated $B_1$-$C_1$ and $B_2$-$C_1$ (Figure 9). Both sets of data show large variations were measured between profiles.

Comparing spirals $A_1$ and $A_2$ which are at the same point but different in time, it can be seen that the characteristics of the inversion are changing significantly over a period of about three hours.

Figure 11, derived from Figure 9, shows the average profile and the variations which occurred as a result of both spatial and temporal changes. Figures 12 and 13 show the isopleths of constant refractivity derived from the soundings of Figure 9 Superimposed on these latter figures are curves showing the radar horizon for elevation angles of zero, one, and two degrees. In general, tracking below two degrees subjects the radar to sea reflections.

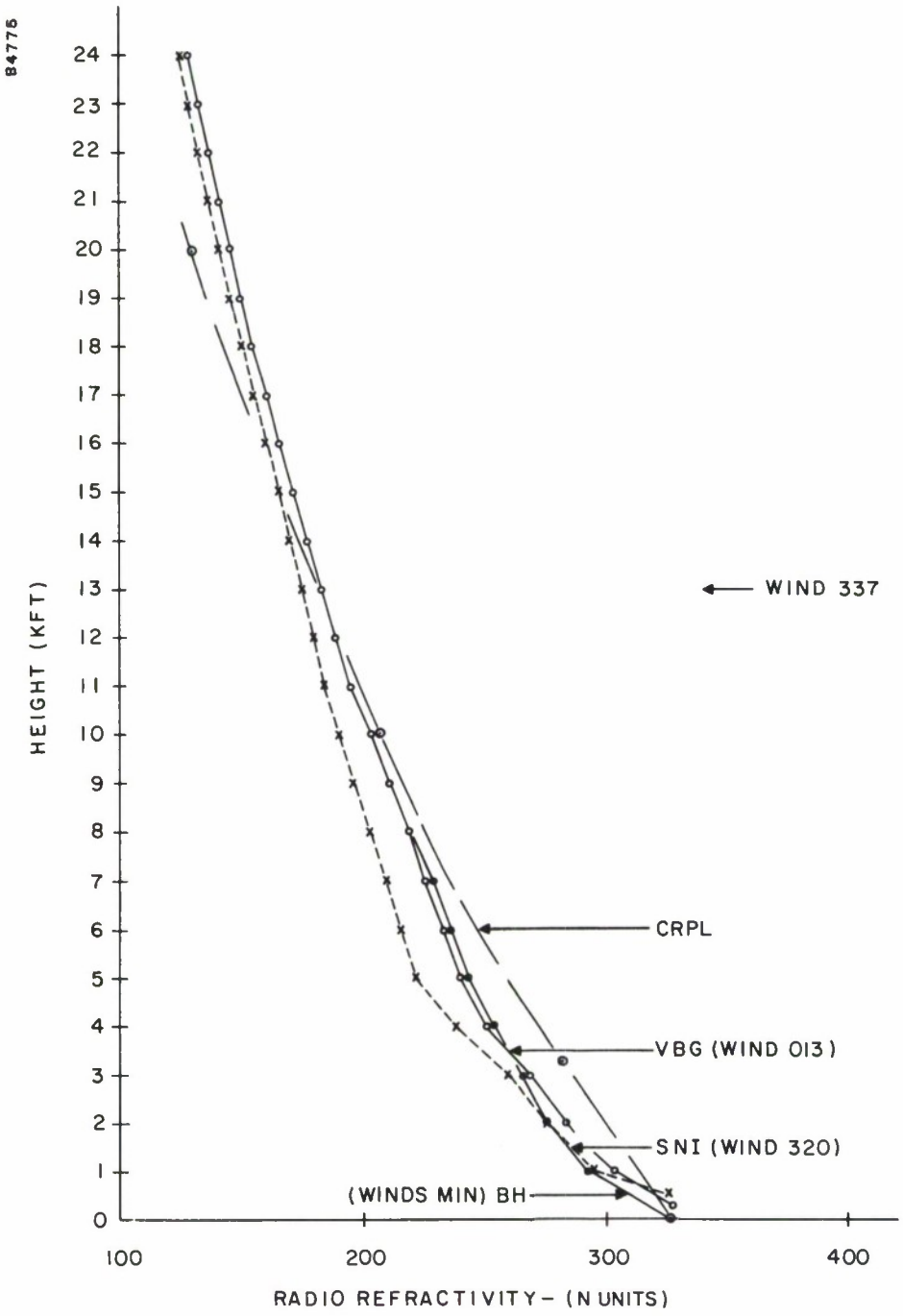


FIGURE 6. RADIOSONDES OCTOBER 23, 1967 1715Z

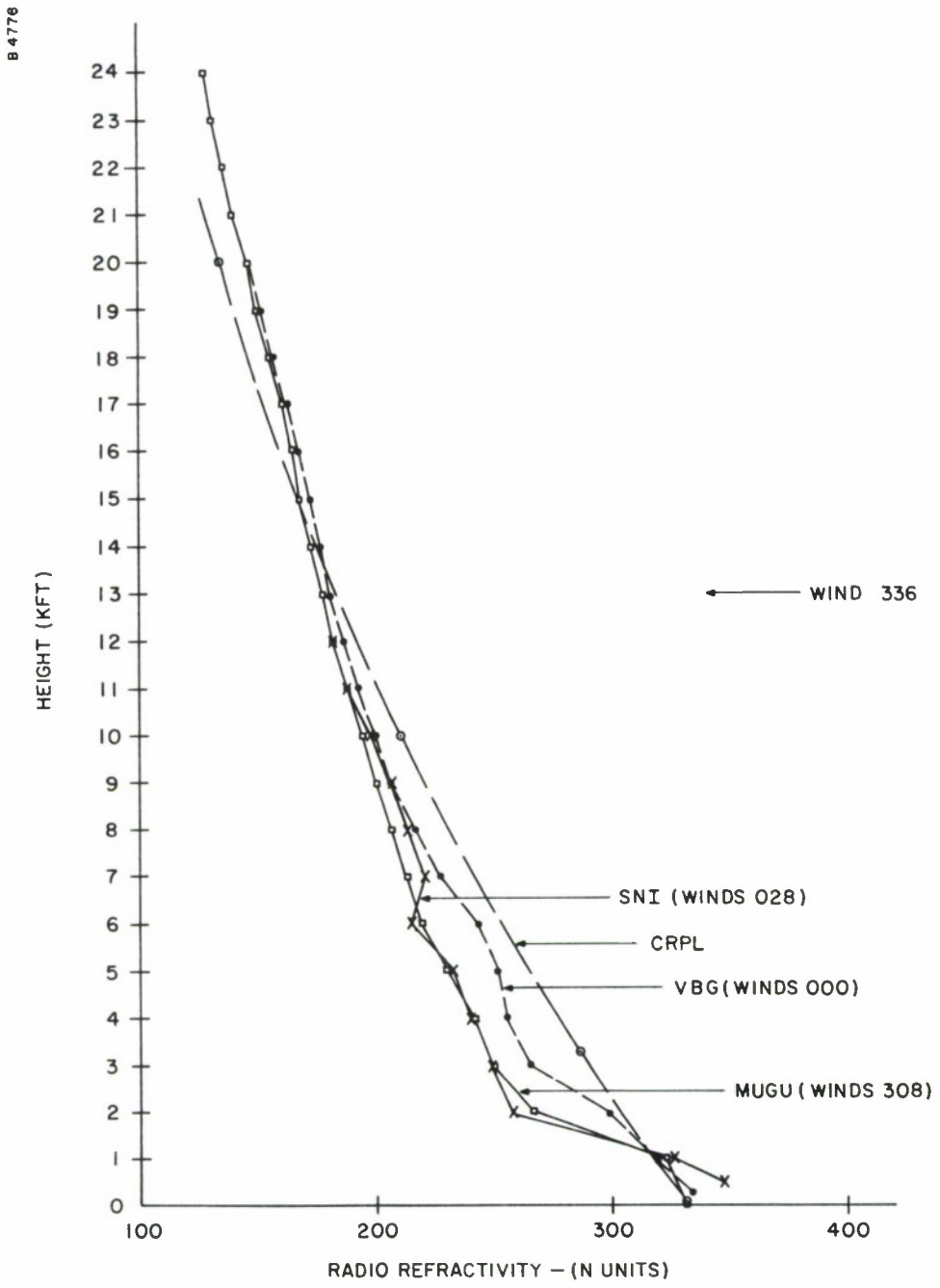


FIGURE 7. RADIOSONDES OCTOBER 23, 1967 1100Z

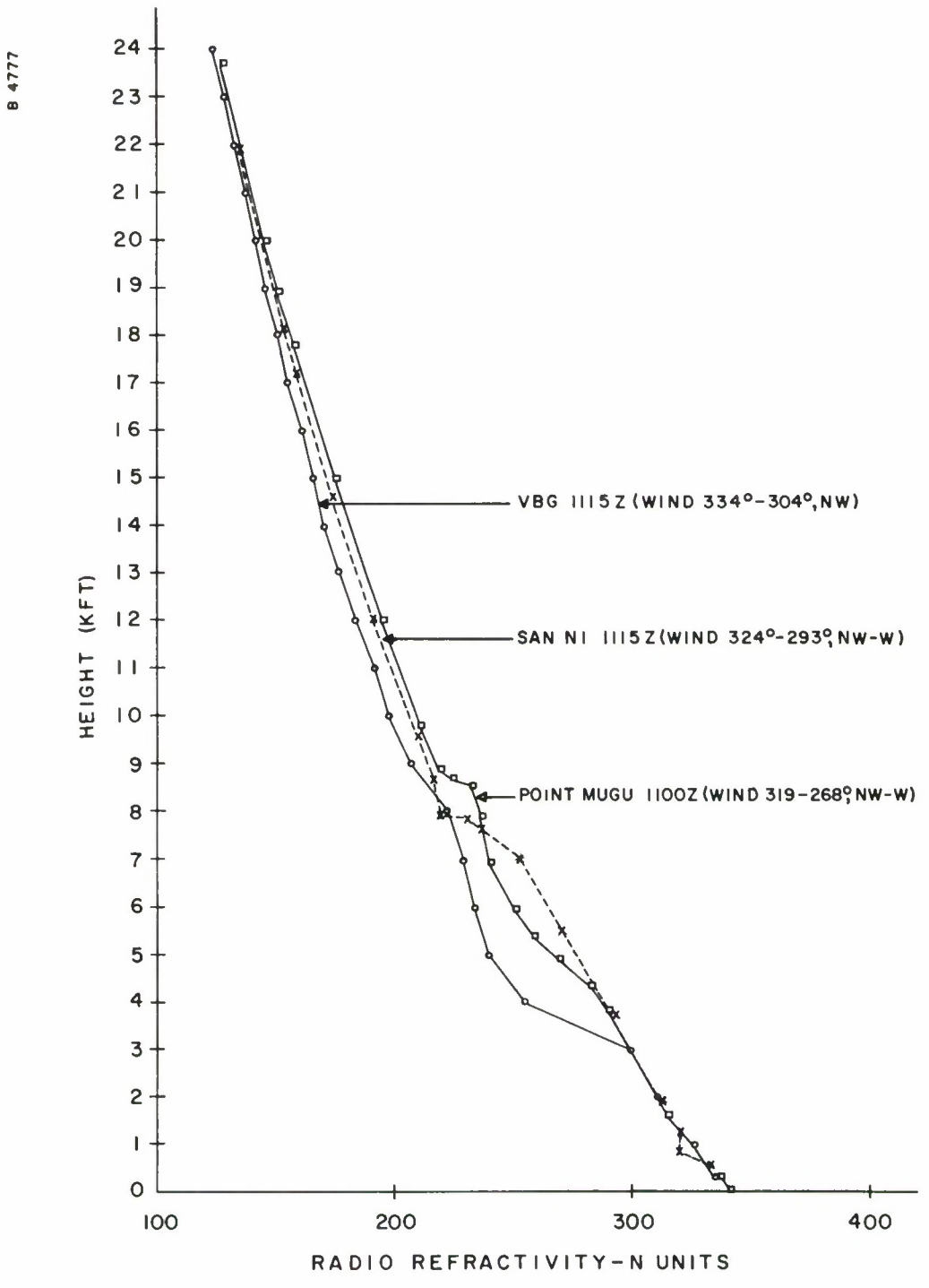


FIGURE 8. RADIOSONDE JUNE 13, 1967

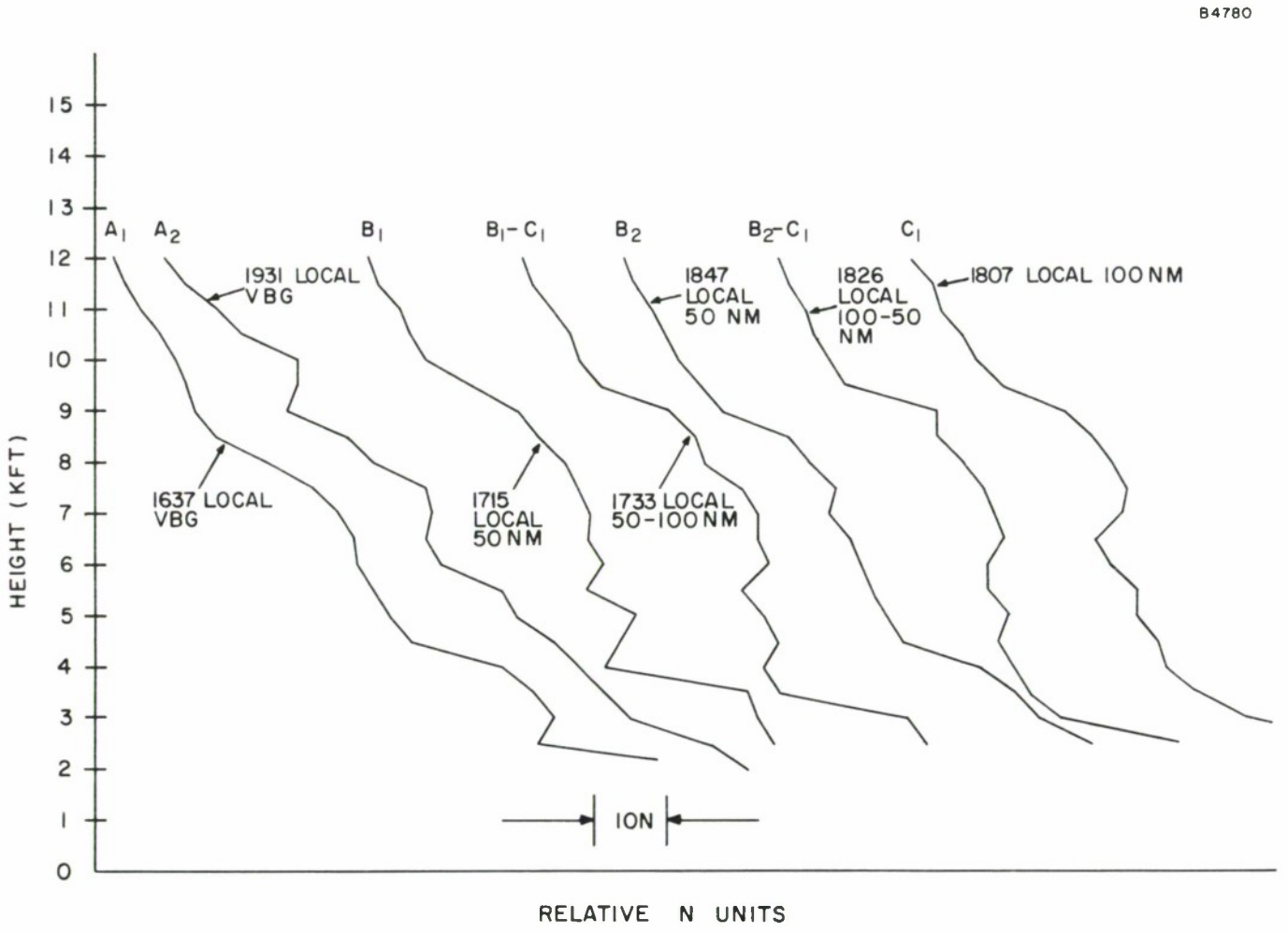


FIGURE 9. RADIO REFRACTIVITY PROFILES WEST FROM VANDENBERG, JUNE 26, 1968

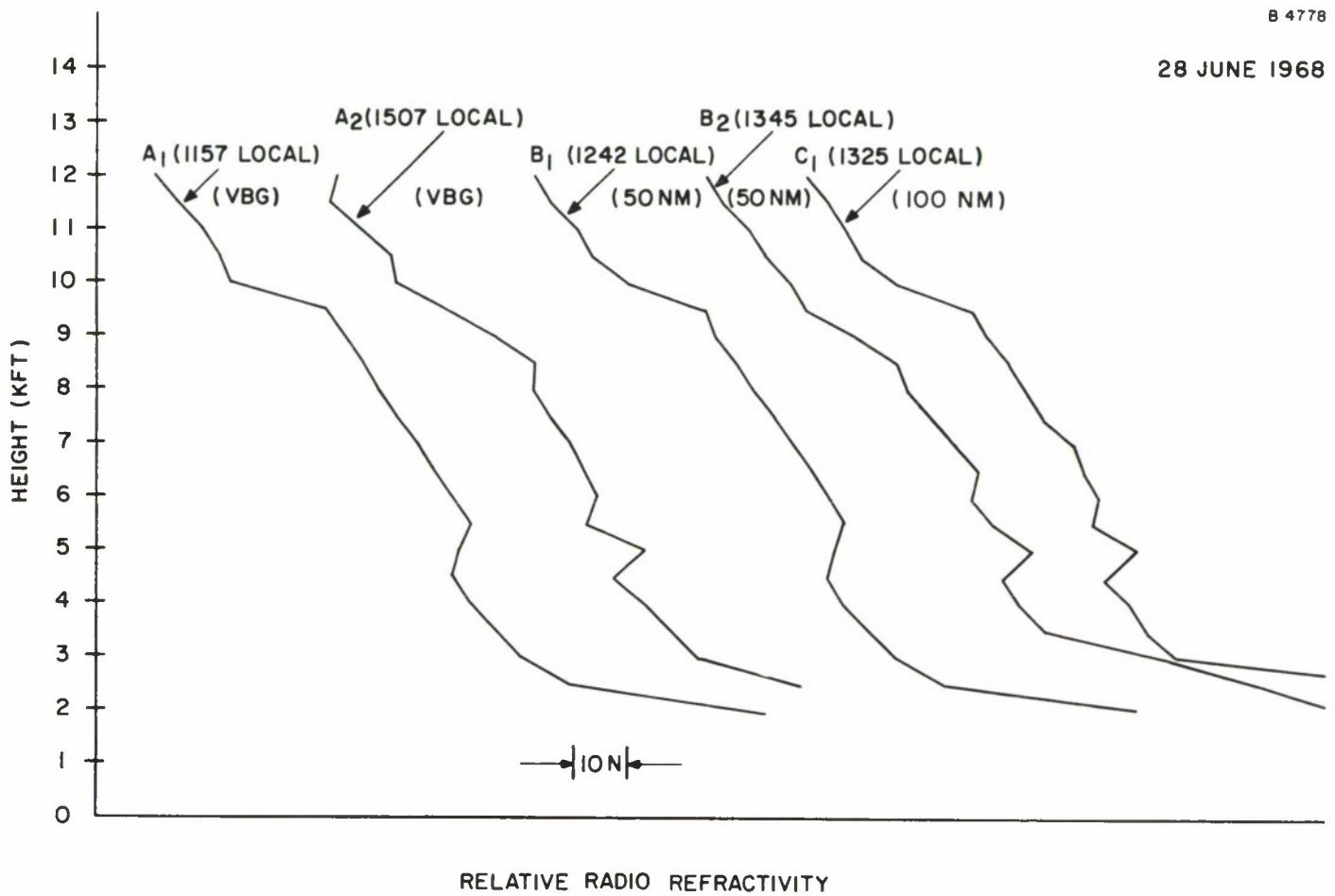


FIGURE 10. SPIRALS OUTBOUND FROM VANDENBERG

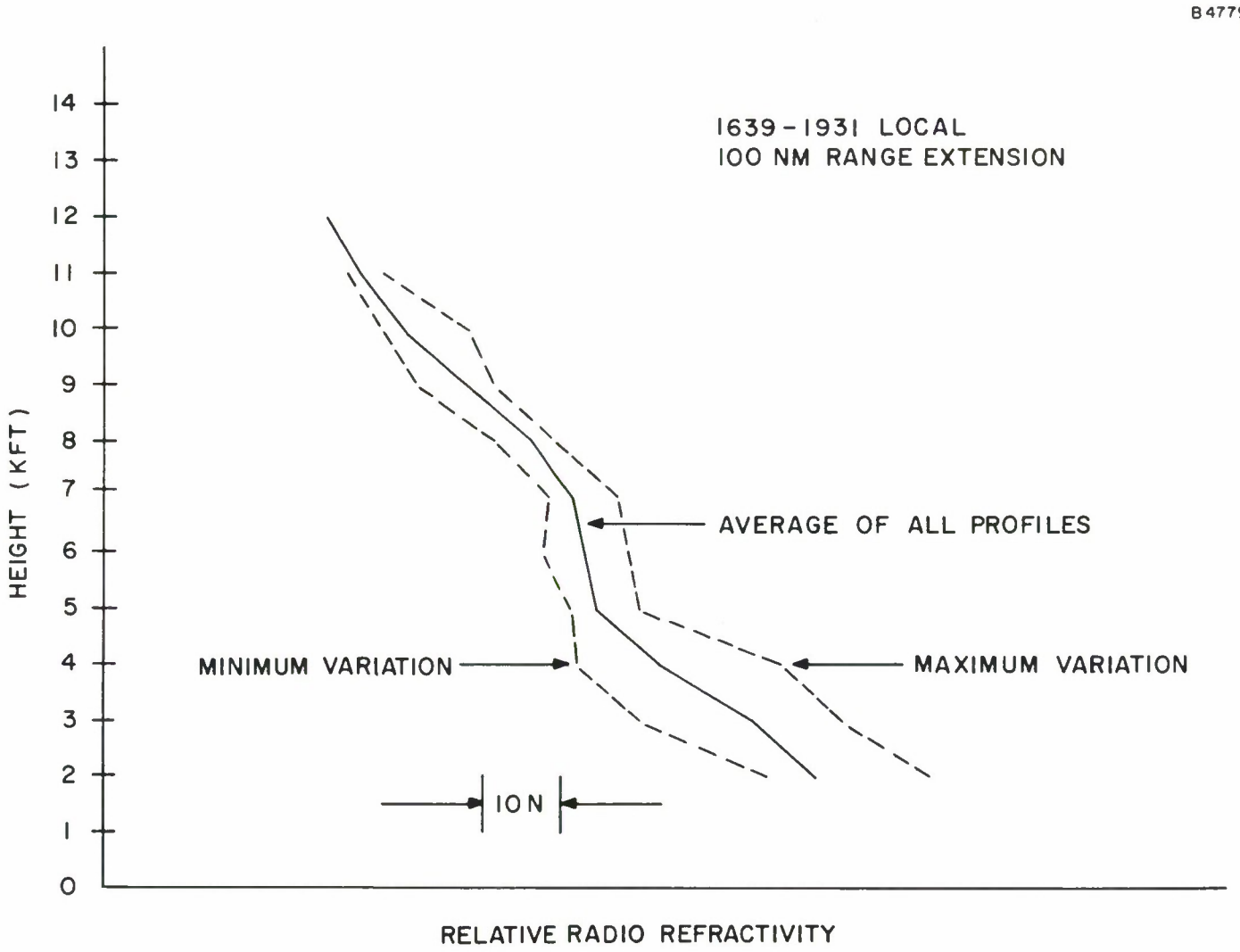


FIGURE 11. AIRCRAFT SOUNDINGS JUNE 26, 1968

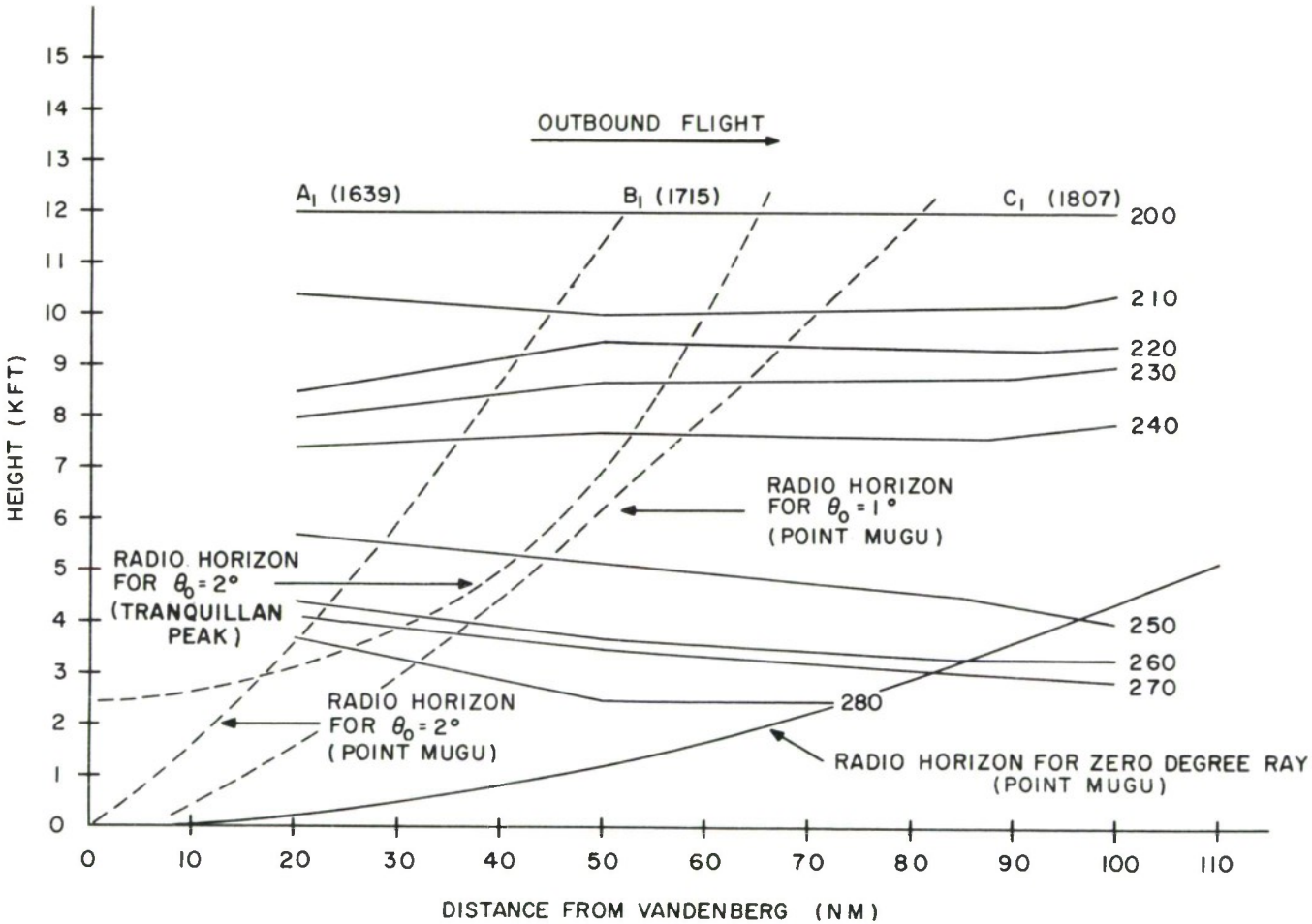


FIGURE 12. ISOPLETHS OF RADIO REFRACTIVITY
JUNE 26, 1968

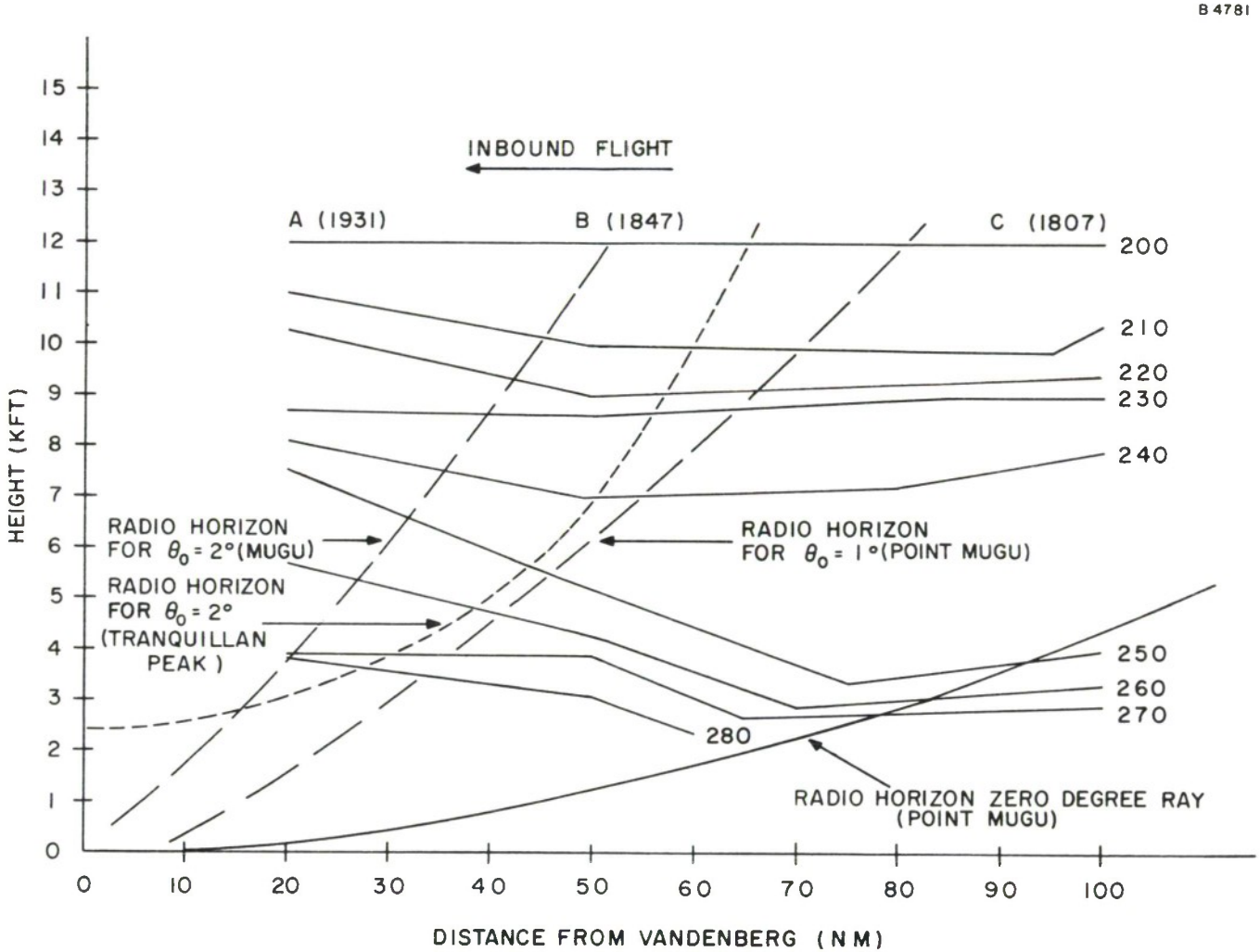


FIGURE 13. ISOPLETHS OF RADIO REFRACTIVITY
JUNE 26, 1968

Figure 14 shows a typical range-height plot from the Tranquillan Peak radar. The aircraft made an initial upward spiral at a point 10 nautical miles from the radar and terminated the spiral at 15,000 feet above sea level. The aircraft then descended to reach a coordinate approximately 85 miles from the radar where a second spiral was initiated. Since no earth curvature or refraction correction was used, the plot shows the top of the second spiral to be approximately 10,000 feet above sea level whereas the true height is 15,000 feet.

Using a simple 4/3 effective earth radius[7] the effect of sea reflections on the radar elevation angle data was pronounced for apparent elevation angles below 1.5 degrees.

Figure 15 shows the ray path geometry where the true earth radius has been replaced by an effective earth radius. The Tranquillan Peak radar is about 2500 feet above sea level. From Figure 15 it is apparent that the angle between the direct and reflected signals, $\alpha$, becomes less as the height of the antenna above the reflecting sea surface decreases. For tracking stations at Point Mugu and San Nicolas Island, which are at lower heights above sea level, the reflected signal arrives much closer to the direction of the main beam. If the sidelobe level is not very far down from the main beam, the behavior of these monopulse tracker systems can be severely disturbed in the elevation angle measurement.

It is, therefore, reasonable to suggest that tracking below 1.5 degrees apparent elevation angle cannot be carried out with the existing radars in the AFWTR system. Only when the target is on the sea surface would multipath propagation be prevented. In fact, the radars can track ships without serious elevation angle fluctuations.

3. The Effect of Time and Space Variations of the Refractivity Profile

Let it be assumed that Profile $A_1$, Figure 9, represents an accurate determination of radio propagation conditions pertaining to the Tranquillan Peak radar at 1639 hours. Restricting tracking to two degrees elevation angle or greater it is reasonable to assume that Profile $A_1$ represents spatial conditions out to 50 nautical miles (reference Figure 12).

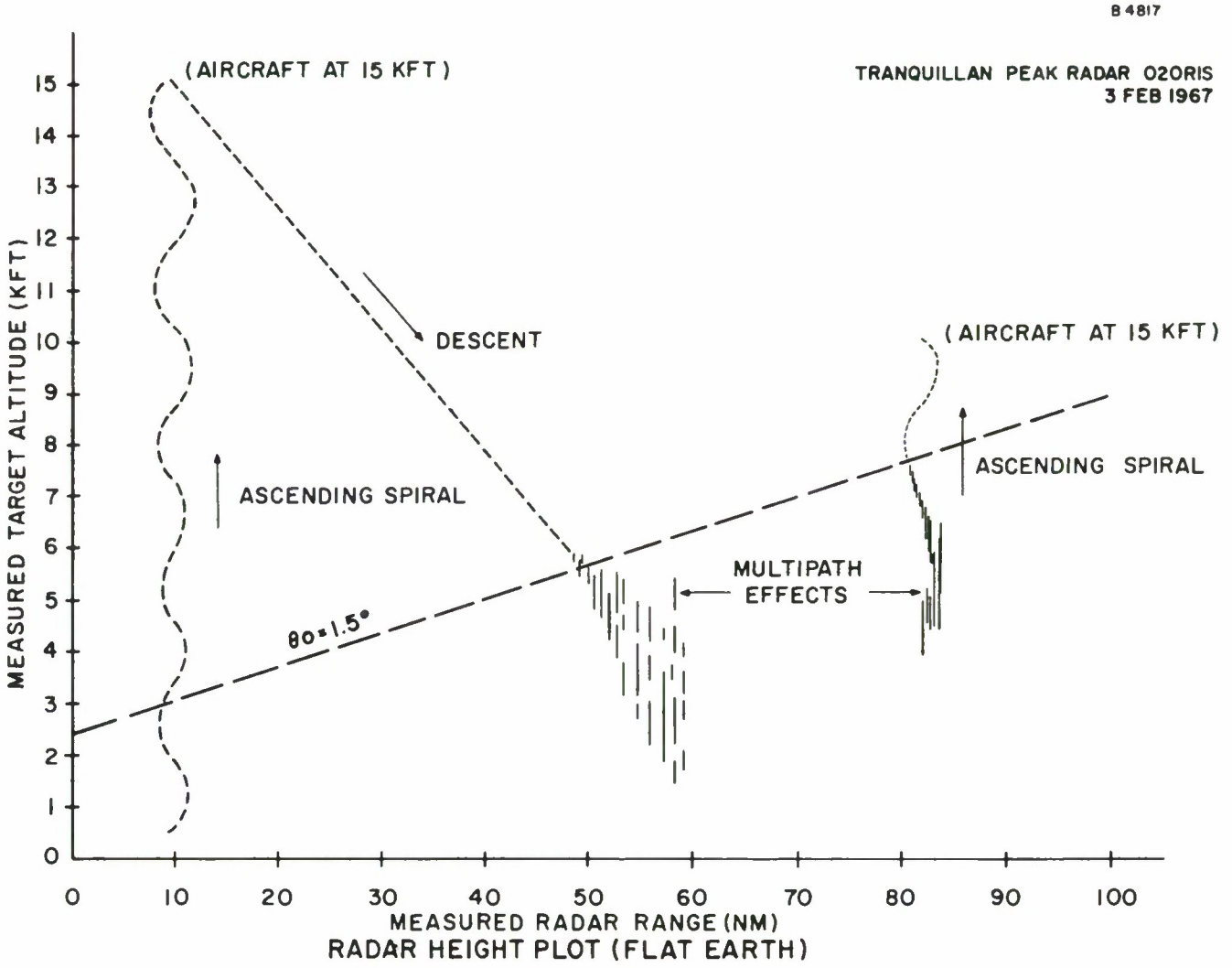


FIGURE 14. RADAR HEIGHT PLOT (FLAT EARTH)

A4816

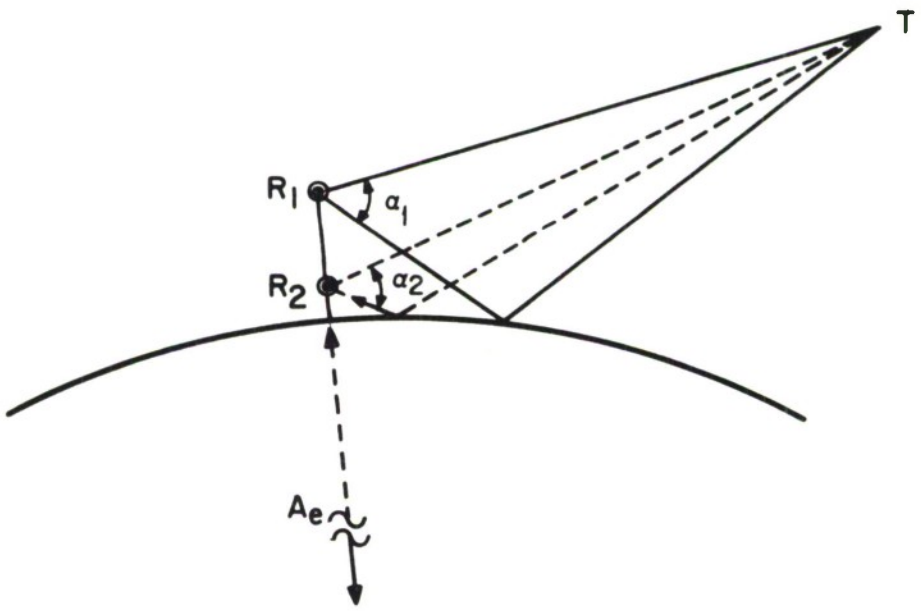


FIGURE 15. MULTIPATH GEOMETRY

Suppose that the application of this profile in the refraction correction program does not take place until 1931 hours. By this time, Profile $A_2$ (Figure 9) is now assumed to be a correct description of the radio propagation conditions. What errors occur as a result of the changes in refractivity between 1639 and 1931 hours?

Figure 16 shows the difference in the elevation angle errors, $\Delta\epsilon$, as a function of the initial elevation angle, $\theta_o$, for the Tranquillan Peak radar. At the smallest tracking angle of two degrees a 0.25 milliradian error would exist as a result of the above time variations in the propagation conditions.

Figure 17 shows that a 2.25 foot range error difference ($\Delta(\Delta R)$), would exist at two degrees elevation angle. Ray tracing analyses were not carried out above 12,000 feet because radio refractivity variations above this level were insignificant. Since the aircraft measurement accuracy is rechecked after each flight, the above profile variations were determined to be due to temporal changes and not due to instrumentation errors in the aircraft.

With one aircraft it is not possible to obtain time invariant spatial measurements; therefore, the information presented in Figures 12 and 13 includes some time variation effects. Let it be assumed that the measurement of refractivity, Profile $A_1$ (Figure 9), is again put into the tracking system refraction correction program. Approximately one hour later, a second measurement, Profile $B_1$, is obtained at 50 nautical miles range from the tracking station. A comparison of these profiles on the elevation angle error differences, $\Delta\epsilon$, and the range error difference, $\Delta(\Delta R)$, is shown in Figures 18 and 19, respectively. Obviously, from Figure 12, the only variations affecting tracking at two degrees occur above 7,000 feet altitude.

At two degrees initial elevation angle the elevation angle error difference is 0.15 milliradian and the range error difference is 0.42 feet.

For tracking stations operating closer to sea level the radio horizon at two degrees elevation angle provides even greater restriction on the effect of spatial variations. As shown by Figure 12, for the Point Mugu radar, variations below 7,000 feet would not be significant for ranges beyond 35 nautical miles.

It is apparent that spatial variations, which occur largely at low altitudes, are prevented by the earth's curvature from having a significant effect on the radar tracking accuracy. However, temporal effects can produce large errors and should be constrained by incorporating refractivity

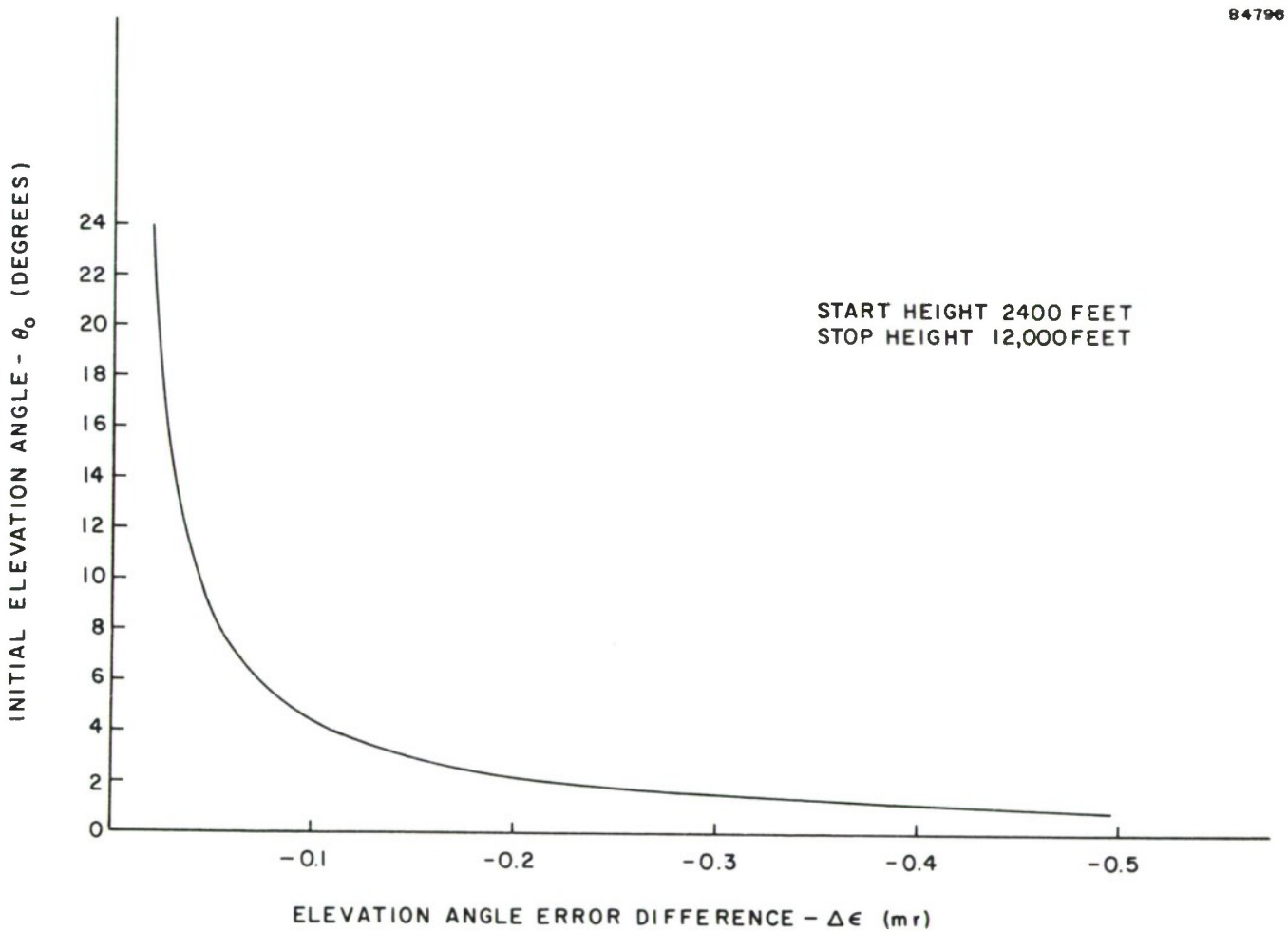


FIGURE 16. ELEVATION ANGLE ERRORS PRODUCED BY TIME VARIATIONS OF REFRACTIVITY

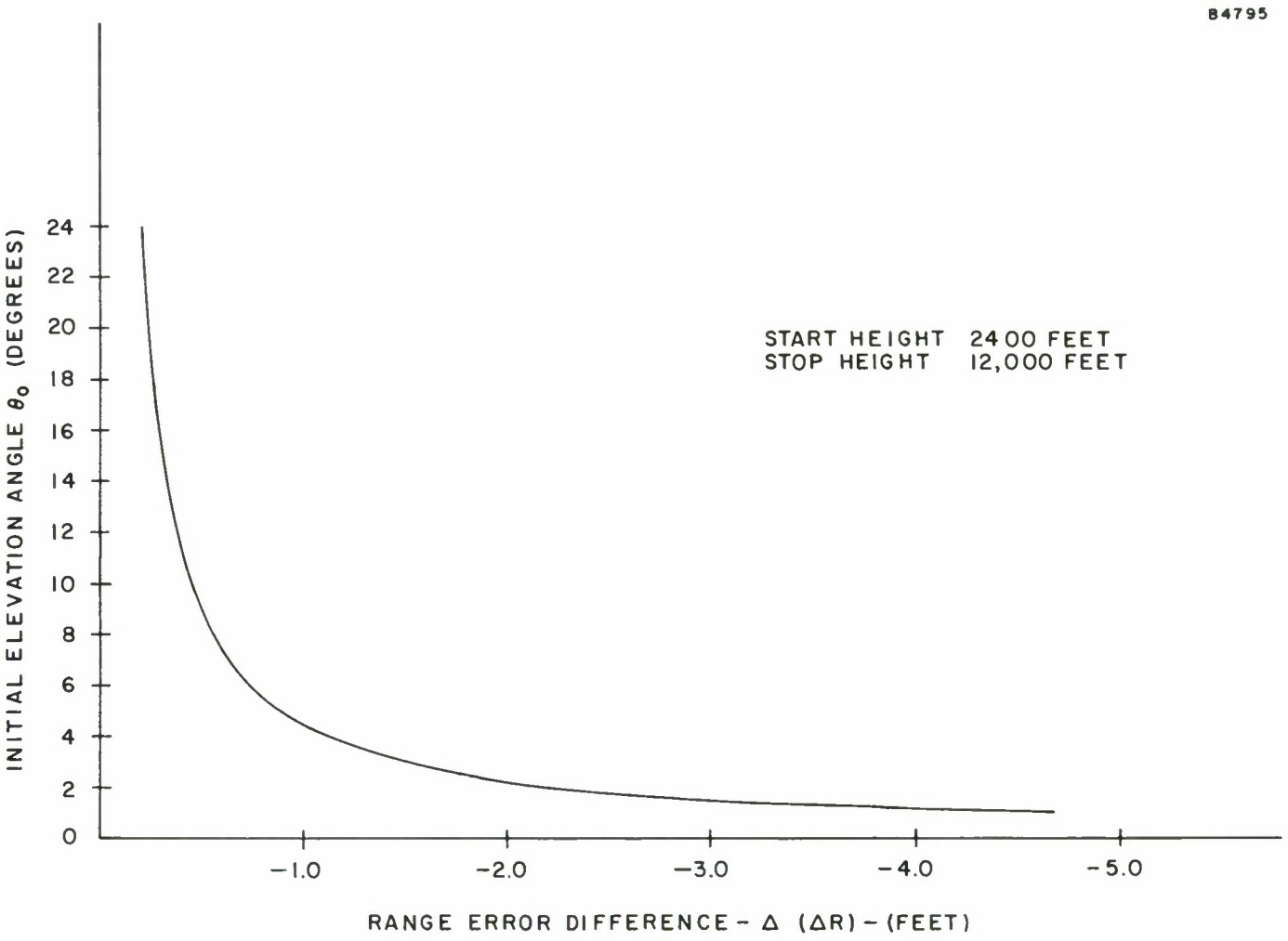


FIGURE 17. RANGE ERRORS PRODUCED BY TIME VARIATIONS OF REFRACTIVITY

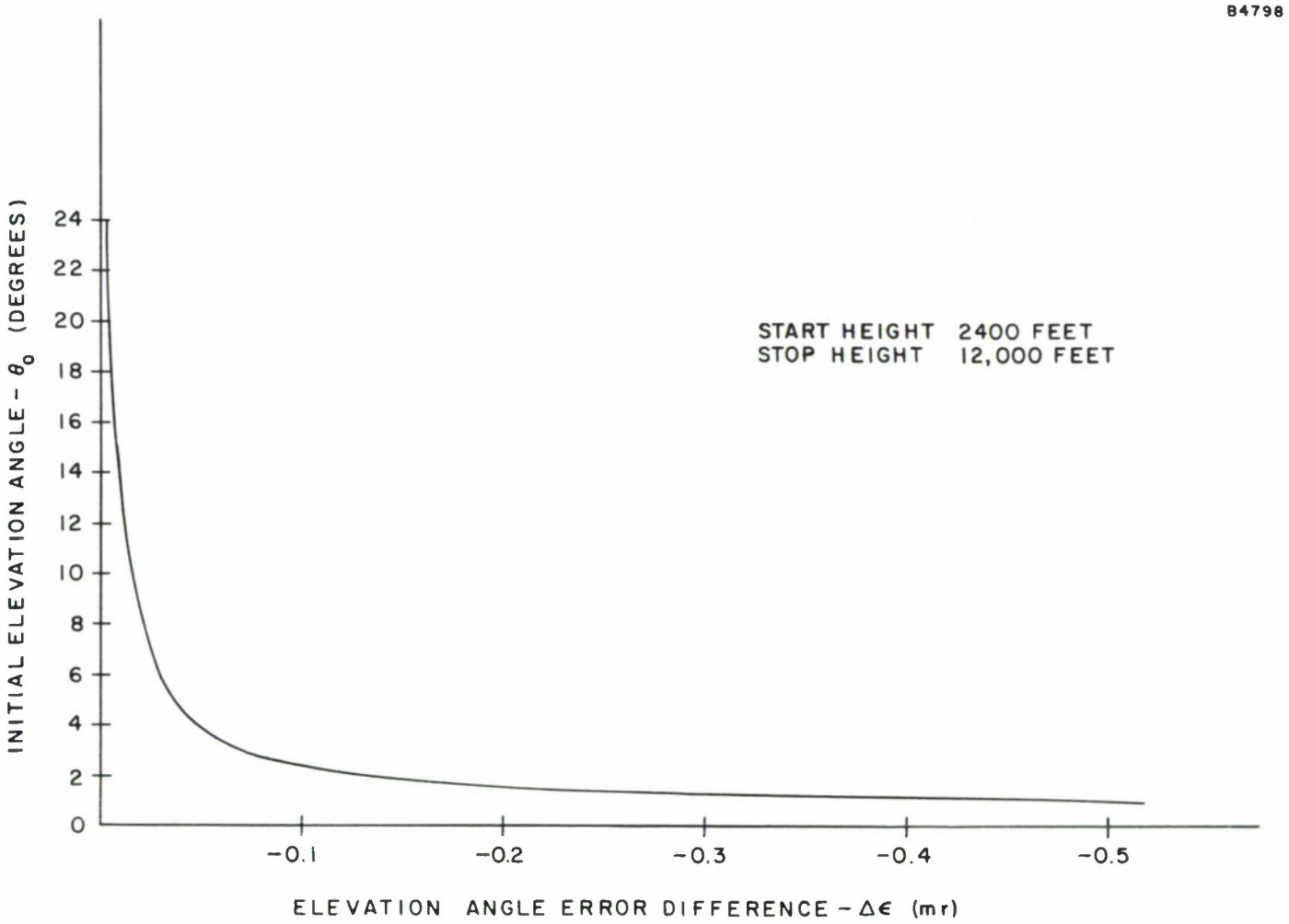


FIGURE 18. ELEVATION ANGLE ERRORS PRODUCED BY SPACE VARIATIONS OF REFRACTIVITY

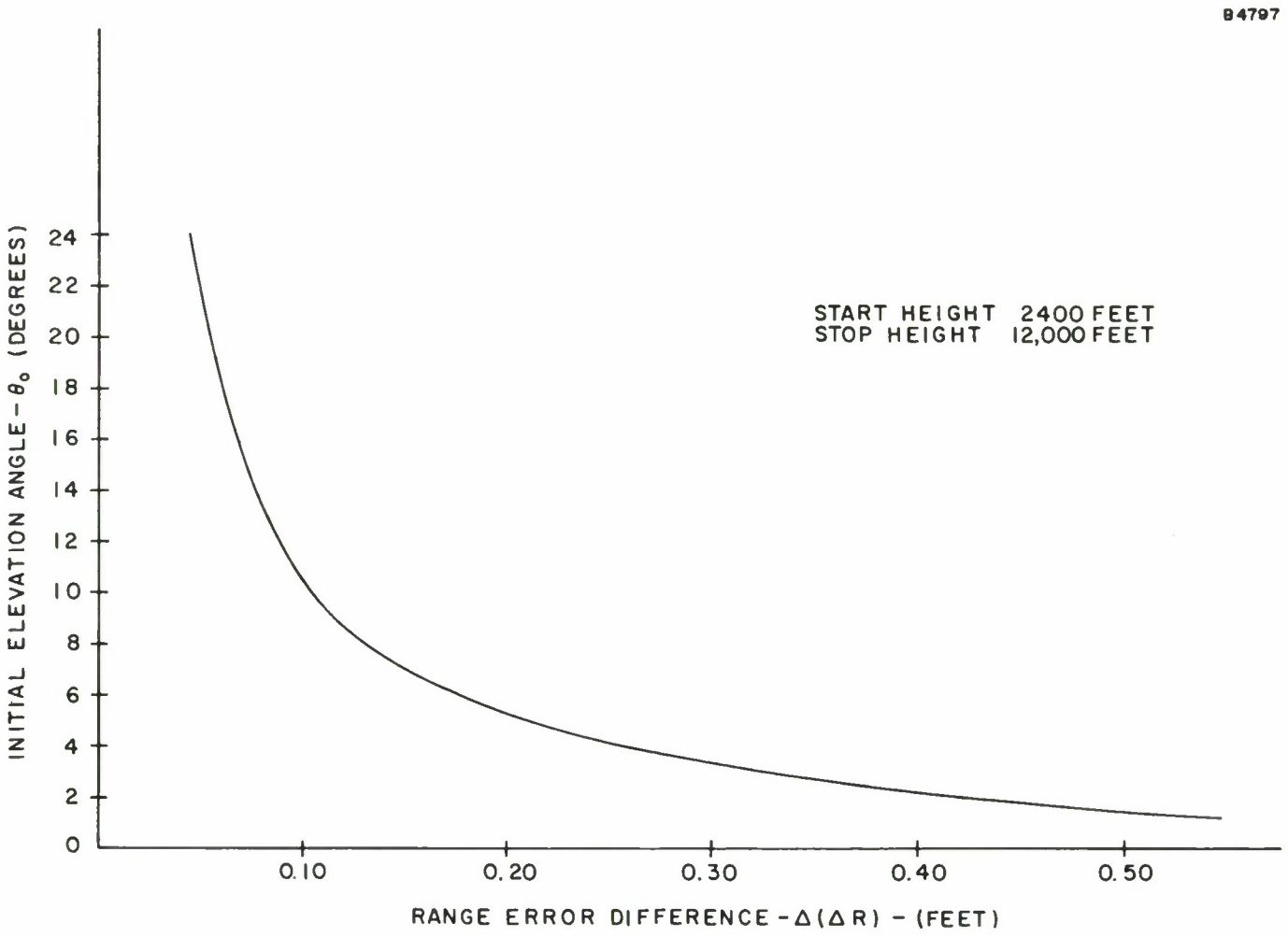


FIGURE 19. RANGE ERRORS PRODUCED BY SPACE VARIATIONS OF REFRACTIVITY

profile information into the tracking system as close as possible to the time of application. It is well known that ray bending near the radar produces larger height errors than bending which occurs far from the radar. This is simply because the height error is the product of the angle error and the distance from this bending disturbance to the target.

In summary, the effects of temporal variations near the radar site are most effective in producing elevation angle errors and, therefore, height errors. For tracking above two degrees elevation angle spatial variations have a secondary effect in the tracking accuracy. Therefore, evidence indicates that to determine refractivity profiles for the correction of refraction-induced errors, measurements should be made close to the radar site and along a bearing of the expected azimuth tracking sector. Finally, the refractivity data should be collected and used as close as possible to the time of tracking application in order to constrain temporal errors.

## SECTION IV

## A COMPARISON OF METHODS TO CORRECT REFRACTION ERRORS AT RADIO FREQUENCIES

At radio frequencies we are concerned with the behavior of the total index of refractivity, $N_T$, given by Equation (2). From the analysis and discussion of spatial refractivity effects it will be assumed that a profile can be measured which represents a description of spherically stratified radio propagation conditions.

The first method to correct refraction induced errors uses a ray-tracing analysis. Range and angle errors are calculated for tracking elevation angles and radar ranges corresponding to the trajectory of a hypothetical missile launch. This analysis was carried out by Gardner[4] and his ray-tracing data will be used to compare with an alternative method to calculate tracking errors, described below.

### 1. Refraction Error Calculations in an Exponential Atmosphere

Let it be assumed for the moment that the vertical decrease of refractivity can be expressed in terms of an exponential function[8] relative to the tracking station, where

$$N = N_s \, e^{-ch_s} \tag{6}$$

and $N_s$ = the surface refractivity at the tracking station
$h_s$ = the height above the elevation of the station (km) and
$c$ = the appropriate exponential decay constant ($km^{-1}$).

From Figure 1 it is apparent that the height, h, of any point, P, on the slant path, $R_o$, can be expressed in terms of the earth radius, $r_o$, the station elevation, $H_s$, the true elevation angle, $\beta_o$, and the geometrical distance, S, of the point, P, from the station. In this way the variation of N (Equation (6)), can be expressed in terms of the distance, S, along $R_o$ which is now taken to be the variable.

From ray theory it can be shown that the range error due to retardation $\Delta R$ is given by

$$\Delta R \simeq 10^{-6} \int_o^{R_g} N \, ds \tag{7}$$

where, from previous discussion (reference Section J) the geometrical error, $R_g - R_o$, is neglected.[7] Since $R_g$ and $R_o$ are very nearly equal, it is convenient to rewrite Equation (7) where

$$\Delta R \simeq 10^{-6} \int_{o}^{R_o} N . ds \tag{8}$$

and integration takes place along the slant path, $R_o$, rather than along the ray path, $R_g$. Since N can be expressed as a function of distance along $R_o$, the integral (Equation (8)) can be solved exactly.

Freeman's development of this method[14] and solution showed that the range error due to retardation could be expressed in terms of error functions. Recognition should be given to Thayer's earlier investigations which simulated these further analyses.[15]

Freeman's solutions are given by the following equations where

$$\Delta R = \frac{10^{-6} N_s \sqrt{\pi}\ g .\ \exp(g^2)}{c \sin \beta_o} \left[\operatorname{erf}\left(R_o \cos \beta_o \sqrt{\frac{c}{2r_o}} + g\right) - \operatorname{erf}(g)\right] \tag{9}$$

$$\text{where} \quad \operatorname{erf} g = \frac{2}{\sqrt{\pi}} \int_{o}^{g} \exp(-x^2)\, dx \tag{10}$$

$$g = \tan \beta_o \sqrt{\frac{c r_o}{2}} \tag{11}$$

and it is assumed that $r_o >> H_s$.

For our present discussion, we are dealing with tracking stations located near sea level so the above equations apply.

In a separately reported analysis, Freeman showed that the overall path bending, $\tau$, (Figure 1) was given by [16]

$$\tau \simeq 10^{-6} \int_{\theta_o, N_s}^{\theta_r, N_r} \cot \theta \, dN \tag{12.1}$$

$$\simeq \frac{10^{-6} N_s \sqrt{\pi}\ g \exp(g^2)}{\tan \beta_o} \left[\operatorname{erf}\left(R_o \cos \beta_o \sqrt{\frac{c}{2r_o}} + g\right) - \operatorname{erf}(g)\right] \tag{12.2}$$

where $\theta_r$ and $N_r$ are defined at the target location.

These equations were found to be in error since the values of refractivity along $R_o$ are larger than they would be along the higher path, $R_e$. Therefore, an empirically determined adjustment was made to give agreement with published data and for targets above the troposphere.

To make these equations more useful for real-time tracking error corrections, Rowlandson[17] took advantage of the fact that the error function was asymptotically bounded.[18]

From the equation

$$\frac{1}{x + (x^2 + 2)^{\frac{1}{2}}} \leq \exp(x^2) \int_x^\infty \exp(-t^2).\, dt \leq \frac{1}{x + (x^2 + 4/\pi)^{\frac{1}{2}}} \tag{13}$$

for the condition that

$$x^2 >> 2 \tag{14}$$

then $$\exp(x^2) \int_x^\infty \exp(-t^2)\, dt \simeq 1/2x \tag{15}$$

Since $$\operatorname{erf}(x) = 1 - \frac{2}{\sqrt{\pi}} \int_x^\infty \exp(-t^2)\, dt \tag{16}$$

Equations (9) and (12) with the substitution of (15) and (16) become

$$\Delta R \simeq \frac{10^{-6} N_s}{c \sin \beta_o} \left[1 - \frac{g \exp[g^2]}{(k + g) \exp[(k + g)^2]}\right] \tag{17}$$

and $$\tau \simeq \frac{10^{-6} N_s}{\tan \beta_o} \left[1 - \frac{g \exp[g^2]}{(k + g) \exp[(k + g)^2]}\right] \tag{18}$$

where $$g = \sqrt{\frac{c r_o}{2}} \tan \beta_o \tag{19}$$

and $$k = R_o \sqrt{\frac{c}{2 r_o}} \cos \beta_o \tag{20}$$

Since corrections to tracking errors must use the measured radar data, these equations were further modified to replace $R_o$ by the measured radar range, $R_e$, hereafter called R, and the apparent elevation angle, $\theta_o$, instead of the true elevation angle, $\beta_o$.

Ray tracing data for the NBS-CRPL surface corrected exponential atmosphere[12] was used to determine a new angle, $\gamma$. This new angle replaces $\beta_o$ and was empirically developed to provide meaningful error data for a wide range of tracking conditions, where

$$\sin \gamma = \sin \theta_o + [K_o + K_2 \exp(-K_3 R^2)] \exp(-K_1 \theta_o^2) \tag{21}$$

Except for the propagation constants, $N_s$ and c, the range and path bending equations are now a function of the measured radar range, R, and the apparent elevation angle, $\theta_o$, where

$$\Delta R \simeq \frac{10^{-6} N_s}{c \sin \gamma} \left[1 - \frac{g \exp [g^2]}{(k+g) \exp [(k+g)^2]}\right] \tag{22}$$

$$\tau \simeq \frac{10^{-6} N_s}{\tan \gamma} \left[1 - \frac{g \exp [g^2]}{(k+g) \exp [(k+g)^2]}\right] \tag{23}$$

where $g = \sqrt{\frac{cr_o}{2}} \tan \gamma$ (24)

$$k = R \sqrt{\frac{c}{2r_o}} \cos \gamma \tag{25}$$

and $\gamma$ is given by Equation (21).

For station values of $N_s$ in the range from 340 to 375 N units, corresponding to AFWTR conditions, comparisons with CRPL ray tracing data generated constants $K_o$ through $K_3$, where

$$K_o = 0.0175 \tag{26.1}$$
$$K_1 = 245.0 \tag{26.2}$$
$$K_2 = 0.045 \tag{26.3}$$
$$K_3 = 0.370 \times 10^{-4} \tag{26.4}$$

From Equation (14) it can be shown that a theoretical restriction is placed on the minimum value which g can have, namely,

$$g = \sqrt{\frac{cr_o}{2}} \tan \gamma >> \sqrt{2} \tag{27}$$

For elevation angles of four degrees and less, Equation (27) is far from satisfied, in which case the accuracy of the calculations would be in error. However, careful selection of the above constants $K_o$ through $K_3$ has permitted the equations for range error and path bending to be extended into the small angle region.

Under long range tracking conditions, k, (Equation (25)) becomes much larger than g. This situation causes a very great simplification to Equations (21), (22), and (23) which then become

$$\sin \gamma \simeq \sin \theta_o + K_o \exp (-K_1 \theta_o^2) \tag{28}$$

$$\Delta R \approx \frac{10^{-6} N_s}{c \sin \gamma} \tag{29}$$

$$\tau \approx \frac{10^{-6} N_s}{\tan \gamma} \tag{30}$$

It was shown by Rowlandson[17] that the elevation angle error, $\epsilon$, can be calculated from the equation

$$\epsilon = \theta_o - \sin^{-1} \left[\frac{1}{R} \int_o^R \sin (\theta_o - |\tau|) \, dR\right] \tag{31}$$

In the long range case, $|\tau|$, is independent of range and Equation (31) becomes

$$\epsilon = \theta_o - \sin^{-1} [\sin (\theta_o - \tau)] \tag{32}$$

or $$\epsilon \propto \tau \tag{33}$$

Ray tracing results show that $\epsilon$ approaches $\tau$ only for ranges in excess of 3000 km.

2. A Comparison of Errors Calculated From Ray Tracing Analysis and Rowlandson's Equations

For the hypothetical missile trajectory postulated by Gardner[4], Figure 20 shows the magnitude of the true elevation angle, $\beta_o$, as a function of flight time. (See Gardner's report[4] for additional tracking parameters.) The radio refractivity profile is defined by a West Coast rawinsonde profile shown in Figure 21. It may be observed that there is a strong inversion present and, therefore, the profile represents very non-standard propagation conditions. Superimposed on the profile is the NBS-CRPL surface-corrected exponential model profile. Gardner uses a tracking station at 1,000 feet above mean sea level and located on San Nicolas Island. Therefore, to calculate with Rowlandson's equations, the station value for $N_s$ from the exponential is 340 units. The surface value for N is found by extrapolation to be approximately 360 units from which the decay constant, c, is equal to 0.1548 $km^{-1}$.[12]

During the flight time from 200 to 475 seconds the range and tracking angles to the vehicle are sufficiently large to permit Equations (28), (29), and (30) to be used to calculate the range error, $\Delta R$, and the total path bending, $\tau$. It should be mentioned at this point that all calculations and parameter definitions use the metric system. However, for the application to AFWTR

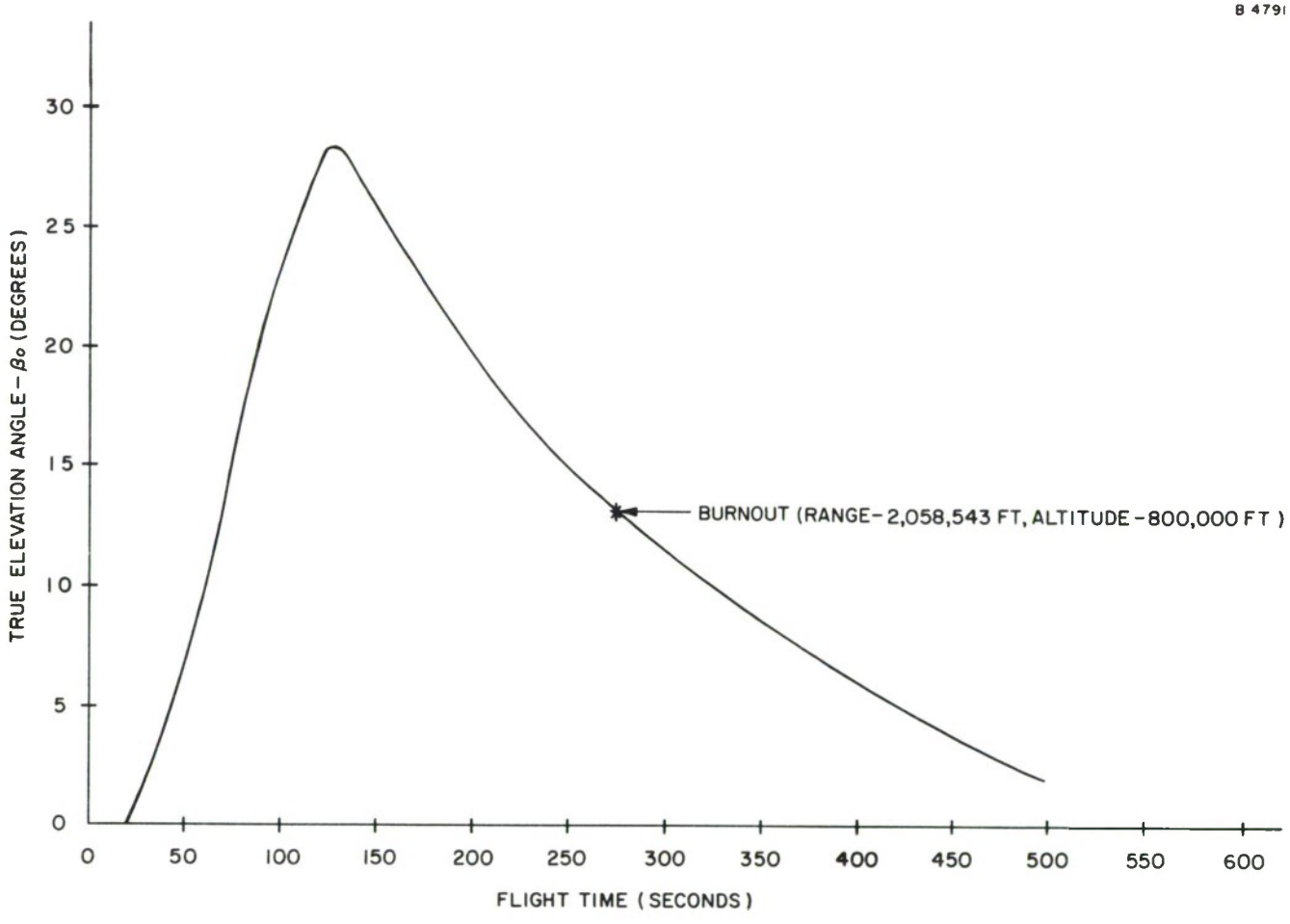


FIGURE 20. HYPOTHETICAL MISSILE LAUNCH TRACKED FROM SAN NICOLAS

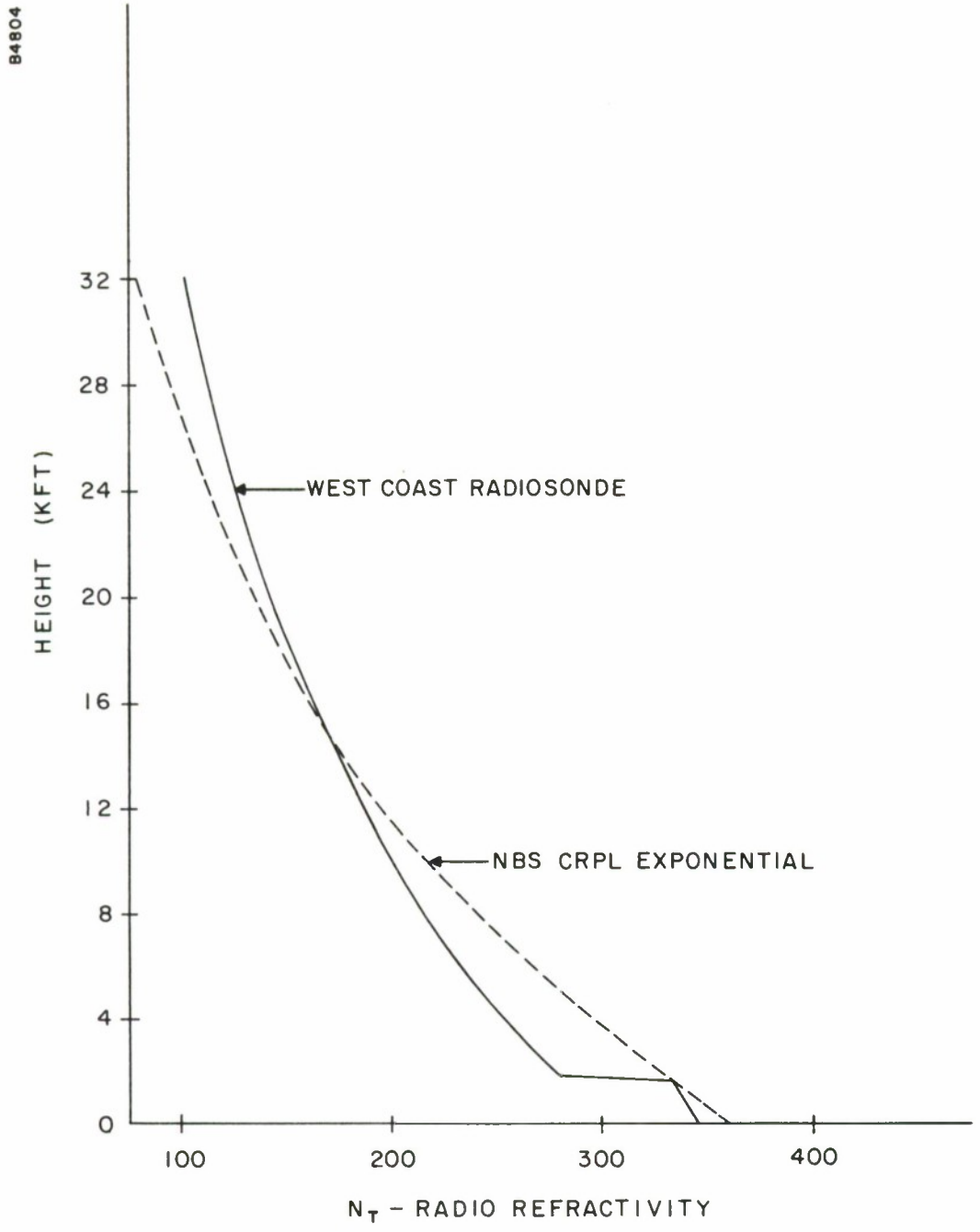


FIGURE 21. WEST COAST RADIOSONDE VERSUS NBS-CRPL EXPONENTIAL

tracking analysis we have generally presented the final results in the English system of units.

Figure 22 shows a comparison of range error calculations with Gardner's ray tracing results. The agreement is seen to be very good down to elevation angles of four degrees. At 2.5 degrees the error difference corresponds to 20 feet at a measured range of $5.75 \times 10^6$ feet. Figure 23 shows a comparison of elevation angle errors, $\epsilon$. The agreement is within 0.10 milliradians down to four degrees elevation angle. For a burnout at 275 seconds, the difference between curves represents a 250 foot height error at a missile altitude of 800,000 feet.

A second comparison is presented where an East Coast rawinsonde was used to represent the refractivity profile. Figure 24 shows the rawinsonde profile with the NBS-CRPL model profile superimposed. In this case the tracking site was selected at 44 feet above mean sea level which corresponds to Gardner's analysis using the Point Mugu tracking radar. This analysis could equally well be applied to the Eastern Test Range tracking system (MISTRAM) which is located near sea level.

Figure 25 shows a comparison of the range errors and agreement is very good down to elevation angles of four degrees. Figure 26 shows a comparison of the elevation angle errors with good agreement maintained to elevation angles just under four degrees.

During the first 100 seconds of flight the range to the target is too small to permit the use of the simplified Equations (28), (29), and (30). A set of calculations over this time period required using the original Equations (21), (22), (23), and (31). Figures 27 and 28 show a comparison of calculations with Gardner's ray tracing results. The West Coast rawinsonde was used to define the propagation conditions for the ray tracing analysis and the tracking radar at San Nicolas Island (1000 feet elevation) was selected for the comparative analysis. The elevation angle error differences at short ranges and low tracking elevation angles is not as good as in the long range cases. However, when the range is small one can tolerate a larger elevation angle error since the height position error is the product of the elevation angle error and range.

As the tracking elevation angle decreases the ray path makes a smaller angle, $\theta$, with respect to the inversion layer. Referring to the bending Equation (12.1) the magnitude of $\cot \theta$ and $dN$ become large as the ray path begins to graze the inversion layer. The increase in ray path bending therefore becomes very large as the ray passes through the inversion at these

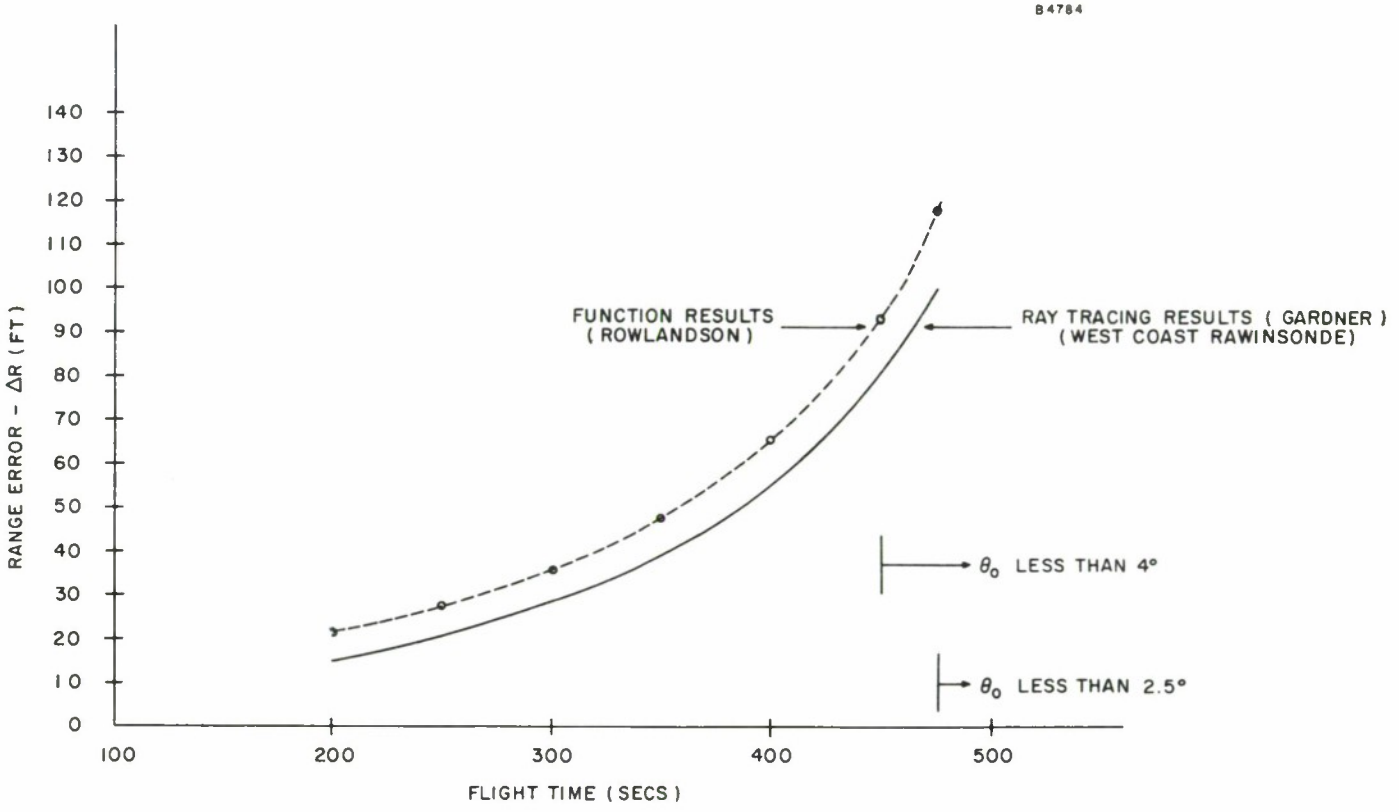


FIGURE 22. A COMPARISON OF RANGE ERRORS FOR RADIOSONDE AND EXPONENTIAL PROFILES

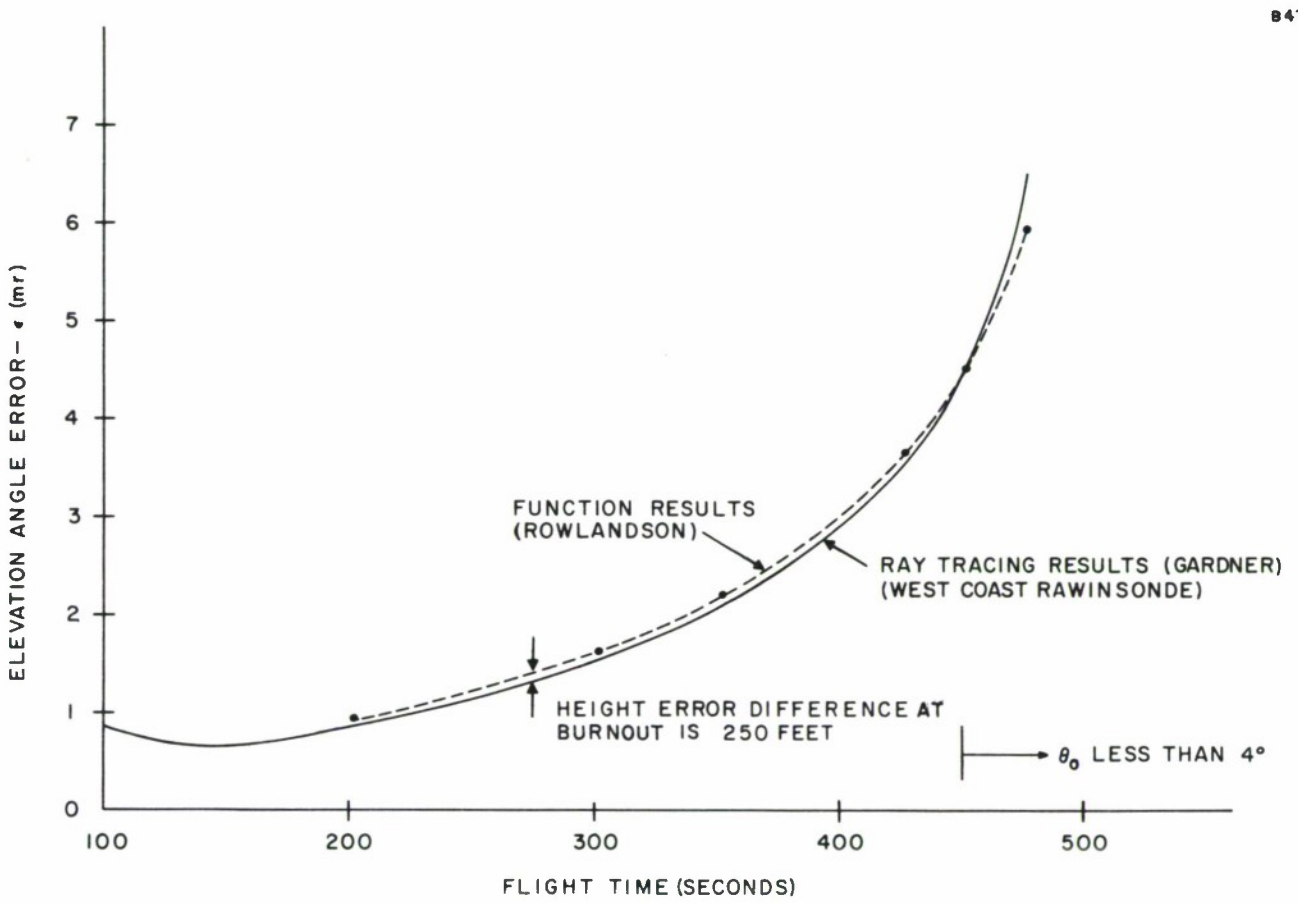


FIGURE 23. A COMPARISON OF ELEVATION ANGLE ERRORS FOR RADIOSONDE AND EXPONENTIAL PROFILES

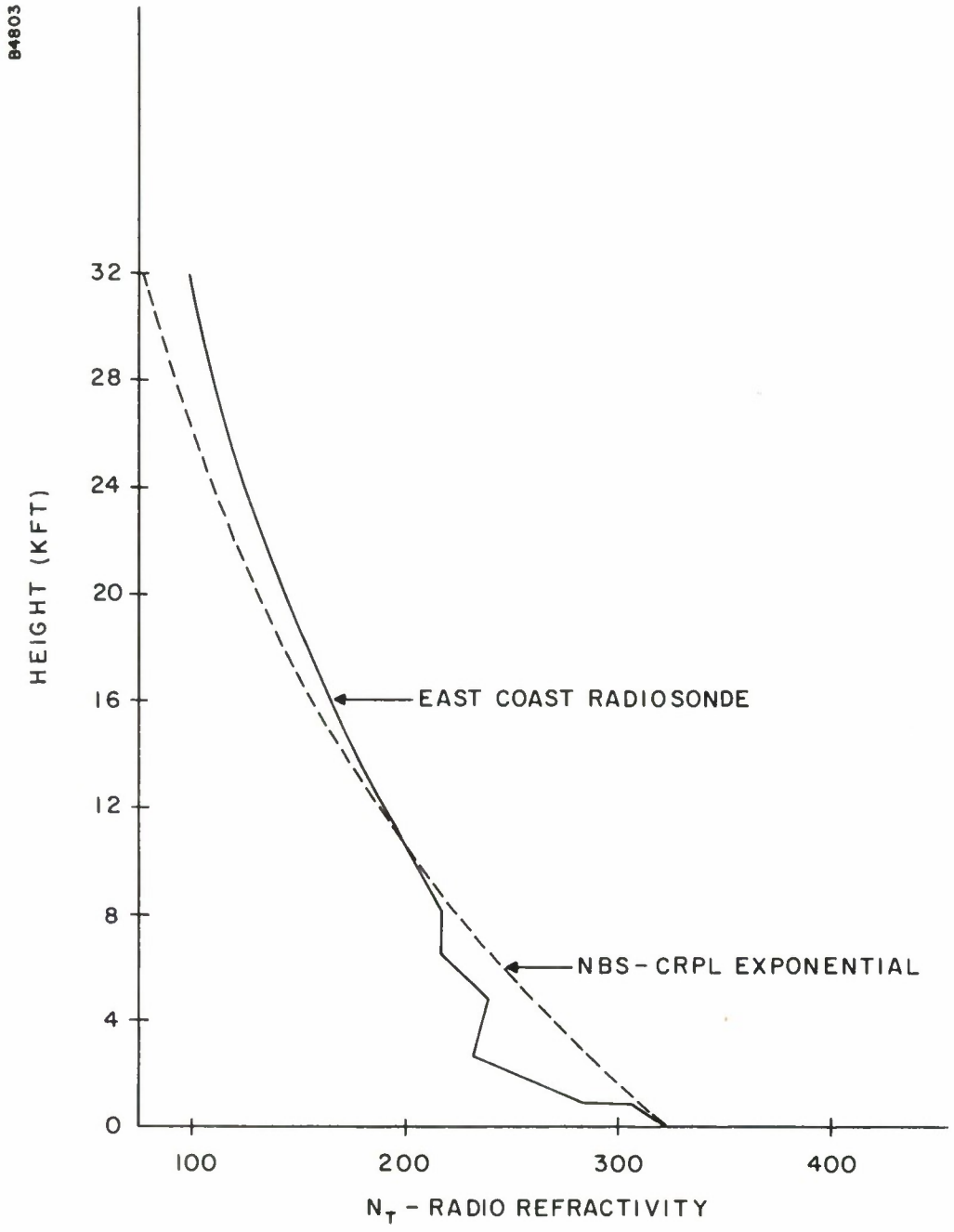


FIGURE 24. EAST COAST RADIOSONDE VERSUS NBS-CRPL EXPONENTIAL

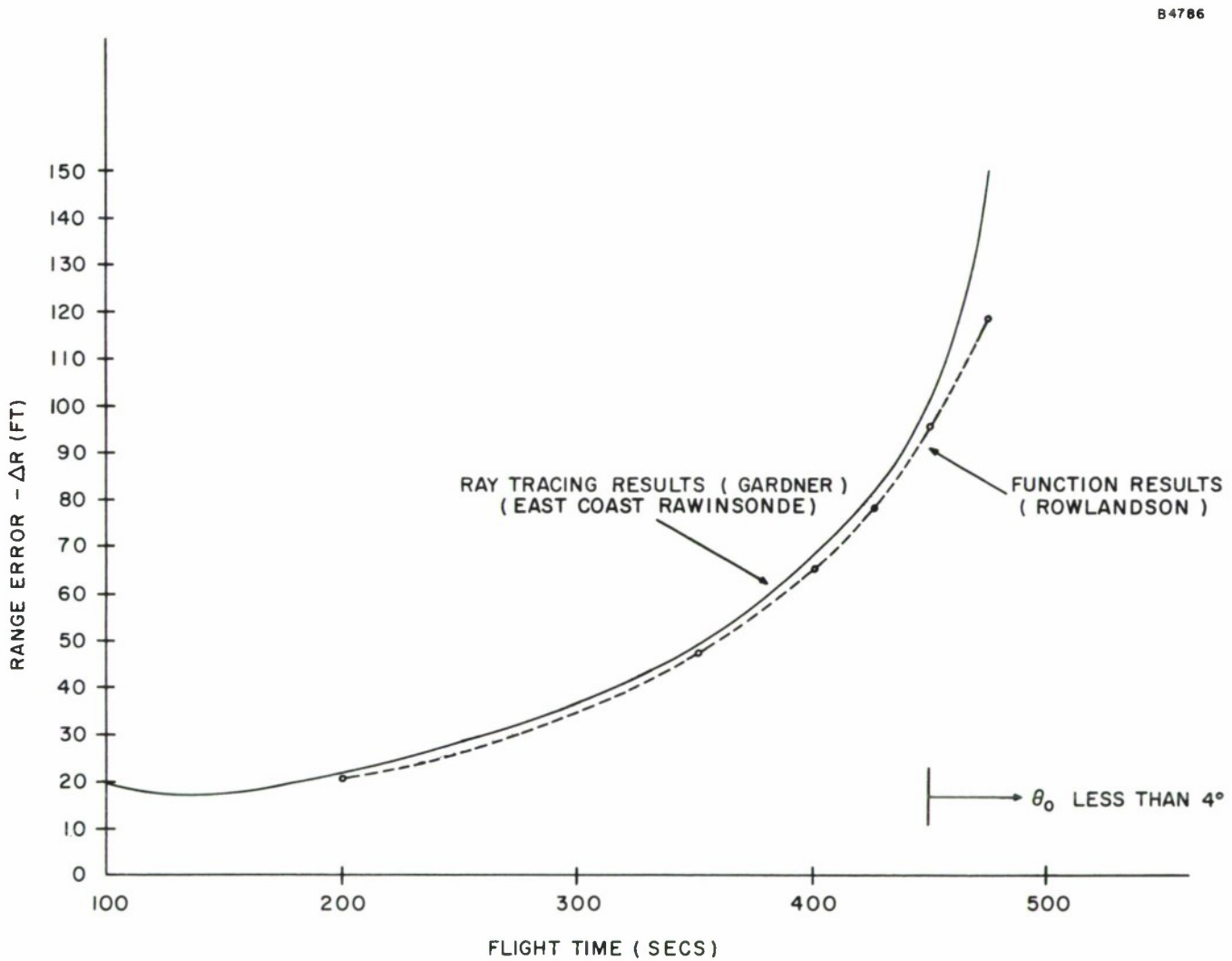


FIGURE 25. A COMPARISON OF RANGE ERRORS FOR RADIOSONDE AND EXPONENTIAL PROFILES

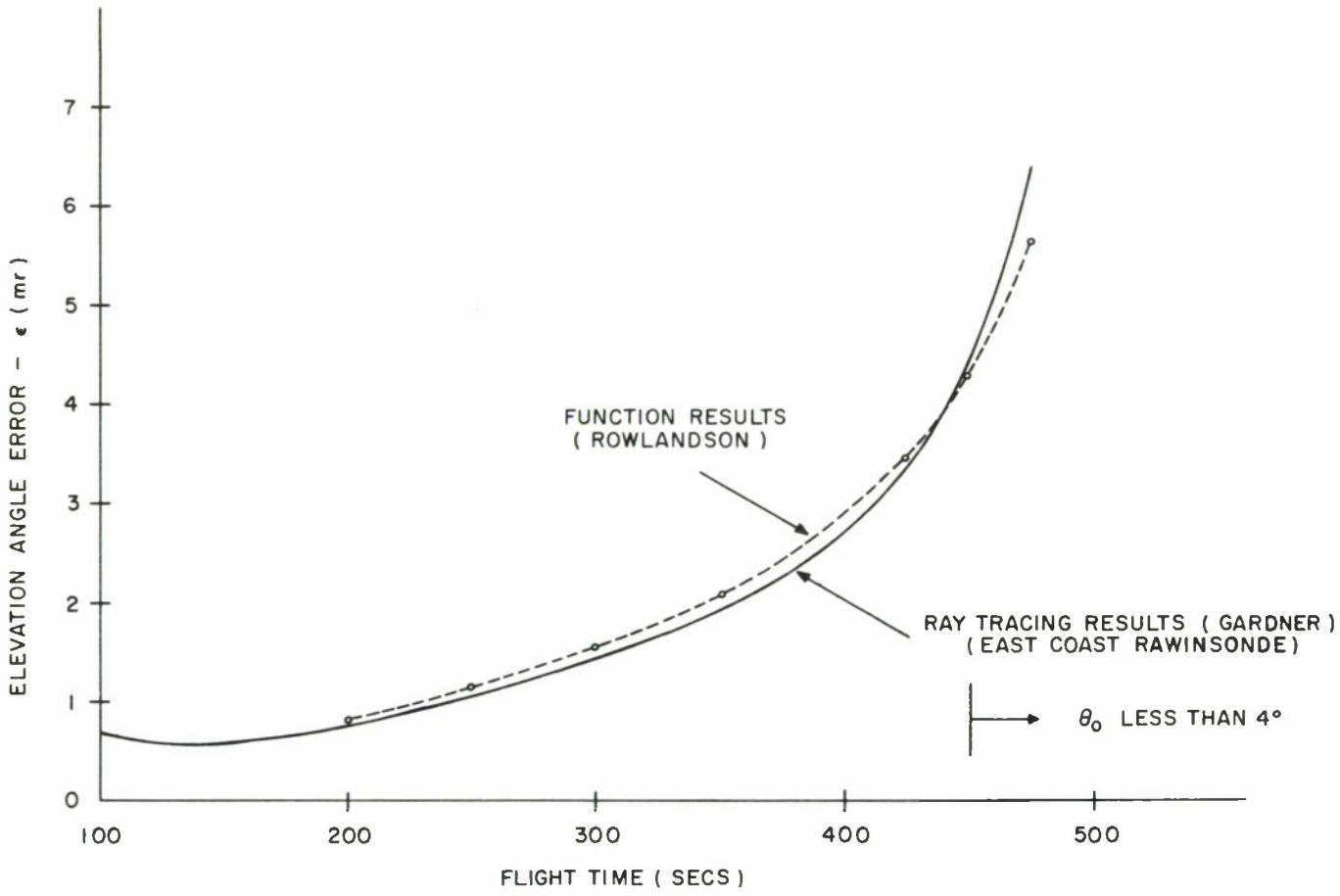


FIGURE 26. A COMPARISON OF ELEVATION ANGLE ERRORS FOR RADIOSONDE AND EXPONENTIAL PROFILES

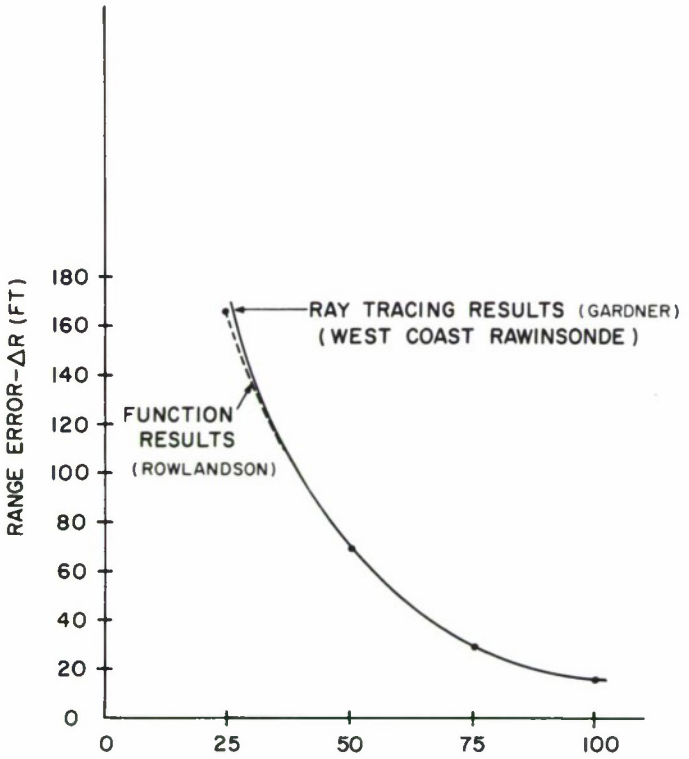


FIGURE 27.

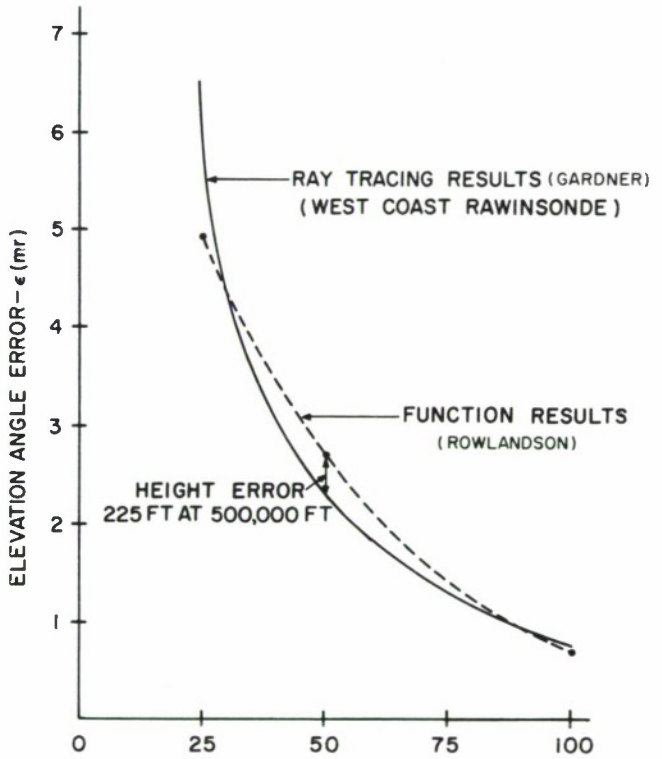


FIGURE 28.

A COMPARISON OF RANGE AND ANGLE ERRORS DURING INITIAL FLIGHT

shallow angles. The elevation angle error, $\epsilon$, correspondingly increases as shown by Equation (33). Therefore, in the presence of large inversions such as exhibited by the rawinsonde profiles the elevation angle error, $\epsilon$, will increase very rapidly as the tracking elevation angle becomes small. The exponential model for refractivity cannot represent refractivity gradients of a magnitude which commonly occur in an inversion and at the same time represent the rest of the more-standard propagation conditions.

Gardner's summary and conclusions were: "...A comparison between actual extreme refractive conditions for the Eastern Test Range (ETR) and the Pacific Missile Range (PMR) in relation to ETR and NBS exponential atmosphere was made for a hypothetical satellite launch as seen by two widely separated radars. It has been shown that for tracking elevation angles greater than five degrees, either type of exponential atmosphere, originating from a measured surface index, can be used for position determination within 100 feet. Consequently, the only variable atmosphere input required for this accuracy is the current surface refractive index. Below five degree elevation angle, refraction corrections should only be made with the use of detailed rawinsonde plus refractometer refractive index profiles using standard ray tracing techniques."

Based on the comparisons of Rowlandson's calculations with Gardner's ray tracing results, we concur that the exponential models can be used to calculate meaningful propagation errors for tracking elevation angles down to about four degrees. The position accuracy in range is generally much better than the elevation angle accuracy since the latter is so greatly affected by variations in the vertical refractivity profile.

The comparison also demonstrates that above five degrees tracking elevation angle the propagation errors can be calculated without using standard ray tracing techniques.

With reference to the earlier discussion on temporal effects it is suggested that if more detailed refractivity profiles are required (for low angle tracking) that rawinsonde data be used. The rawinsonde measurement would be made in front of the tracking radar and at some convenient distance within 20 nautical miles.

Refractometer measurements of the refractivity are not recommended for two reasons. In the first instance, the microwave refractometer requires a great deal of maintenance and calibration and without special ducting facilities on the aircraft it cannot be used to measure refractivity in the presence of visible moisture. Second, the time required to make the airborne

measurements, then to reduce and correct the data, would not permit the application of this information in the tracking system in near-real-time.

### 3. Comments on the Optimization of Rowlandson's Equations

A least squares optimization program was used to determine the constants $K_0$ through $K_3$ to give the best possible agreement with published CRPL model ray trace data.[12] Constants were determined corresponding to each exponential model listed in the CRPL Monograph.

Figures 29, 30, and 31 show the comparison for range error, $\Delta R$, total path bending, $\tau$, and elevation angle error, $\epsilon$, respectively. These figures pertain to a surface refractivity condition of 313 N units. The agreement was found to be equally good for the other model conditions.

It was also determined during this analyses that the sin $\gamma$ function could be simplified without losing comparative accuracy. The final form for sin $\gamma$ which will be used hereafter is

$$\sin \gamma = \sin \theta_0 + [K_0 + K_2 \exp(-K_3 R)] \exp(-K_1 \theta_0) \qquad (34)$$

Figure 32 shows the values for the optimized constants versus surface refractivity, $N_0$.

The graphical results presented above were derived with this new expression for sin $\gamma$, replacing the earlier expression shown by Equation (21). In all cases the differences between computed elevation angle and ray tracing calculations remain below 0.04 milliradians.

The excellent agreement between the sets of data clearly demonstrate that refraction-induced radar propagation errors can be accurately calculated without ray tracing analysis. It is understood, of course, that the equations and constants developed in this latter instance are designed to work with the CRPL surface-corrected exponential model atmosphere.

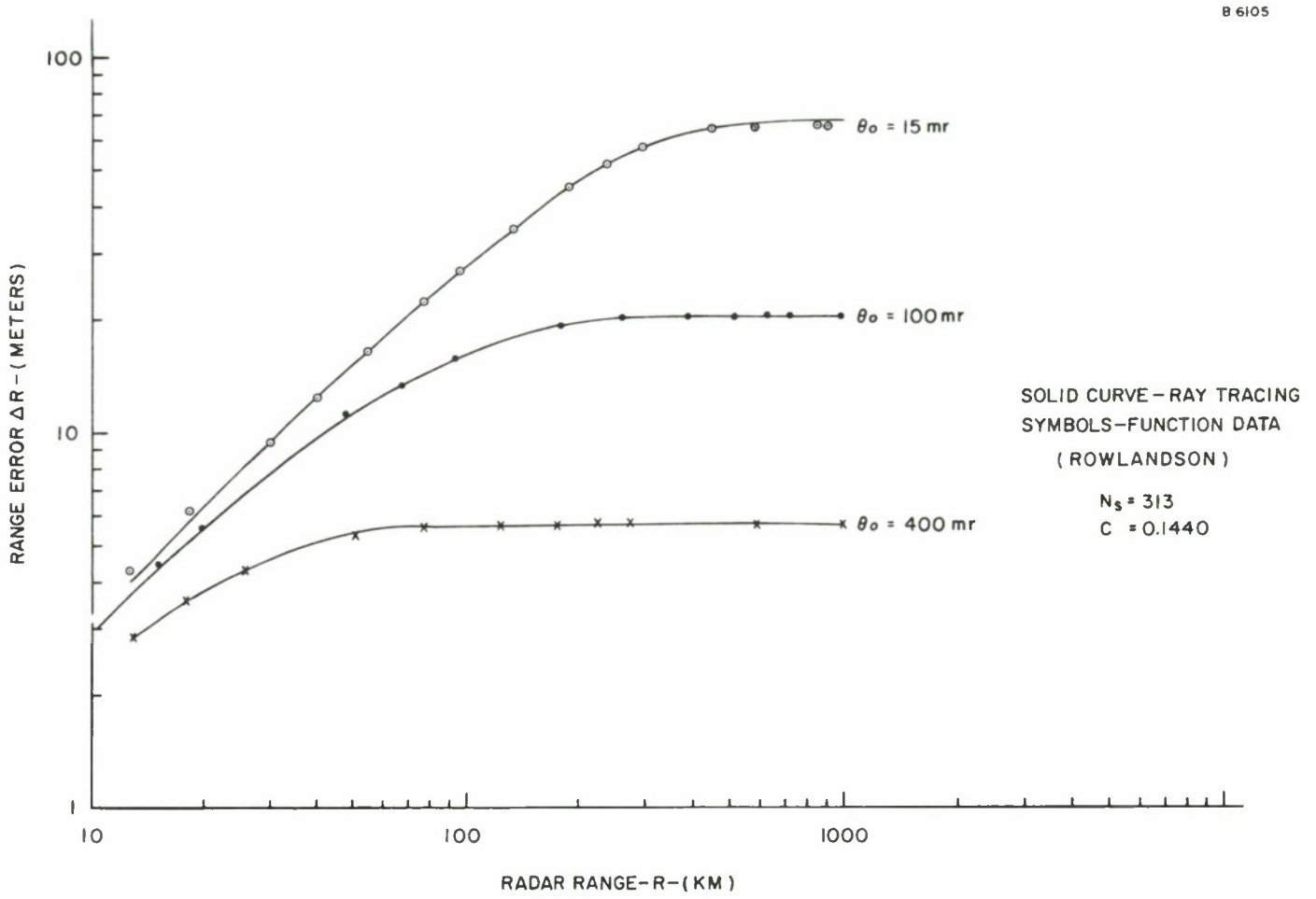


FIGURE 29. A COMPARISON OF RANGE ERRORS VERSUS RANGE FOR RAY-TRACED AND ROWLANDSON'S EQUATION

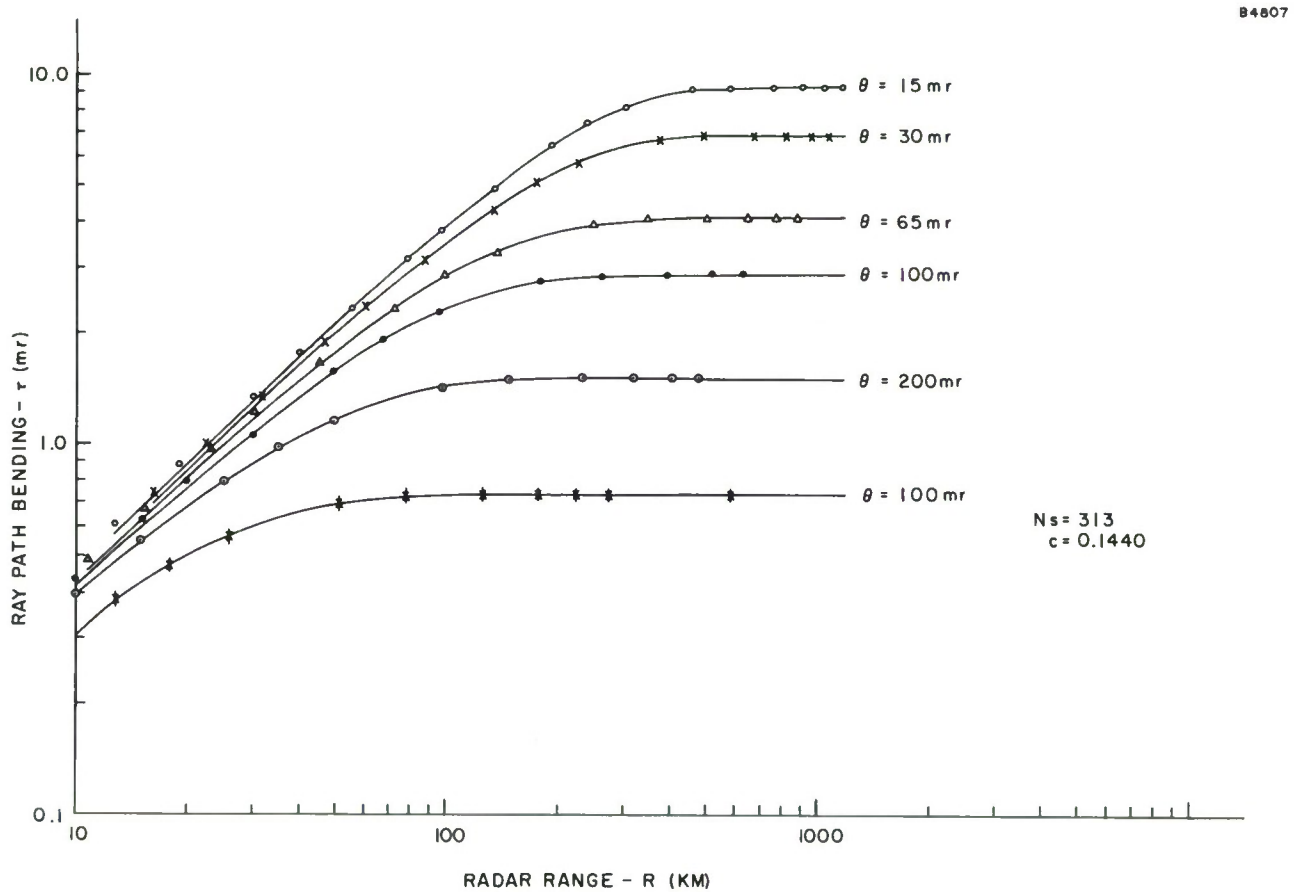


FIGURE 30. A COMPARISON OF RAY BENDING VALUES VERSUS RANGE FOR RAY-TRACED AND ROWLANDSON'S EQUATION

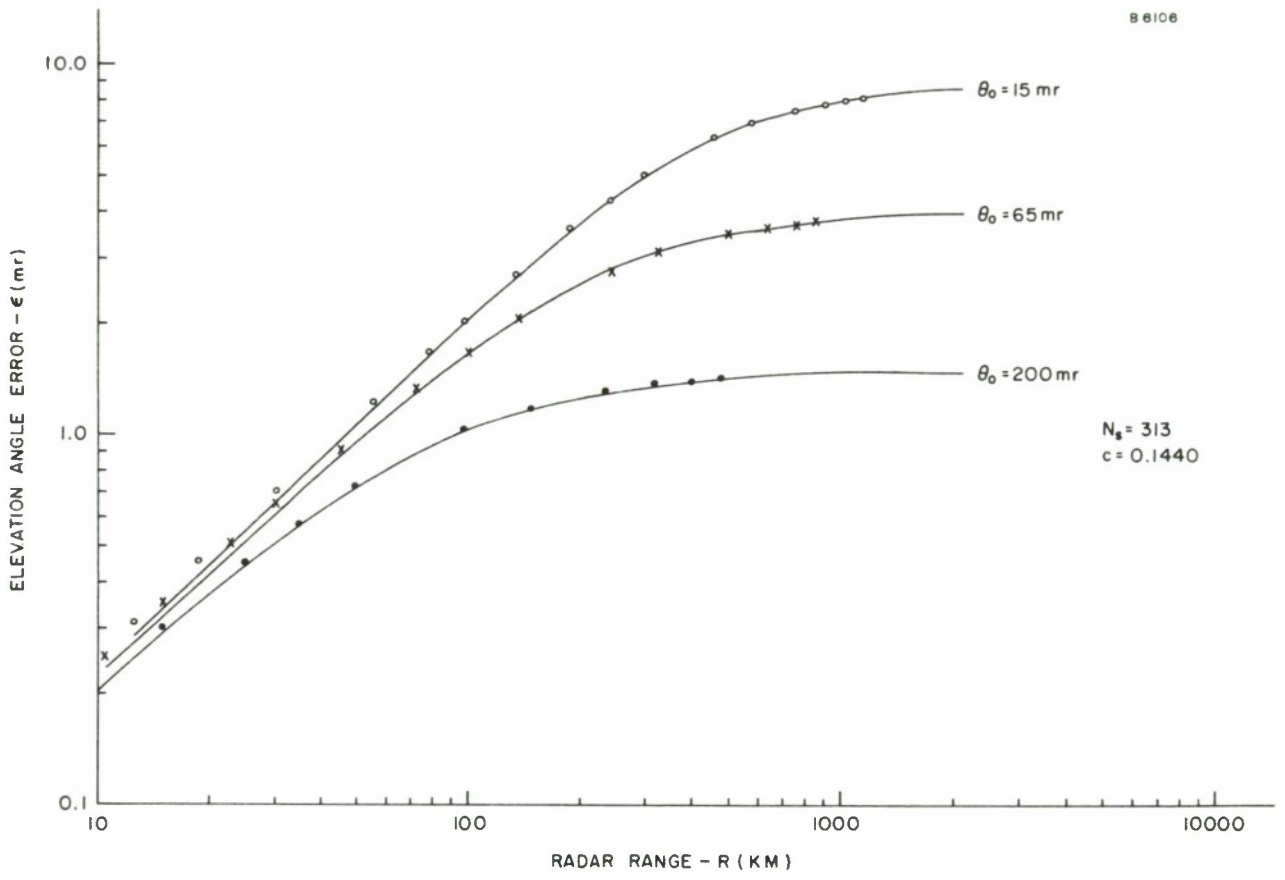


FIGURE 31. A COMPARISON OF ELEVATION ANGLE ERRORS VERSUS RANGE FOR RAY-TRACED AND ROWLANDSON'S EQUATIONS

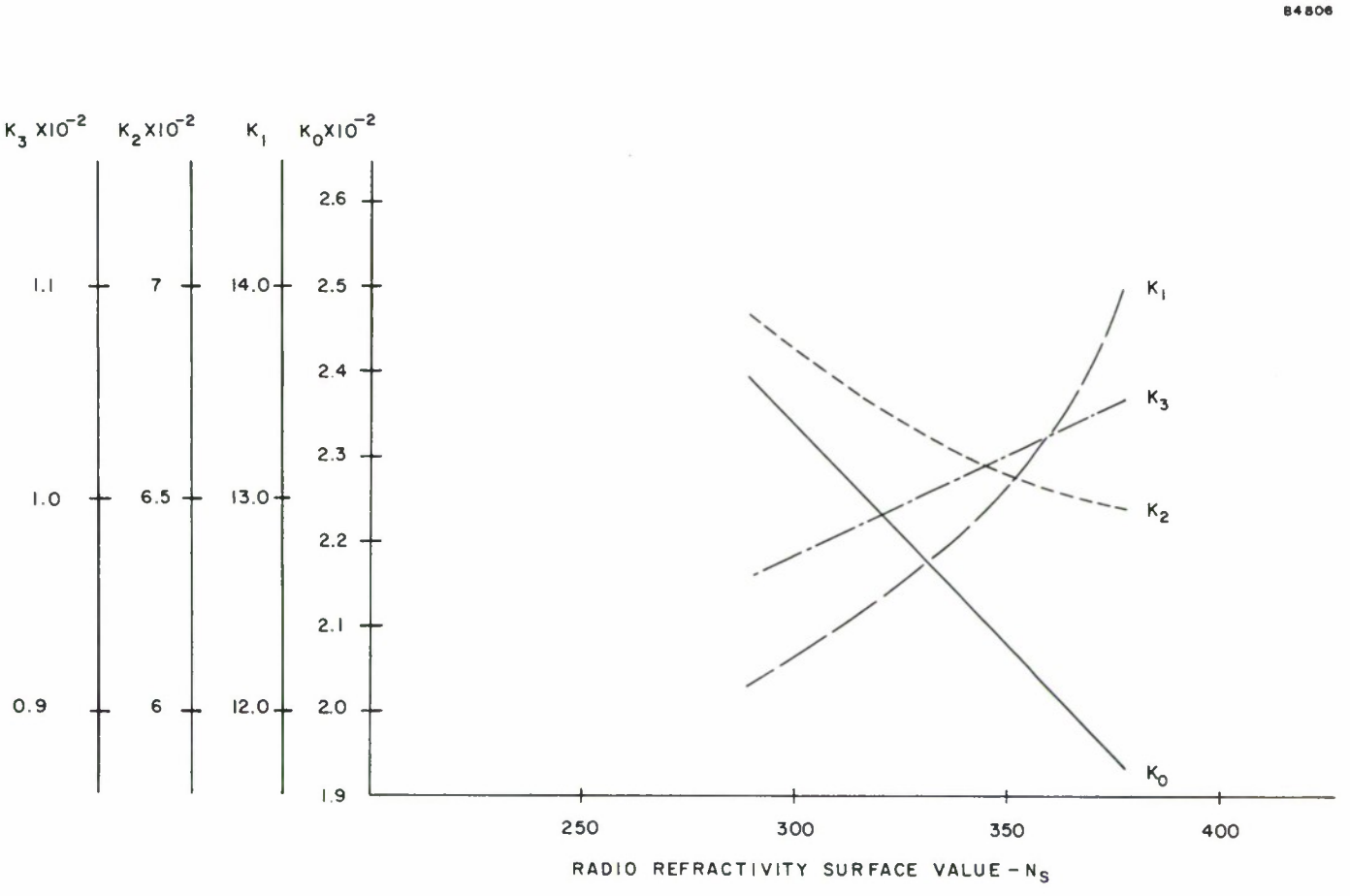


FIGURE 32. VARIATION OF EMPIRICAL CONSTANTS WITH SURFACE REFRACTIVITY

## SECTION V

# AN ANALYSIS OF REFRACTION-INDUCED ERRORS USING AIRBORNE REFRACTOMETER MEASUREMENTS AND A COMPARISON WITH THE CRPL MODEL

During the period from 19 January through 29 May 1967, a total of 16 airborne missions were flown in the AFWTR sector. From these flights the measurements made in close proximity to the Tranquillan Peak radar site were analyzed to determine the magnitudes of tracking errors produced by refraction. With reference to the effect of spatial and temporal variations, the selected profiles nearest to the radar were considered to give the most meaningful description of propagation conditions affecting this radar.

Figures 33 through 36 show examples of the presentations used to describe the magnitudes of elevation angle and range errors for each measurement. Since the total compendium of such data is of little general interest the complete set of such data is not included in this report.

In lieu of a direct graphical presentation, the errors were compiled statistically to show the average behavior of the elevation angle and range errors together with the standard deviation about the average.

Figure 37 shows the average elevation angle error behavior with height for two groups of test periods. The first group covered the period from 20 January to 8 February and the second group from 28 March to 29 May 1967. The presentation shows the angle error data for apparent elevation angles of 100 and 200 milliradians.

Figure 38 shows the average range error variation with height for the two seasons and for apparent elevation angles of 100 and 200 milliradians.

The vertical bars on the curves define the standard deviation of the data about the average values.

From reference 19, the average value of surface refractivity for Santa Maria, California, is listed as 319.8 and 322.7 N units for January and February, respectively. Since Santa Maria is close to the Vandenberg Base and near sea level (258 feet msl) it is useful to determine whether or not these near-surface readings can be used to generate a meaningful CRPL profile.

Using the average Santa Maria surface value for January-February of 321.25, the CRPL exponential decay constant, c, is[12] 0.1471 $km^{-1}$. For the Tranquillan Peak radar at 2500 feet above msl (0.761 km) the CRPL profile gives a corresponding station value of 287 N units.

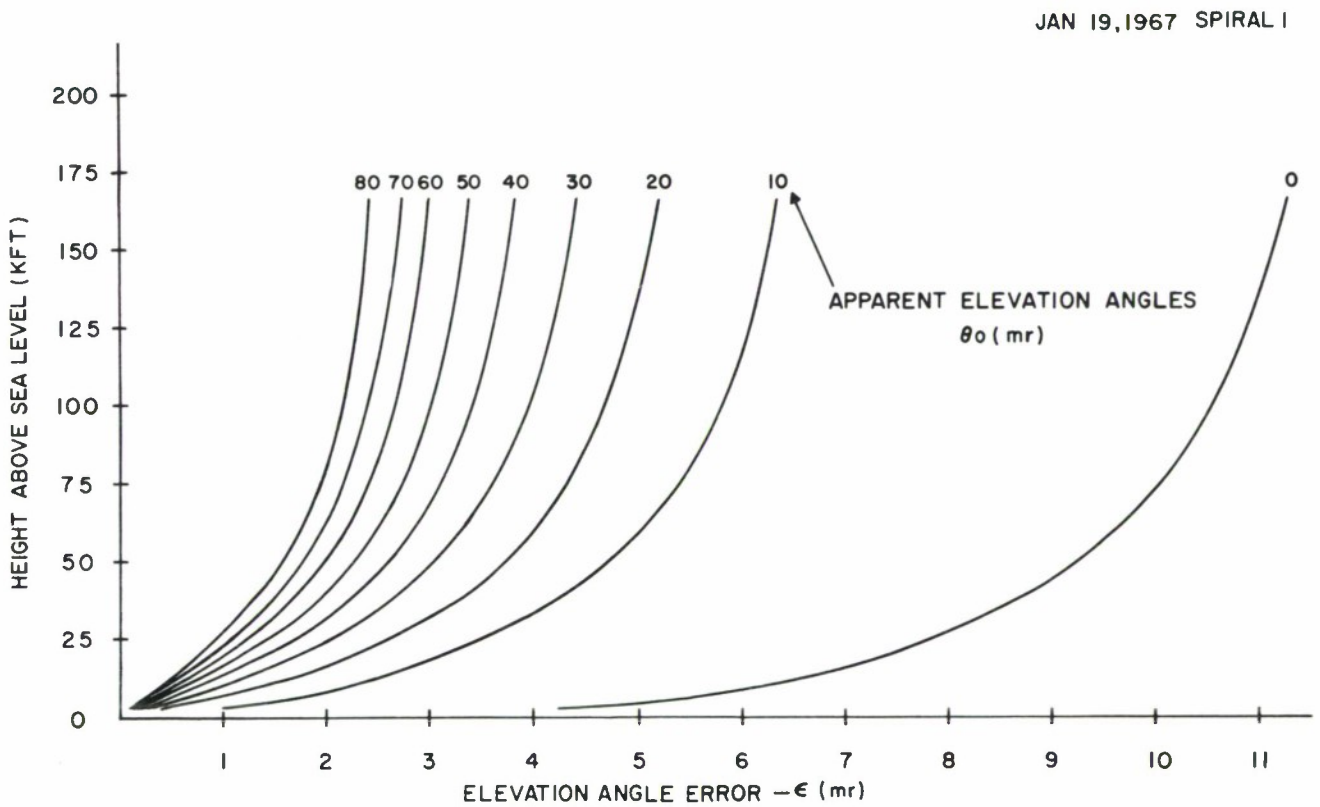


FIGURE 33. THE VARIATION OF ELEVATION ANGLE ERROR WITH HEIGHT FOR VARIOUS APPARENT ELEVATION ANGLES

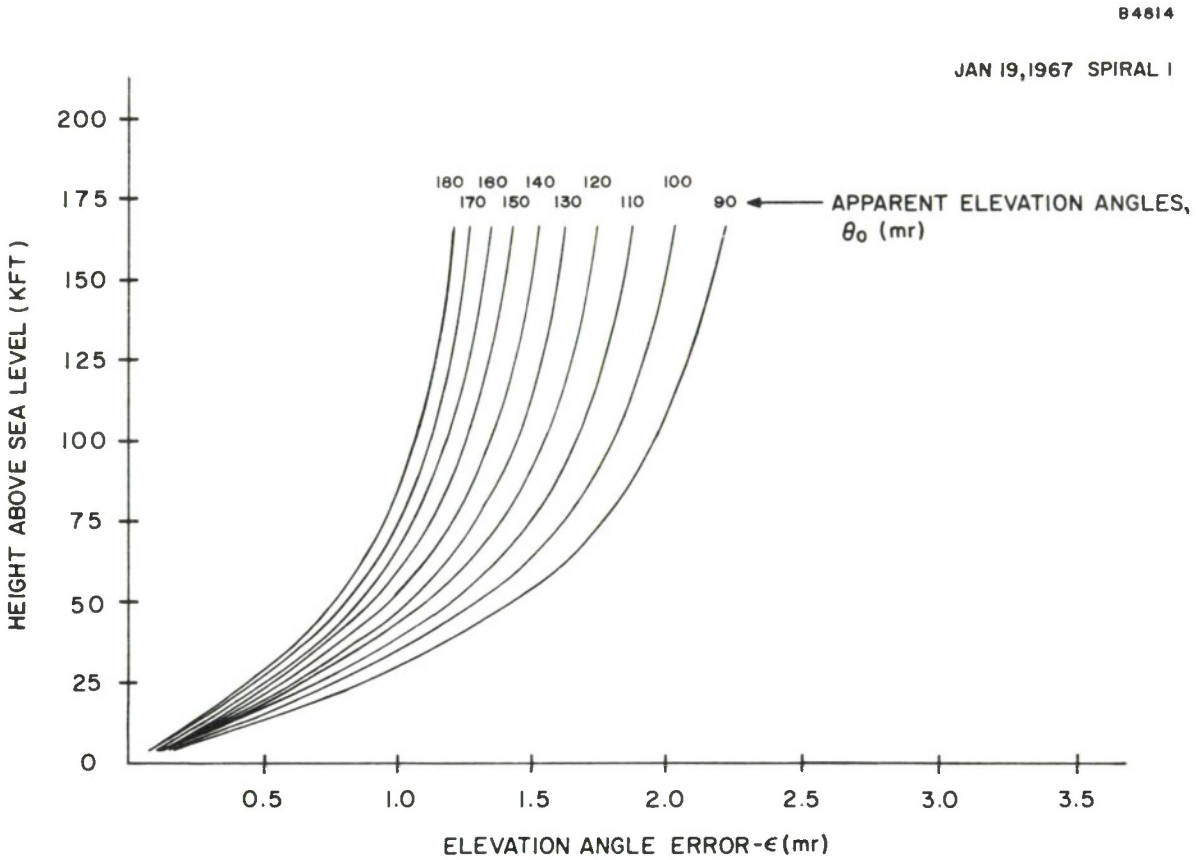


FIGURE 34. THE VARIATION OF ELEVATION ANGLE ERROR WITH HEIGHT FOR VARIOUS APPARENT ELEVATION ANGLES

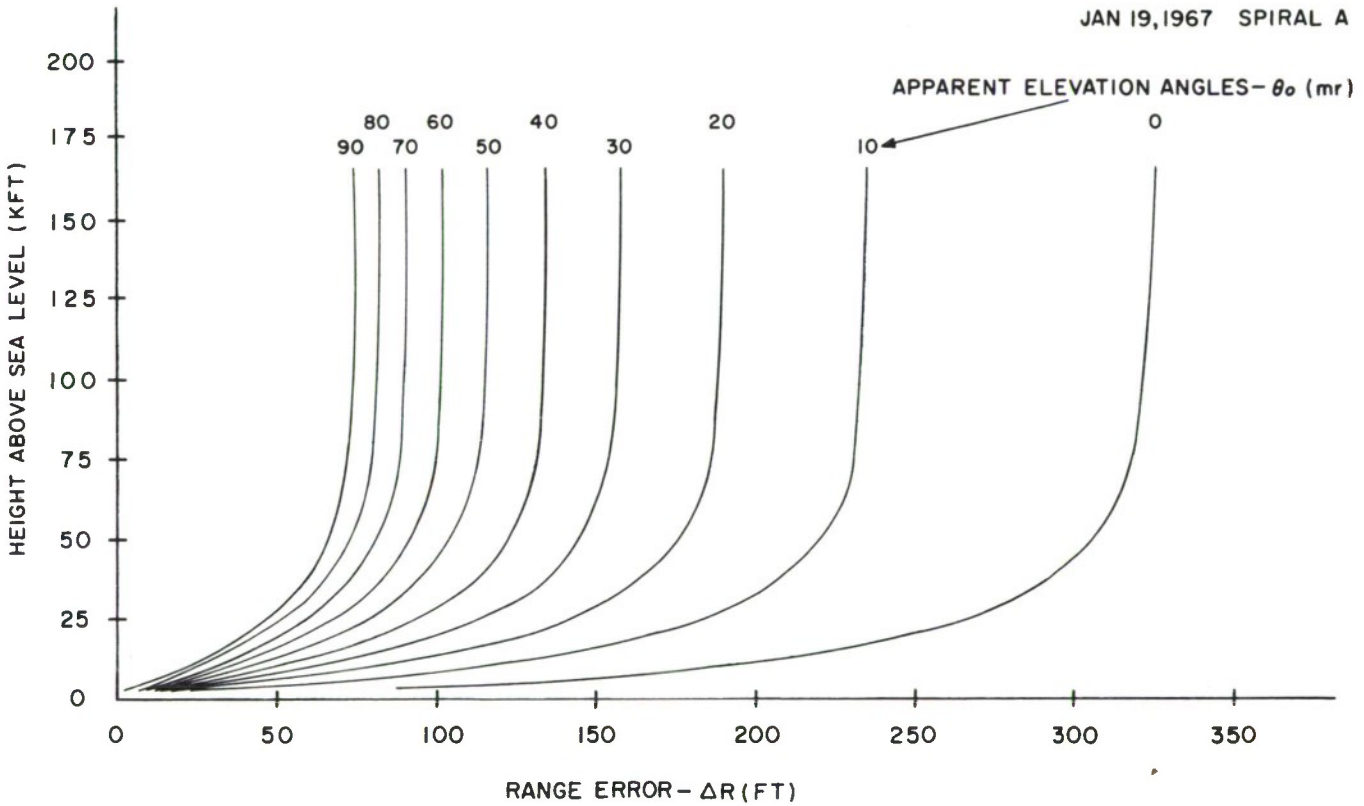


FIGURE 35. VARIATION OF RANGE ERROR WITH HEIGHT FOR VARIOUS APPARENT ELEVATION ANGLES

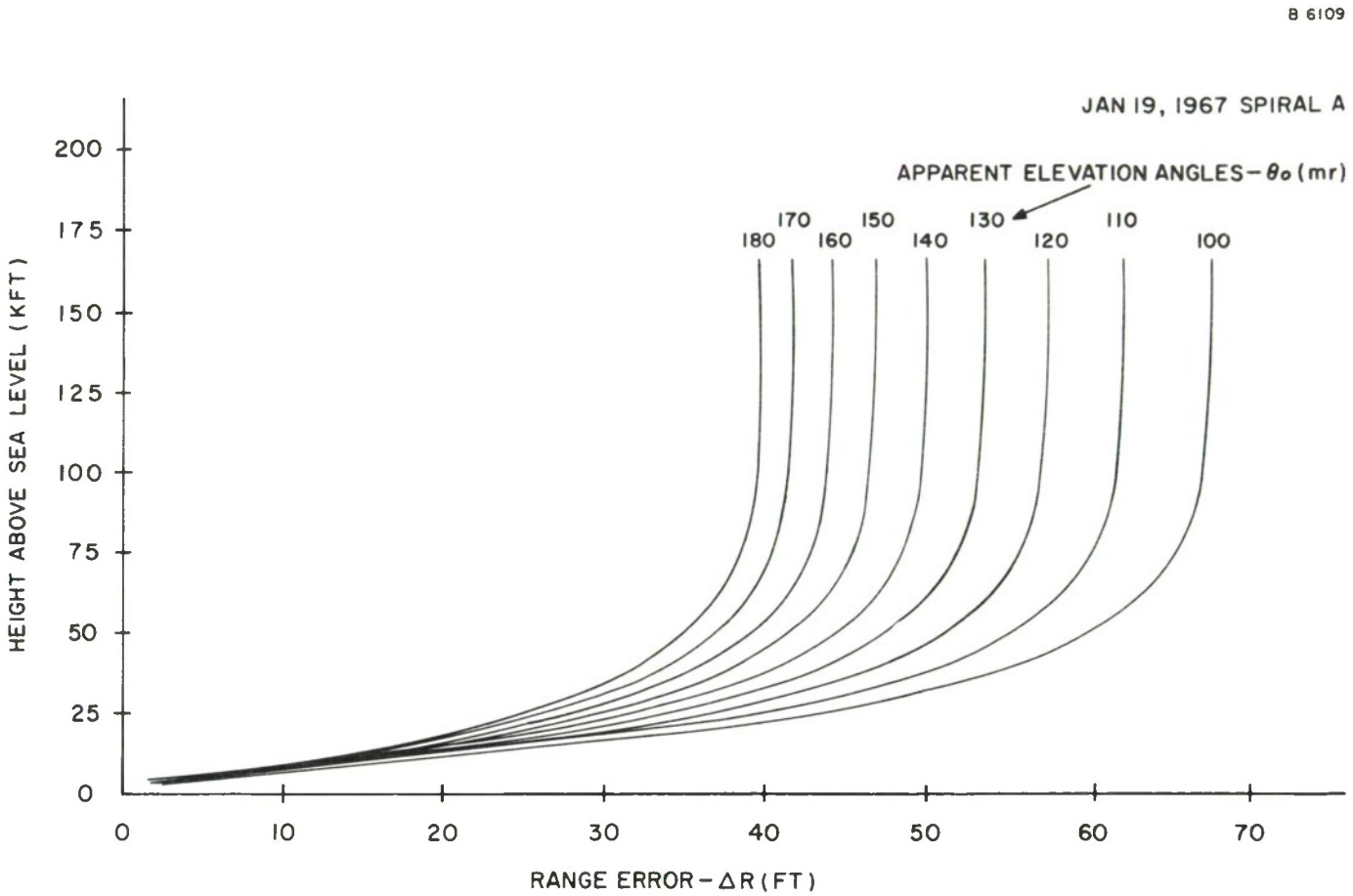


FIGURE 36. VARIATION OF RANGE ERROR WITH HEIGHT FOR VARIOUS APPARENT ELEVATION ANGLES

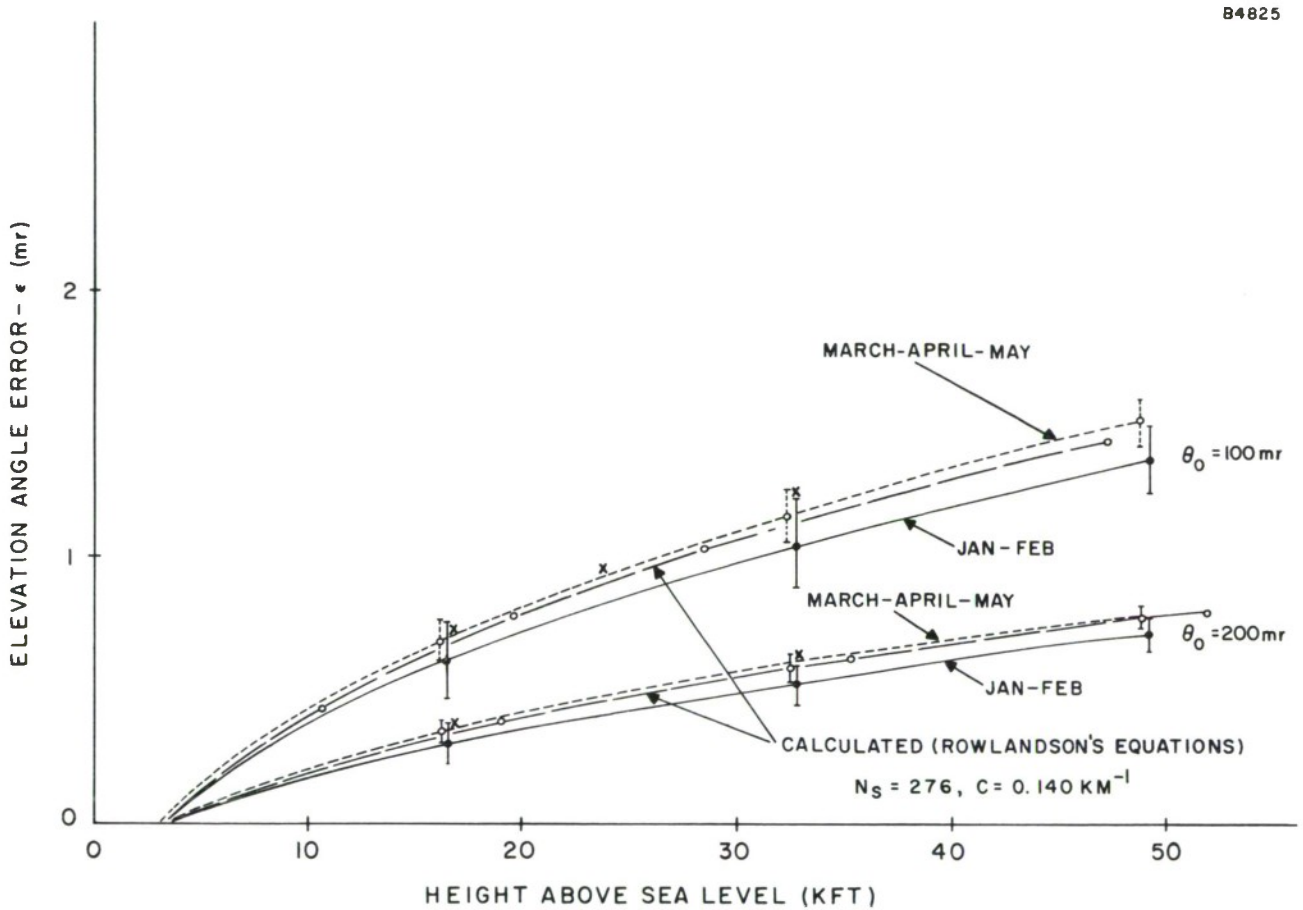


FIGURE 37. SEASONAL EFFECTS ON THE ELEVATION ANGLE ERROR VERSUS HEIGHT (TRANQUILLAN PEAK RADAR, HEIGHT 2400 FEET)

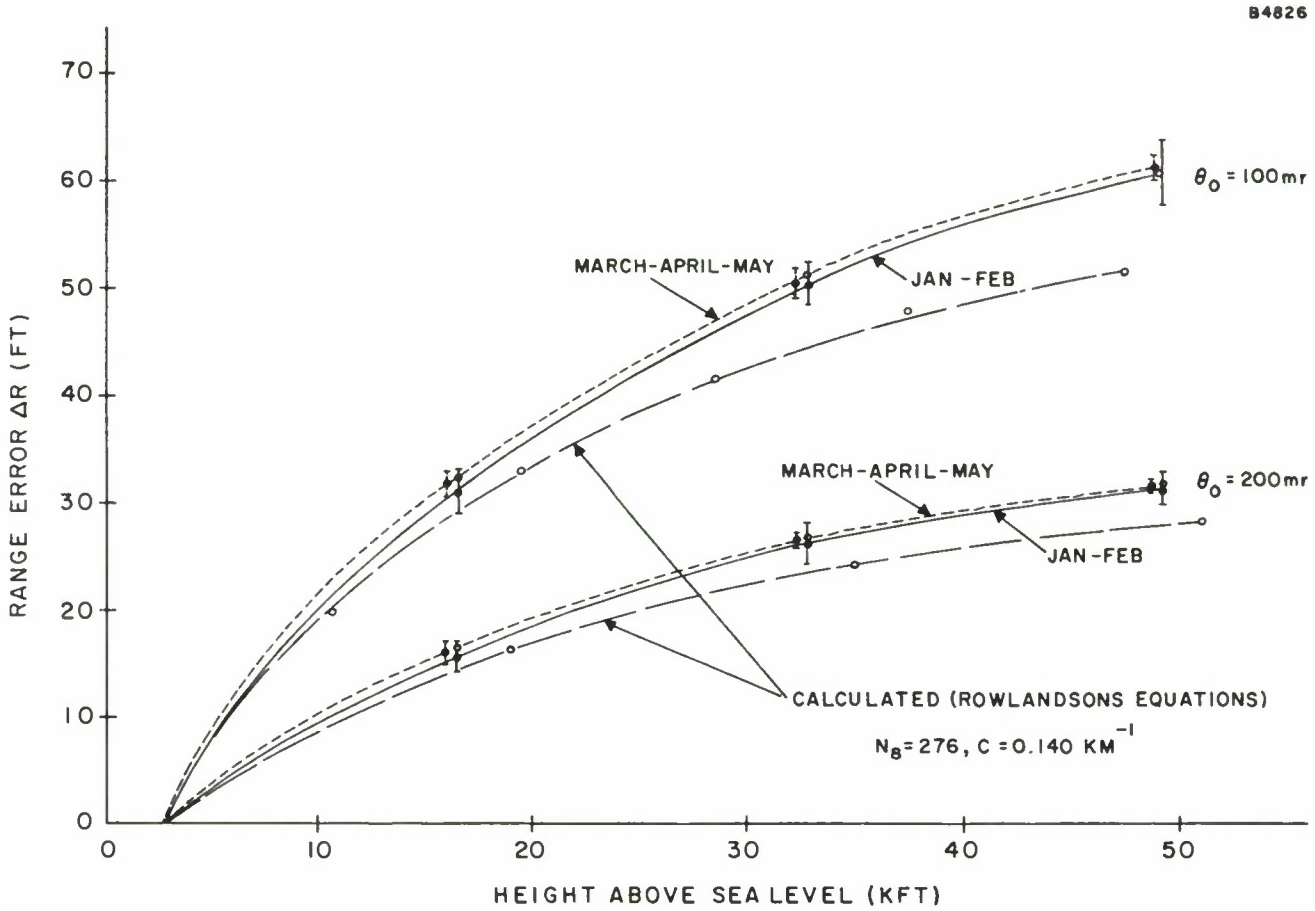


FIGURE 38. SEASONAL EFFECTS ON THE RANGE ERROR VERSUS HEIGHT (TRANQUILLAN PEAK RADAR, HEIGHT 2400 FEET)

Using all available airborne refractometer measurements made close to the Tranquillan Peak radar and all Vandenberg radiosonde data for the period 20 January to 8 February, the average station value is calculated to be 276 N units. The standard deviation about this average is 7.65 N units.

It therefore appears that the station value of refractivity, 276 N units, is less on the average then would be determined from the CRPL exponential model and a surface value of about 321 N units (Santa Maria). Radiosonde launch data over the January-February period also shows surface values around 320 N units from Vandenberg and the Boathouse.

1. Refraction Errors Calculated from Rowlandson's Equations

The elevation angle and range errors were calculated using the closed form equations developed in Section IV (Rowlandson's equations) where sin $\nu$ is now given by Equation (34). The appropriate CRPL model is defined by the following method.

(i) From aircraft and radiosonde measurements the average station value is determined to be 276 N units.

(ii) The index at 100,000 feet, from standard tables, is constrained to be 3.8 N units for all occasions.[20]

(iii) The simple exponential model becomes a straight line on a semi-logarithmic plot, shown on Figure 39. Projecting the line from 3.8 N units at 100,000 feet and 276 N units at 2500 feet, an equivalent surface value, $N_o$, is 302 N units.

(iv) The CRPL exponential decay constant, c, is then 0.140 $(km^{-1})$[12] for this equivalent surface value of 302 N units.

The calculations are shown on Figures 37 and 38 for the elevation angle and range errors, respectively. The elevation angle calculations agree with the average January-February results to within 0.1 milliradians. Referring to Figure 23, this agreement is essentially the same as that obtained for the hypothetical missile trajectory analysis. Similarily, the range error differences between calculations and the January-February average (Figure 38) is representative of the differences obtained for the hypothetical missile trajectory analysis, Figure 22. The differences between the calculations and ray tracing results become less as the apparent elevation angle, $\theta_o$, is increased as shown on Figures 37 and 38.

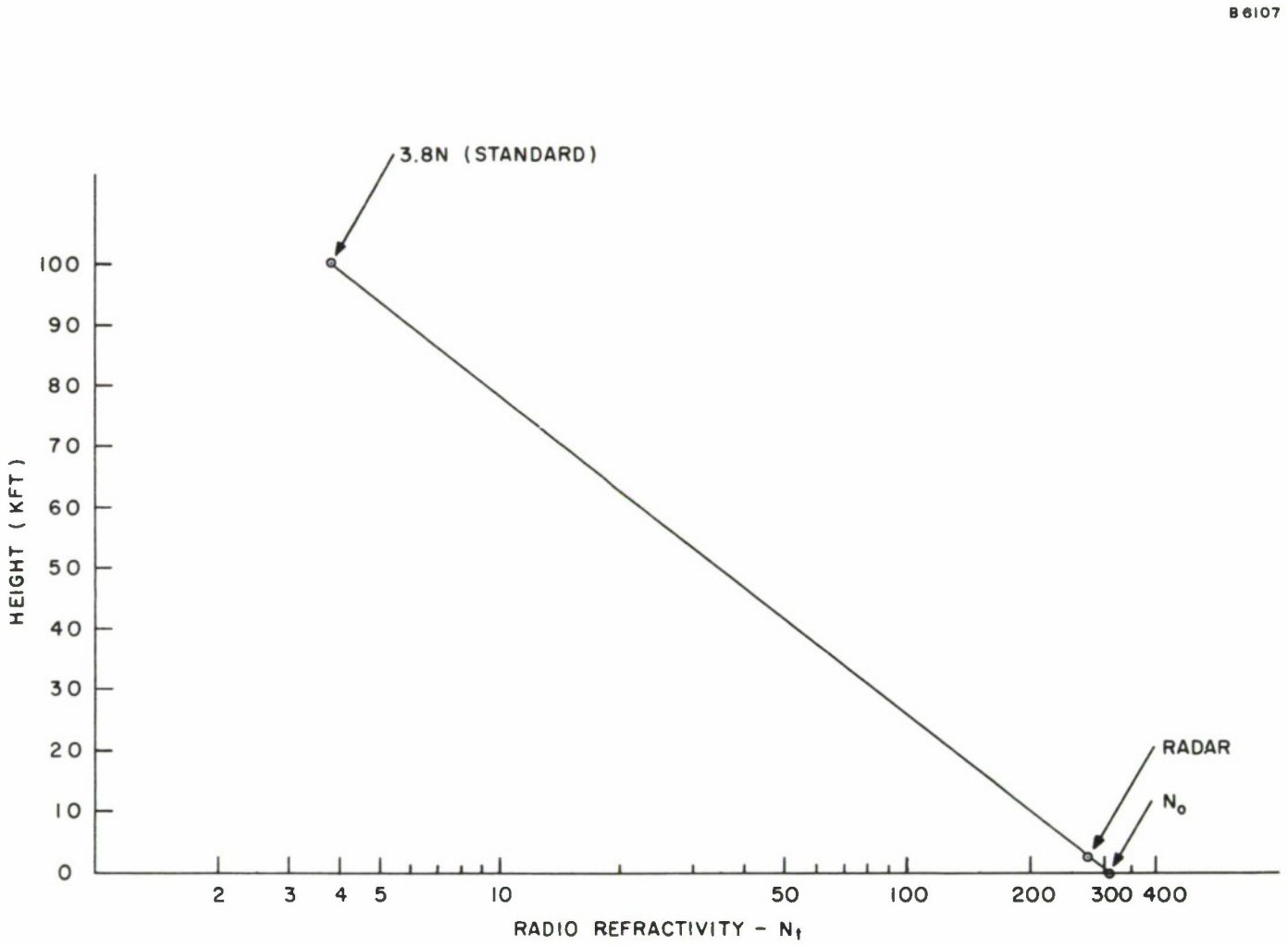


FIGURE 39. DETERMINATION OF SEA LEVEL REFRACTIVITY WITH A SIMPLE EXPONENTIAL MODEL PROFILE

This comparative analysis again shows that the elevation angle and range errors can be determined to a high degree of accuracy with the closed form equations.

It should also be pointed out that the optimization of the constants $K_0$ through $K_3$ (Equation (34)) used the available CRPL ray tracing data[12] which pertains to a radar at sea level. In the above analysis the constants were chosen for a station value, $N_s$, of 276 N units (Reference Figure 32). The decay constant, c, was determined for a surface value, $N_0$, of 302 N units. To obtain a final optimization of these equations it will be necessary to generate a set of ray tracing data pertaining to a station height of 2500 feet above mean sea level (Tranquillan Peak radar) and for propagation in a series of different CRPL model atmospheres.

Since the analyses show very good agreement between the data from ray tracings and the closed form equation we do not feel that such an additional optimization program can be justified at this time.

## SECTION VI

## THE CORRECTION OF TRACKING ERRORS AT VISIBLE OPTICAL FREQUENCIES

When visibility conditions permit, it may be required to track vehicles with ballistic cameras. Refraction induced errors are produced by variations in the dry term of the index of refractivity given by Equation (3).[6]

$$N_{DRY} = \frac{77.6\ P}{T} \tag{35}$$

It can be shown[21] that in an isothermal atmosphere the air pressure, P, decreases exponentially with height in order to maintain hydrostatic equilibrium. A plot of the variation of $N_{DRY}$ with height would then be represented by a straight line on the semi-logarithmic plot of Figure 40. These conditions occur above 40,000 feet altitude as shown by both the NACA standard atmosphere[20] and typical radiosonde measurements from Vandenberg.

Below 30,000 feet the air temperature (degrees Kelvin) tends to decrease linearly with height in which case the pressure decreases with height according to[21]

$$p = p_0 \left(\frac{T}{T_0}\right)^{g/R\gamma} \tag{36}$$

where $p_0$ = the surface pressure (mb)
$T_0$ = the surface temperature ($^\circ$ K)
$T$ = the air temperature at a given altitude ($^\circ$ K)
$g$ = the acceleration of gravity (m/sec$^2$)
$R$ = the specific gas constant (m$^2$/sec$^2$/$^\circ$ K)
$\gamma$ = the constant lapse rate of temperature T ($^\circ$ K/m)

Therefore, the dry term of refractivity does not follow a simple exponential dependence with height over the first 40,000 foot height interval. Analysis shows that the dry term behavior with height can be given by an empirically determined expression

$$N_{DRY} \simeq N_0 \exp\left[-0.0167\ (h^{1.21})\right] \tag{37}$$

where $N_0$ is the dry term of refractivity at the surface and h is the height.

In order to use Rowlandson's equations it would be advantageous if the vertical variation of $N_{DRY}$ could be expressed as a simple exponential function of height. A comparison was made between the propagation errors using the rawinsonde measurements and a simple exponential model. The exponential model is shown by the straight line on Figure 40 originating at a surface value of 274 N units and passing through 3.8 N units at 100,000 feet in height.

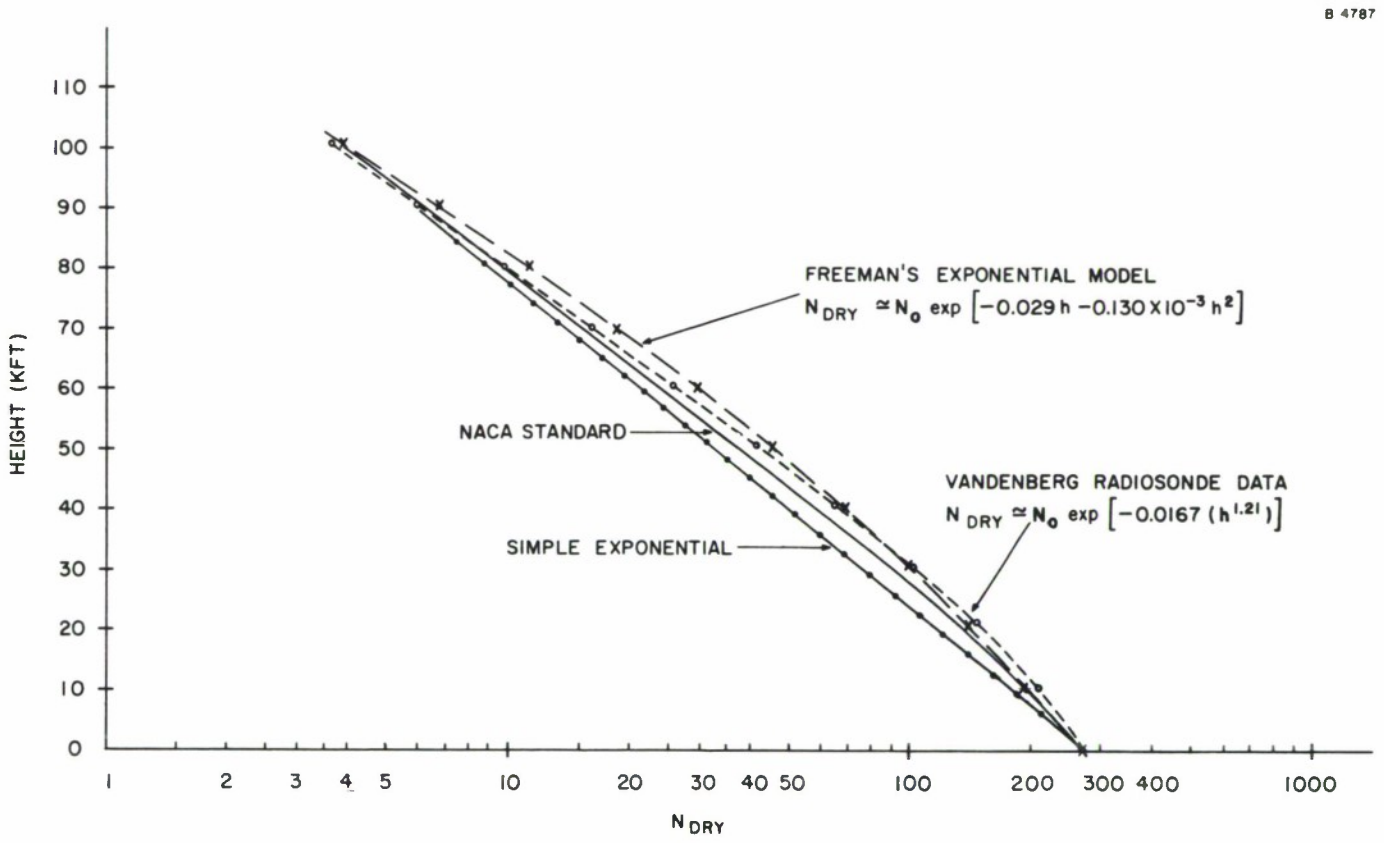


FIGURE 40. A COMPARISON OF DRY REFRACTIVITY MEASUREMENTS WITH MODELS

Figure 41 shows the elevation angle error differences, $\Delta\epsilon$, as a function of elevation angle, $\theta_o$. Ray tracings were carried out with the target at 30,000 feet altitude and the tracking camera at 100 feet above the surface.

A second comparison in Figure 42 places the target at 100,000 feet above sea level.

Comparing Figures 41 and 42, the elevation angle error differences are smaller under the longer range tracking conditions. This indicates that the effective gradients of refractivity which produce ray bending are more nearly equal as the height interval is increased. Referring to Figure 40, it is seen that the magnitude of the radiosonde gradient is less than the simple exponential gradient certainly over the first 30,000 foot height interval. Above this height the magnitude of the radiosonde gradient becomes larger than the gradient of the simple exponential function. Therefore, when ray tracing over the 100,000 foot height interval, the opposing radiosonde gradients tend to average out and provide an overall effective gradient which is closer to the gradient of the simple exponential function.

Figure 43 shows a comparison of the range errors for the radiosonde and the simple exponential profile. In this case the total range error differences, $\Delta(\Delta R)$, increase as the height interval is increased. The range error, $\Delta R$, is a direct function of the magnitudes of refractivity along the ray path where (reference Equation (7))

$$\Delta R = \frac{1}{10^6} \int_o^{R_g} N.\, ds \qquad (38)$$

From Figure 40 it is apparent that the absolute differences on the dry refractivity for the profiles in question continue to be significant above 30,000 feet with the radiosonde data always larger than the simple exponential data.

Therefore, the total range error given by Equation (38) increases at a greater rate along the path when radiosonde data are used than it does when the simple exponential is used. The range error difference, $\Delta(\Delta R)$, therefore increases directly as the path length increases.

The magnitudes of the elevation angle differences are significant even for tracking conditions above two degrees elevation angle. Therefore, the use of a simple exponential function to correct propagation errors in the visible region is not recommended.

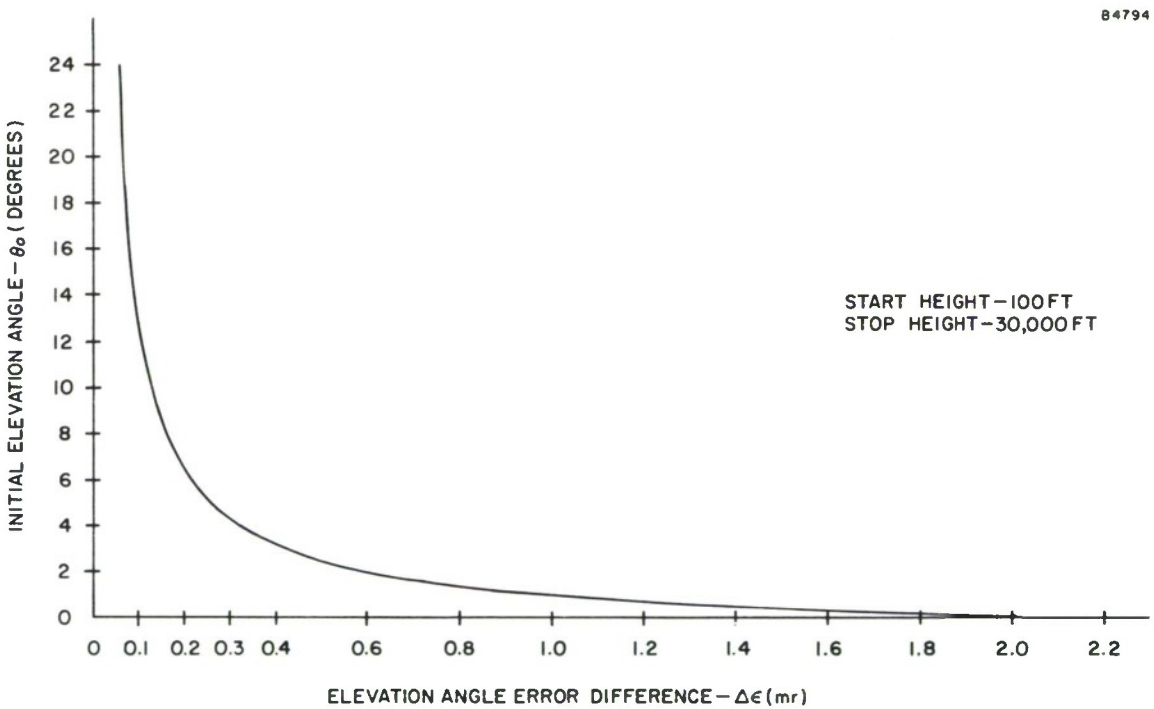


FIGURE 41. ELEVATION ANGLE ERROR DIFFERENCE BETWEEN RADIOSONDE AND EXPONENTIAL MODEL (OPTICAL TRACKING)

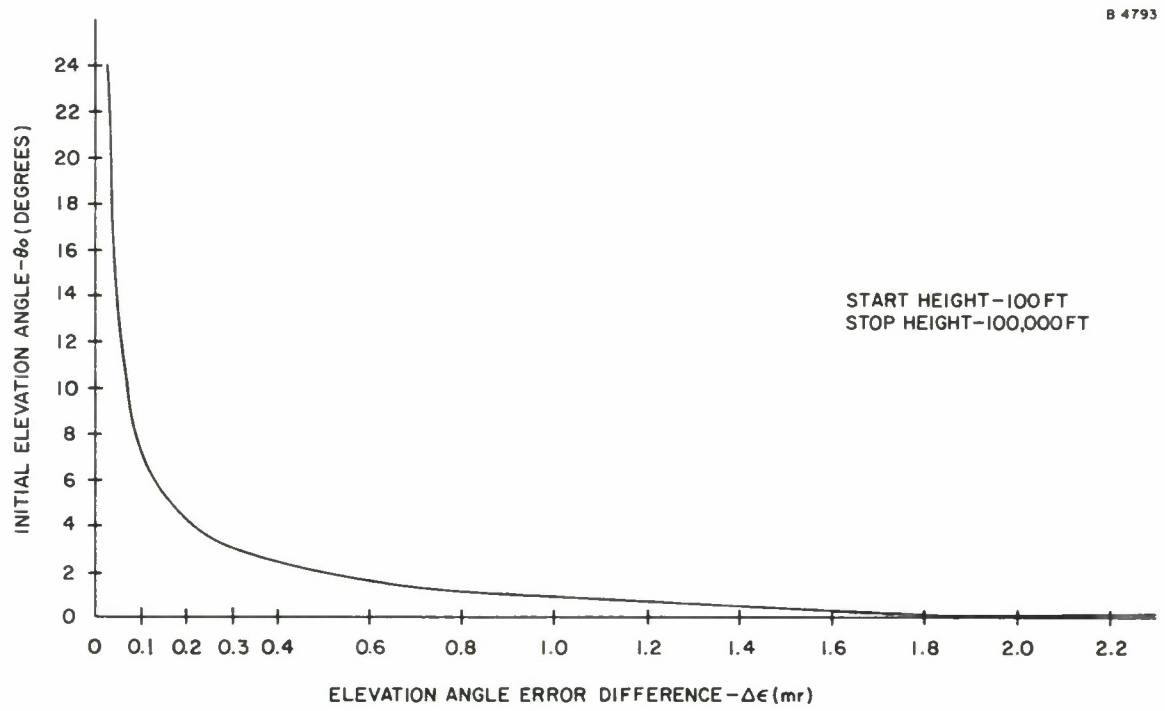


FIGURE 42. ELEVATION ANGLE ERROR DIFFERENCE BETWEEN RADIOSONDE AND EXPONENTIAL MODEL (OPTICAL TRACKING)

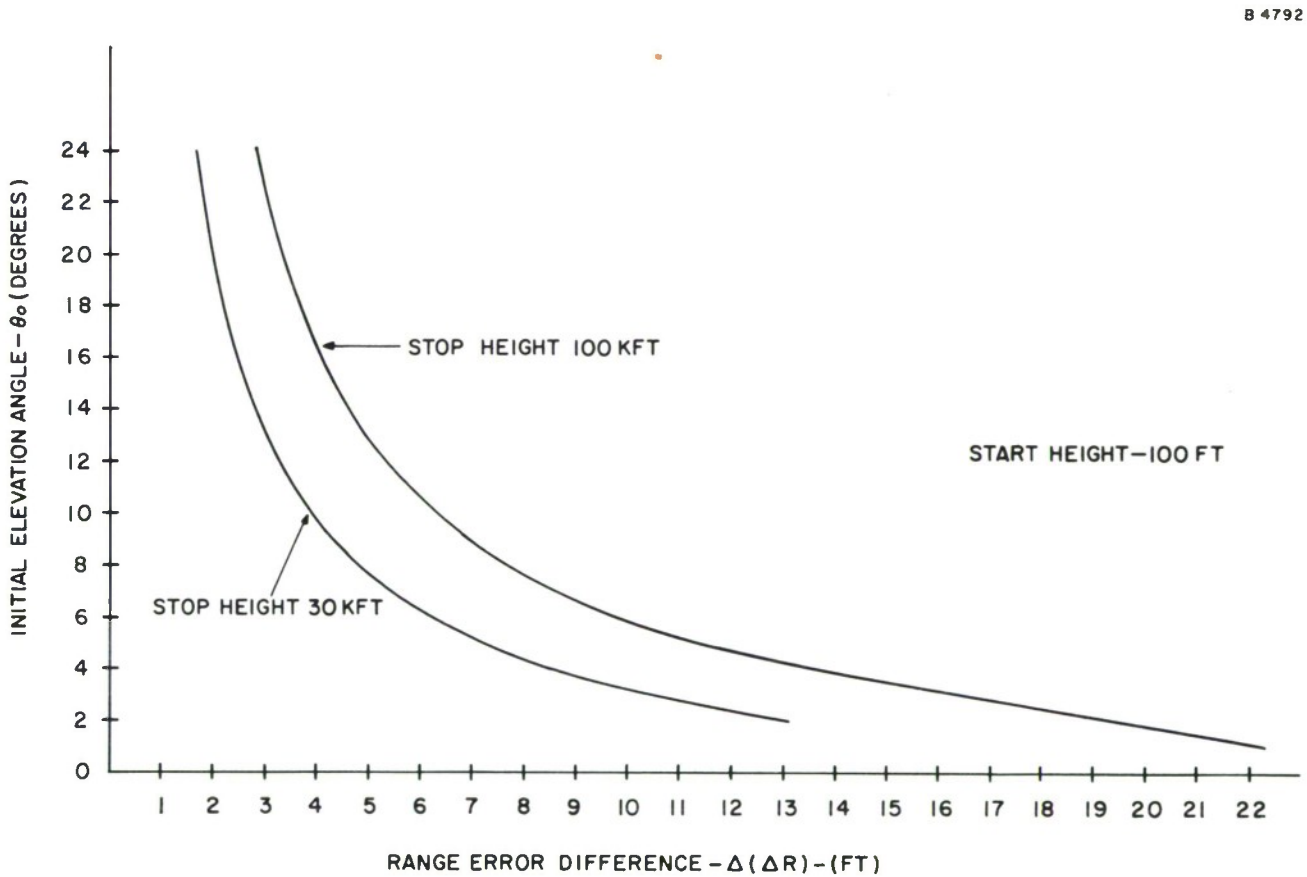


FIGURE 43. RANGE ERROR DIFFERENCE BETWEEN RADIOSONDE AND EXPONENTIAL MODEL (OPTICAL TRACKING)

## 1. The Calculation of Optical Propagation Errors With a Quadratic Exponential Function

Freeman showed that a solution to the ray tracing integrals (Equations (7) and (12.1) could be found by again integrating along the slant path, $R_o$, but with a quadratic exponential function to describe the vertical variation of N.[14] This equation is given by

$$N = N_S \exp(- ch_s - dh_s^2) \tag{39}$$

where $N_S$ is the station value of refractivity
$h_S$ is the height above the station (km)
and c and d are decay constants.

Figure 44 shows the vertical variation of the dry term of refractivity measured by the radiosonde. Using the quadratic exponential function (Equation (39)), it is almost possible to match the radiosonde results. Care was taken to get good agreement near the surface since the elevation angle errors are very dependent upon the initial index gradient.

## 2. Some Considerations on the Use of a Bi-Exponential Atmosphere

This section deals with a refractivity profile defined by the sum of two terms each one expressing an exponentially height-dependent refractivity profile.[7] Let the total refractivity be given by

$$N = N_0 e^{-c_1 h} + N_W e^{-c_2 h} \tag{40}$$

The first term represents the dry term and the second the wet term of refractivity. Figure 45 shows the total value of refractivity obtained from a radiosonde (13 June 1967, SNI). In the discussion on optical tracking corrections it was shown that the dry term of refractivity could not be expressed as one simple exponential function over the whole height interval.

If the interval is broken into two height sections, the dry term can be approximated by two simple exponentials, where

$$N_0 \simeq 280\, e^{-0.0329h} \qquad (0 \leq h \leq 40 \text{ k ft}) \tag{41}$$

$$N_0 \simeq 76\, e^{-0.0508h} \qquad (40 \leq h \leq 100 \text{ k ft}) \tag{42}$$

The wet term which is plotted on the lower left side of the figure is approximated by an exponential

$$N_W \simeq 62\, e^{-0.1375h} \tag{43}$$

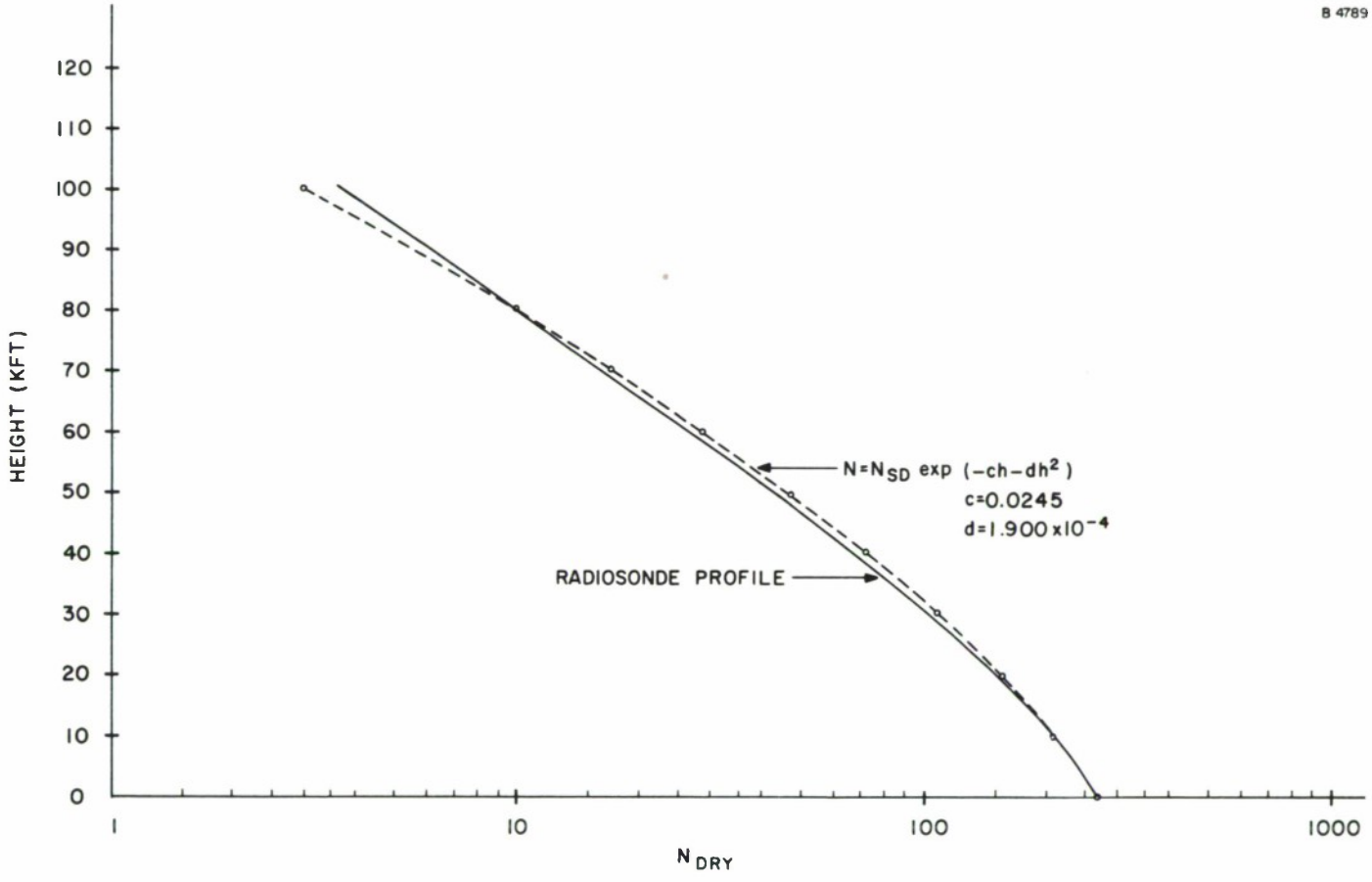


FIGURE 44. THE DRY TERM OF REFRACTIVITY

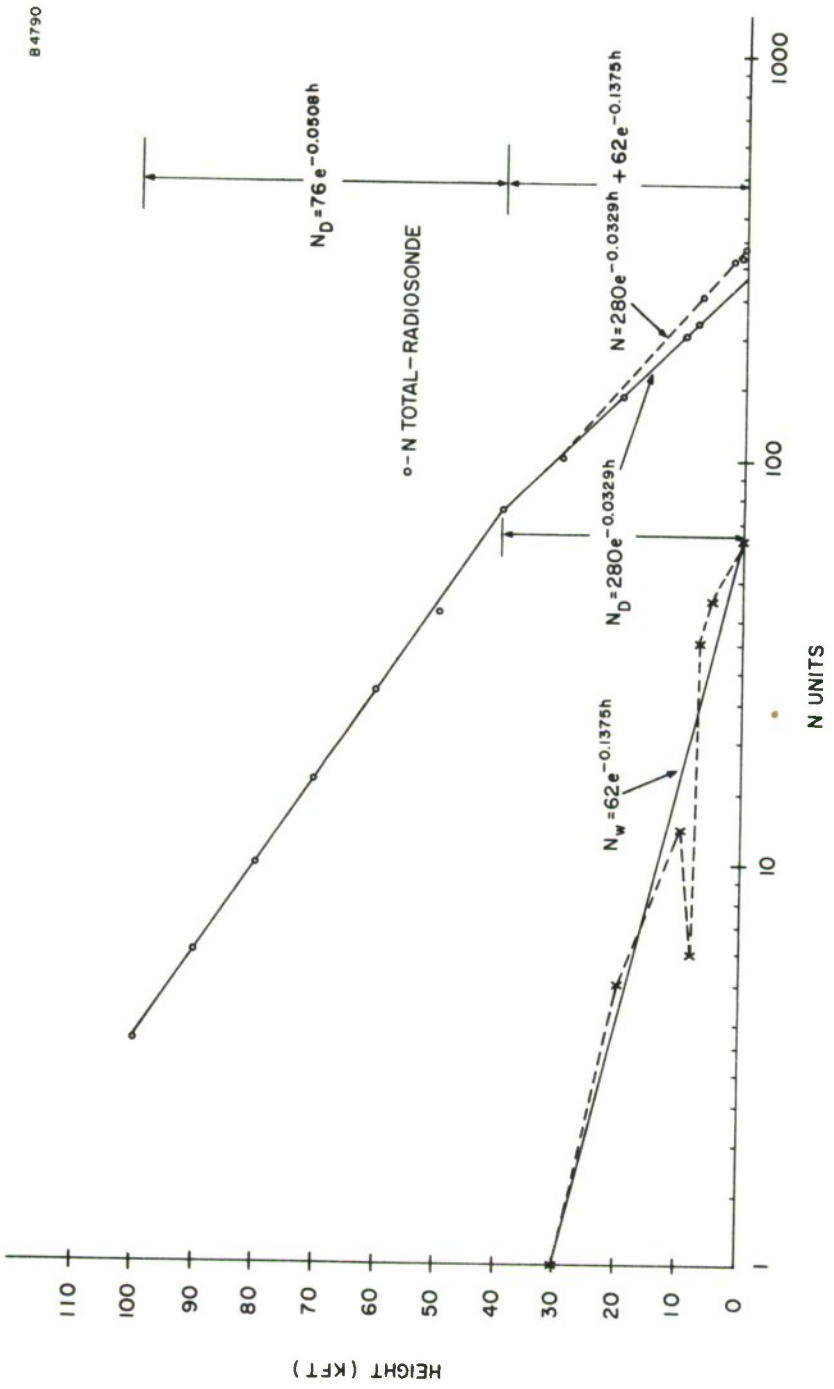


FIGURE 45. A BI-EXPONENTIAL REFRACTIVITY MODEL

The contribution of the wet term above 30,000 feet is negligible so there is no restriction on the height interval.

Using simple exponentials the total value of refractivity could be expressed by

$$N_T \simeq 280\, e^{-0.0329h} + 62\, e^{-0.1375h} \qquad (0 \leq h \leq 40 \text{ k ft}) \qquad (44)$$

$$\simeq 76\, e^{-0.0508h} \qquad (40 \leq h \leq 100 \text{ k ft}) \qquad (45)$$

It was shown previously that the dry term over the whole height interval could be expressed as

$$N \simeq N_{sd}\, e^{-(ch + dh^2)} \qquad (46)$$

Therefore, another bi-exponential form for the total refractivity could be given by

$$N_T \simeq N_{sd}\, e^{-(ch + dh^2)} + N_{ws}\, e^{-bh} \qquad (47)$$

Using Freeman's development it is apparent that either of the bi-exponential models can be directly integrated to give an expression for the retardation error, $\Delta R$, and the total ray path bending, $\tau$.[14,16] These equations may then be put into the form of Rowlandson's equations and empirically fitted to ray tracing data.[17]

It was already demonstrated that the simple exponential model for total refractivity (CRPL surface corrected model) provides a meaningful description of the propagation conditions for tracking elevation angles down to around four degrees. Therefore, at this point there is no justification to further complicate the calculations through the use of a bi-exponential model.

However, if greater accuracy requirements are found to be necessary at low tracking angles the bi-exponential model permits greater flexibility to describe propagation conditions as measured by radiosondes.

## SECTION VII

## VELOCITY MEASUREMENT ERRORS

The apparent radial velocity of a target can be determined by either differentiating the range data or by measuring the doppler frequency shift on the returned carrier signal. The doppler method is generally preferred because of greater inherent measurement accuracy and because differentiation tends to produce additional noise in the measurement.

Referring to Figure 46, a target velocity V has a component Vu in the direction away from the radar. Following the method of Fannin and Jehn[23], let $\tau$ be the time required for a signal to travel from the radar to the target and back. It can be shown[24] that the doppler frequency shift, $\Delta f$, is related to $\tau$ by the expression

$$\frac{d\tau}{dt} = \frac{\Delta f}{f + \Delta f} \tag{48}$$

From Figure 46, if u is in the radial direction and v in the tangential direction

$$\frac{d\tau}{dt} = \frac{\partial \tau}{\partial u} \cdot V_u + \frac{\partial \tau}{\partial v} \cdot V_v \tag{49}$$

However, $\partial\tau/\partial v$ is zero since motion in the tangential direction does not change the distance between the target and the radar. If the index of refraction is $n_t$ at the target the velocity of electromagnetic propagation is then $c/n_t$ at the target. Then

$$\frac{d\tau}{dt} = \frac{2n_t}{c} \cdot V_u \tag{50}$$

or

$$V_u = \frac{c}{2n_t} \cdot \frac{d\tau}{dt} \tag{51}$$

Since the true value of $n_t$ is generally unknown, the apparent velocity, $V_{ua}$, is then

$$V_{ua} = \frac{c}{2n_a} \cdot \frac{d\tau}{dt} \tag{52}$$

The velocity error from Equations (51) and (52) is then

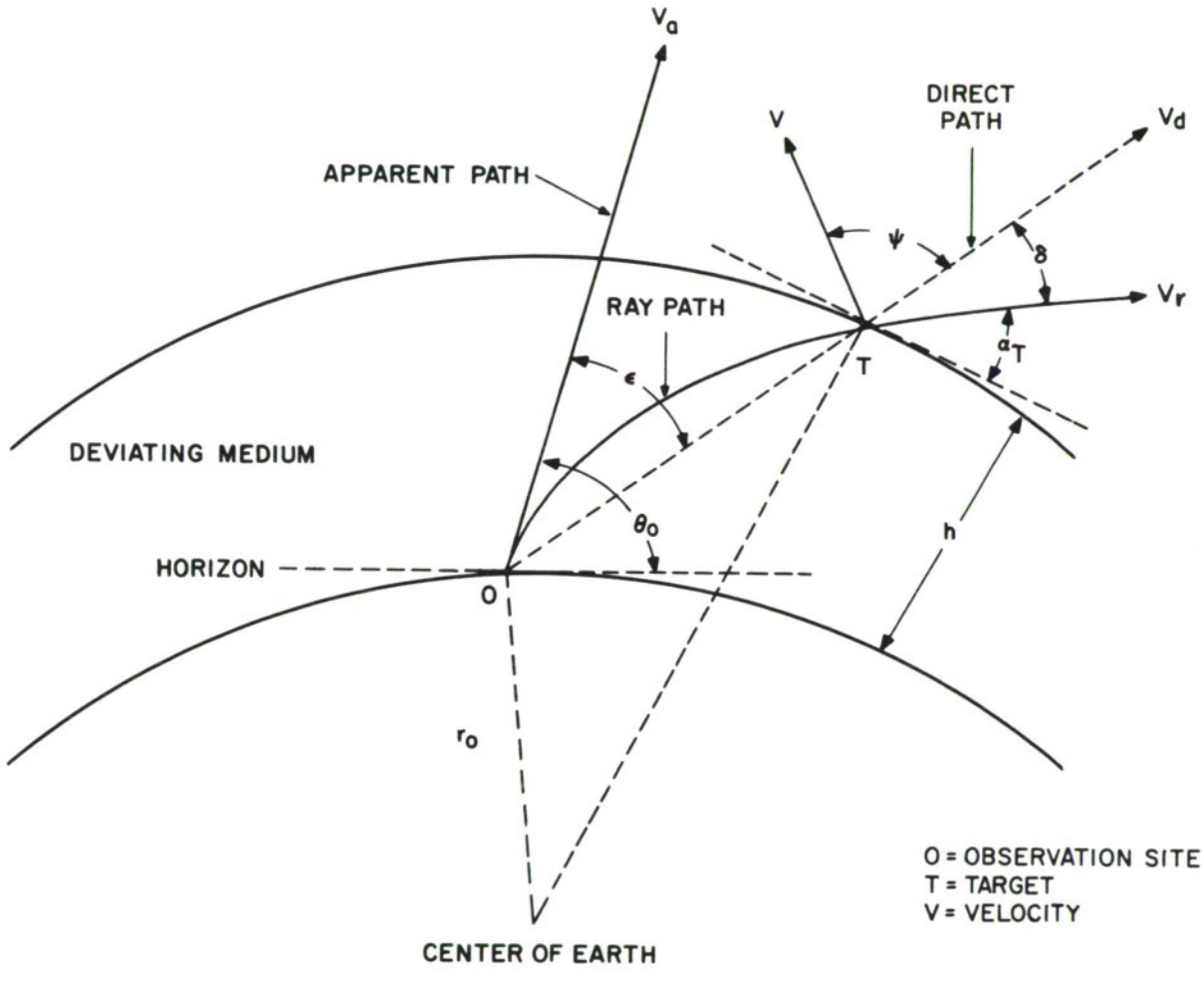


FIGURE 46. RAY PATH GEOMETRY

$$\Delta V = V_{ua} - V_u$$

$$= \frac{c}{2}\left(\frac{1}{n_a} - \frac{1}{n_t}\right) \cdot \frac{d\tau}{dt}$$

$$= \left(\frac{n_t - n_a}{n_a}\right) \cdot V_u \qquad (53)$$

At high altitudes n is very close to unity, to within a few parts per million. Therefore, the radial velocity measurement error due to the uncertainty in knowing the index of refraction at the target would be small for targets at very great heights.

The other terms neglected in the above derivation is that the round trip time, $\tau$, will be increased by the retardation error, $\Delta R$, ( reference Section IV ), by the difference in geometric path length, $R_g - R_o$, and by the fact that the retardation error, $\Delta R$, is increasing in a direction along the ray path rather than along $R_o$. However, one can readily determine that these errors are negligible in comparison with the effect of ray bending which is now presented.

Using the methods of Millman[26], it is apparent from Figure 46 that

$$V_r = V \cos(\psi + \delta) \qquad (54)$$

$$V_u = V \cos \psi \qquad (55)$$

Due to ray bending the target appears to be moving along a path, $V_a$, where

$$V_a = V_u \cos \epsilon \qquad (56)$$

The velocity error due to ray bending is then

$$\Delta V = V_a - V_r \qquad (57)$$

Substituting from Equations (54), (55), and (56) into (57), then

$$\Delta V = V \cos \psi \left[\frac{\delta^2}{2} - \frac{\epsilon^2}{2}\right] + V \sin \psi \cdot \sin \delta \qquad (58)$$

Again, $\delta^2/2$ and $\epsilon^2/2$ are extremely small, therefore

$$\Delta V \simeq V \sin \psi \cdot \sin \delta \qquad (59)$$

The measurement of the radial component of target velocity is, therefore, principally in error due to ray path bending and is directly dependent upon the tangential component of target velocity.

The tangential component of velocity would be measured by noting the rate of change of the true elevation angle, $\beta_o$, at particular ranges, that is

$$V \sin \psi = R \cdot \frac{d\beta_o}{dt}$$

$$= R \cdot \frac{d}{dt} (\theta_o - \epsilon) \tag{60}$$

Methods to compute $\epsilon$ and $\delta$ have been reported by Rowlandson.[17]

The doppler frequency error due to ray bending is then

$$d(f_d) = - \frac{2f}{c} \cdot V \cdot \sin \psi \cdot \sin \delta \tag{61}$$

For a spherically stratified atmosphere, and using Snell's Law in polar coordinates, Millman provides another method to compute $\delta$.

$$\delta = \cos^{-1} \left[\frac{r_s}{r_t} \cos (\theta_o - \epsilon)\right] - \cos^{-1} \left[\frac{n_s \, r_s}{n_t \, r_t} \cdot \cos \theta_o\right] \tag{62}$$

where $r_s$ is the radial distance from the station to the earth's center
$r_t$ is the radial distance from the target to the earth's center
$\theta_o$ is the apparent tracking elevation angle
$\epsilon$ is the elevation angle error
$n_s$ is the station value of refractive index
$n_t$ is the value of refractive index at the target.

For a station height, $H_s$, and a target height, h, relative to the station, then

$$r_s = r_o + H_s$$

$$r_t = r_o + H_s + h$$

also $N_s = 1 + \frac{N_s}{10^6}$

$$N_t = 1 + \frac{N_t}{10^6} = 1 + 10^{-6} N_s \, e^{-ch} \text{ (for an exponential atmosphere)}$$

where $N_s$ is the station value of refractivity
and $c$ is the exponential decay constant.

For most applications we are concerned with herein

$$r_o >> h >> H_s$$

$$1 >> \frac{N_s}{10^6} >> \frac{N_t}{10^6}$$

therefore

$$r_s / r_t \simeq 1 - \frac{h}{r_o} \tag{63}$$

and $$\frac{N_s \; r_o}{N_t \; r_t} \simeq 1 - \frac{h}{r_o} + 10^{-6} (N_s - N_t). \tag{64}$$

To a first order, $\delta$, can then be expressed by

$$\delta = \cos^{-1} [(1 - h/r_o) \cos (\theta_o - \epsilon)] - \cos^{-1} [(1 - h/r_o + 10^{-6} (N_s - N_t)) \cdot \cos \theta_o] \tag{65}$$

The measurement errors produced by refraction apply equally to either doppler or range differentiation methods used to determine target velocity.

## SECTION VIII

## SUMMARY COMMENTS

This report has considered several aspects of the effect of refraction on radar and optical tracking accuracy. The emphasis was placed on methods to correct refraction-induced errors and considerable attention given to the use of closed form equations for the calculation of tracking errors in real-time.

From an operational point of view, it was considered important to evaluate the accuracy of these real-time correction methods because of their greater simplicity over ray tracing methods. In particular, these closed form expressions require a limited amount of meteorological support data which can be interpreted and used in near-real-time.

It should also be pointed out that ray tracing results are only as accurate as the meteorological data and unless exceptional care is taken in the definition of the propagation conditions the ray tracing results cannot be tacitly assumed to give an absolute measure of propagation errors.

Below five degree tracking angles the ray tracing results should provide a more accurate description of the propagation errors than the closed form equations. This is simply because the non-exponential behavior of the vertical variation of refractivity with height becomes more apparent at low altitudes. However, two other considerations may impose a limit on the use of ray tracing methods below five degrees. In the first case, any tendency towards ducting or anomalous propagation will begin to be noticed at these low elevation angles. When these effects are evident, ray tracing methods, as commonly defined, cannot be used.[7] Propagation characteristics must then be determined from the field equations governing electromagnetic signal behavior.[6] In the second case, tracking below five degrees can subject the radar to the effects of multipath propagation and it then becomes difficult to obtain an accurate determination of the apparent elevation angle, $\theta_o$.

Most of the ray tracing results used in the comparison with the closed form equations were derived from radiosonde measurements. It was shown by Bean and Dutton[26] that unless the radiosonde measurements are corrected for the lag constants and the time variation of air temperature on the humidity sensor, the measured gradients can be significantly in error. Carlson[27] shows that with an uncertainty in measuring the refractivity to within $\pm$ 6 N units in the first 1000 feet and $\pm$ 2 N units in each higher 1000 foot layer, that elevation angle errors of $\pm$ 0.05 milliradians would be experienced for tracking angles of 2.5 degrees. The error, of course, falls off as the elevation angle is increased.

Further analyses by Barnett[28], Bean and Cahoon[29], Mayer[30], Rainey and Thorn[31], Cramond, et al[32], Anderson, et al[33], and many others clearly demonstrate the difficulty in determining accurate and representative radio refractivity data for use in real-time ray tracing analysis.

To summarize these comments, I would like to refer to the paper prepared by Ratner and Bower[34] of the PMR Division, FEC, VAFB. Several comments were made in this report which are pertinent to the analysis presented in our (SURC) report.

(a) "Considerable investigation has been conducted at Point Mugu to establish the experimental fact that the exponential atmosphere model introduces sizeable errors because it is too oversimplified."

(b) "Radar tracking errors due to tropospheric refraction can best be handled when the index of refraction profile through the troposphere is determined. The index of refraction profile has a relatively systematic exponential distribution with altitude, together with a superimposed fine-structure, which is not readily amenable to analytical treatment. The fine-structure is due to local variations in temperature, humidity and pressure. The extent to which tracking errors due to refraction can be reduced is, in general, proportional to the amount of meteorological data in conjunction with a tracking operation."

(c) "REFRAC is used for post-flight data reduction, since its execution cycle time is too great to permit real-time analysis."

It has been demonstrated in this (SURC) report by a comparison with Gardner's data[4] that for tracking above five degrees elevation angle that an exponential model can be used to determine refraction-induced errors. Between five degrees and approximately two degrees, directly measured radio refractivity data are required together with ray tracing analysis to obtain accurate tracking error data. The comment, (a), above, is, therefore, conditioned by the requirement to track below five degrees. Tracking below two degrees is considered to be impractical due to multipath propagation effects and limitations on the applicability of conventional ray tracing methods.

Comment, (b), above, reiterates the problem associated with obtaining accurate real-time measurements of the radio refractivity structure.

This report (SURC) has attempted to show that these fine-structure errors can be reduced by using real-time measurements near the site and that spatial effects are constrained by the effect of earth curvature.

Finally, with respect to (c), the use of Rowlandson's equations, particularly when simplifications of these equations can be made for long range tracking, permits real-time calculations of tracking errors to be carried out above five degree elevation angles.

# SECTION IX

## RECOMMENDATIONS

1. A comparison of tracking error data be made using the AFWTR ray tracing program and Rowlandson's equations for representative missile trajectories, initially on a post-flight basis.

2. The comparative data be analyzed with respect to known trajectory data, the latter made available from independent missile guidance and impact coordinate data.

3. The ray tracing and closed form (Rowlandson) methods to derive tracking error data be compared on the basis of real-time data availability. This comparison will be initiated at a pre-designated time and accurate records maintained of the times required to obtain and implement pertinent radio refractivity data and to process the data for tracking correction use.

4. The results of these analyses will be presented to AFWTR at which time a decision will be made to implement a technique or a combination of techniques to support real-time radar and ballistic camera tracking operations.

5. The technique which is selected will then be re-evaluated under live launch conditions.

6. Finally, it is recommended that additional studies be initiated following the complete evaluation of these refraction correction methods towards optimizing the tracking data from independent velocity measuring systems.

## REFERENCES


1. Crain, C. M., "Survey of Airborne Microwave Refractometer Measurements," Proc. IRE 43, No. 10, 1405-1411, (October 1955).

2. Crain, C. M., "Apparatus for Recording Fluctuations in the Reflective Index of the Atmosphere at 3.2 Centimeter Wavelength," Rev. Sci. Instr. 21, No. 5, 456-457, (May 1950).

3. Vickers, W. W., W. A. Carito, and L. G. Rowlandson, Contents of a Briefing Presented to AFWTR, April 1967, "The Effects of Tropospheric Refraction on Vehicle Signal Loss, the Accuracy of Trilateration Tracking and the Magnitudes of Correctable Range and Bending Errors." Mitre Technical Report, MTR-458, 18 August 1967, The Mitre Corporation, Bedford, Massachusetts, [ESD/USAF Contract AF19(628)-5165], (August 1967).

4. Gardner, C., "Comparison of Refraction Effect Correction Techniques," Proc. of Third Tropospheric Refraction Effects Meeting, Vol. II, ESD/USAF Report ESD-TDR-64-148, January 1966, Prepared by the Mitre Corporation, Bedford, Massachusetts, [ESD/USAF Contract AF19(628)-2390], (July 1964).

5. Smith, E. K., and S. Weintraub, "The Constants in the Equation for Atmospheric Refractive Index at Radio Frequencies," Proc. IRE 41, 1035-1037, (August 1953).

6. Born, M., and E. Wolf, "Principles of Optics," Pergamon Press, 1959.

7. Bean, B. R., and E. J. Dutton, "Radio Meteorology," National Bureau of Standards Monograph 92, March 1966, US Government Printing Office.

8. Bean, B. R., and G. D. Thayer, "On Models of the Atmospheric Refractive Index," Proc. IRE 47, No. 5, 740-755, (May 1959).

9. Rainey, R. J., and D. C. Thorn, "A Radar Refraction Correction for Symmetric and Non-Symmetric Tropospheric Index Distribution," Technical Report EE-43, University of New Mexico, Albuquerque, New Mexico, [White Sands Missile Range Contract DA 29-040-ORD-1238], (February 1961).

10. Weisbrod, S., and L. J. Anderson, "Simple Methods for Computing Tropospheric and Ionospheric Refractive Effects on Radio Waves," Proc. IRE, Vol. 47, No. 10, pp 1770-1777, (October 1959).

11. Gardner, C., "Standards for Refraction Correction of Tracking Data," Electromagnetic Propagation Working Group, Inter-Range Instrumentation Group, Range Commanders Council, Preliminary Report, 1966-67, WTN, AFWTR, Vandenberg, California.

12. Bean, B. R., and G. D. Thayer, "CRPL Exponential Reference Atmosphere," NBS Monograph 4, US Government Printing Office, (October 1959).

13. DeMarrais, G. A., G. C. Holzwarth, and C. R. Hosler, "Meteorological Summaries Pertinent to Atmospheric Transport and Dispersion Over Southern California," Technical Paper No. 54, US Department of Commerce, Weather Bureau, US Government Printing Office, (1965).

14. Freeman, J. J., "Range-Error Compensation for a Troposphere With Exponentially Varying Refractivity," Journal of Research, NBS, D. Radio Propagation, Vol. 66D, No. 6, November-December 1962, (June 1962).

15. Thayer, G. D., "A Formula for Radio Ray Refraction in an Experimental Atmosphere," Journal of Research, NBS, D. Radio Propagation, Vol. 65, No. 2, (March-April 1961).

16. Freeman, J. J., "The Real-Time Compensation for Tropospheric Effects on the Measurement of Range and Range Rate," Proceedings of the Second Tropospheric Refraction Effects Technical Review Meeting, Vol. II, ESD/USAF Report ESD-TDR-64-103, April 1964, Prepared by the Mitre Corporation, Bedford, Massachusetts, [ESD/USAF Contract AF19(628)-2390] (November 1963).

17. Rowlandson, L. G., "Simple Analytical Functions Which Provide Magnitudes of Range and Angle Errors for Propagation in an Exponential Atmosphere," ESD/USAF Report ESD-TR-68-308, 19 January 1968, Prepared by Syracuse University Research Corporation, Syracuse, New York, [ESD/USAF Contract F19628-68-C-0209], (January 1968).

18. Abramowitz, M., and J. A. Stegun, "Handbook of Mathematical Functions," NBS Applied Mathematics Series 55, June 1964, Department of Commerce, US Government Printing Office.

19. Bean, B. R., J. D. Horn, and A. M. Ozanich, Jr., "Climatic Charts and Data of the Radio Refractive Index for the United States and the World," National Bureau of Standards Monograph 22, 25 November 1960, US Government Printing Office, Washington.

20. List, R. J., "Smithsonian Meteorological Tables," Vol. 114, Sixth Edition, Smithsonian Institute, Washington, D. C.

21. Hess, S. L., "Introduction to Theoretical Meteorology," (1959), Holt, Rinehard and Winston, New York.

22. National Advisary Committee for Aeronautics, "Standard Atmosphere Tables and Data for Altitudes to 65,800 feet," Report 1235, (November 1952), NACA, Washington, D. C.

23. Fannin, B. M., and K. H. Jehn, "Radar Elevation Angle and Range Errors in Representative Air Masses," Electrical Engineering Research Laboratory, Report No. 7-01, The University of Texas, (30 June 1954).

24. Sommerfield, A., "Optics, Lectures on Theoretical Physics," Vol. IV, Academic Press, Inc., New York, (1964).

25. Millman, G. H., "Atmospheric and Extraterrestial Effects on Radio Wave Propagation," General Electric Report No. R61EMH29, Technical Publications, CSP 9-12, Syracuse, New York.

26. Bean, B. R., and E. J. Dutton, "Concerning Radiosondes, Lag Constants, and Radio Refractivity Index Profiles," Journal of Geophysical Research, Vol. 66, No. 11, (November 1961).

27. Carlson, A. V., "Analysis of the Precision of Atmospheric Refractivity Corrections to Radar Tracking Measurements," USAERDAA-MET-8-64, (May 1964), U. S. Army Electronics Research and Development Activity, Fort Huachuca, Arizona.

28. Barnett, K. M., "An Objective Procedure for Planning Meteorological Observations Needed to Calculate Radar Refraction Errors," USAERDAA-MET-9-64, (June 1964), U. S. Army Electronics Research and Development Activity, Fort Huachuca, Arizona.

29. Bean, B. R., and B. A. Cahoon, "Effect of Atmospheric Horizontal Inhomogeneity Upon Ray Tracing," Journal of Research of the National Bureau of Standards, D. Radio Propagation, Vol. 63D, No. 3, (November-December 1959).

30. Mayer, V. E., "Meteorological Analysis of Selected Offshore California Refractive Index Profiles," AFCRC-TN-55-365, Report No. 6-09, Electrical Engineering Research Laboratory, The University of Texas, (June 1955), Air Force Contract AF19(604)-494.

31. Rainey, R. J., and D. C. Thorn, "A Radar Refraction Correction for Symmetric and Non-Symmetric Tropospheric Index Distributions," Technical Report EE-43, University of New Mexico, Albuquerque, (February 1961), [White Sands Missile Range Contract DA-29-040-ORD-1238].

32. Cramond, W. R., J. E. Leaman, and D. C. Thorn, "Radar Elevation Angle Errors and Refraction Corrections," Technical Report EE-79, University of New Mexico, Albuquerque, (September 1962), [White Sands Missile Range Contract, DA-29-040-ORD-1238].

33. Anderson, W. L., and R. J. Rainey, "Comparison of Experimental With Computed Tropospheric Refraction," Technical Report EE-28, University of New Mexico, Albuquerque, (October 1959), [White Sands Missile Range Contract DA-29-040-ORD-1238].

34. Ratner, M., and T. Bower, "An Investigation Into the Errors of Impact Prediction Due to Errors in Tropospheric Refraction," ADP-64-064, (October 1964), Analysis and Data Processing Department, Federal Electric Corporation, PMR Division, Vandenberg Air Force Base.

# APPENDIX

## A DESCRIPTION OF A C-131 CONVAIR AIRCRAFT USED FOR ATMOSPHERIC RESEARCH

# PREFACE

The following paper describes a C-131 Convair flight facility which was instrumented to obtain meteorological and radio refractivity measurements.

The aircraft, under the direction of the Electronics Systems Division, USAF, is used to support radar refraction studies at the National Ranges and also meteorological investigations for Air Force oriented programs.

Having been completely associated with this facility during and since its inception, my intention herein is to provide a reasonably detailed description of the aircraft's capabilities, its past activities, and to indicate its future potential.

Lyall G. Rowlandson

# A DESCRIPTION OF A C-131 CONVAIR AIRCRAFT USED FOR ATMOSPHERIC RESEARCH

## 1.0 INTRODUCTION

A USAF C-131 Convair (37812), based at L. G. Hanscom Field, Bedford, Massachusetts, was instrumented in 1962 to obtain meteorological measurements associated with radio wave propagation. Figure 1 shows a photograph of the aircraft in flight. To determine propagation characteristics, the fundamental parameter to be measured was the radio refractive index[1,2,3]. However, to obtain accurate measurements it became necessary to also monitor the characteristics of associated air temperature, pressure, and relative humidity. Since these measurements can be in error due to the velocity of the air relative to the sampling probes, the indicated aircraft velocity and air pressure were also required.

The requirement to collect, assimilate and process large quantities of data, together with the requirement to correct the free-air variables due to aircraft motion, led to a digital recording system and an associated data analysis computer program.

The use of the corrected data in propagation analysis requires a knowledge of where the measurements are recorded as a function of time. The facility was, therefore, further modified to include an accurate radar altimeter, 35 mm telescopic camera system and a radio-navigational position.

It is apparent that starting from what initially appeared to be a rather simple requirement led to a much more complicated system. As additional tasks were levied the facility was expanded to include an air sampling system, additional refractometers, tape recorder, accelerometers, drift meter, and radio communications for long over-water operations.

The details of these various instruments and programs will be described later. However, the essential point is that the facility has developed into a flexible and accurate system for investigation of parameter characteristics which affect radio signal propagation. To expand its mission one can think of several additional instruments which are available and which would permit greater involvement in atmospheric measurement programs; namely, a weather-radar, more extensive camera facilities, three directional wind velocity probes (possibly acoustic anemometers), an infrared camera detection system for water temperature recordings, air particle and aerosol samplers, lyman-alpha humidiometer or dew-point hygrometer, water drop size spectrometer, etc.

FIGURE 1

The primary power and distribution system is adequate to meet these further requirements. Since 1962, the advancements in solid-state development could lead to a considerable power, space and weight saving in much of the existing equipment. Certainly the aircraft is large enough to house additional equipment.

To summarize, the existing aircraft equipment has provided an adequate facility for lower altitude tropospheric propagation and meteorological investigations. Its potential in this important lower region of the atmosphere could be greatly expanded by cooperative efforts of the various atmospheric science investigators to serve a much broader field.

## 2.0 SPONSORSHIP

The C-131 aircraft is operated by the United States Air Force under the direction of the Air Force Systems Command. It has been based at L. G. Hanscom Field, Bedford, Massachusetts, and was assigned to support technical investigations of the effect of the troposphere on command and control systems. Its experimental flight function was, therefore, placed under the Electronics Systems Division, Hanscom Field, Bedford. Historically, since 1962, the aircraft has carried out extensive investigations at both the National Ranges (Eastern Test Range, Cape Kennedy, and Western Test Range, Vandenberg, California). Special joint programs have been coordinated with a large cross-section of the scientific community in those areas of investigation where results would have a direct impact on the ESD mission and, at the same time, by agreement, the work could be carried out without jeopardizing the open publication of scientific information.

These programs have been extremely fruitful in that the Electronics Systems Division has gained valuable information and support from the scientific agencies affiliated with the programs and, at the same time, the level of competence of the Air Force-Contractor personnel has been greatly improved.

As an example of some types of joint programs, I might mention the radar-backscatter experiments with AFCRL[4], the water-vapor radiometric program with the Department of Meteorology, MIT, the sea-air and anomalous propagation experiments with the Woods Hole Oceanographic Institution[5], the multipath-propagation experiments with the Defense Research Board and the Royal Canadian Air Force[5,7,8], the DCA experiments with RADC, ESSA[9], etc.

The output from these various activities is reflected in the referenced list of publications, not to mention the associated papers which have been and are being prepared for publication in the scientific journals.

It has been a real credit, in my opinion, to the Electronics Systems Division of USAF and to the administering project officers that a reasonable degree of joint scientific effort has been permitted without jeopardizing the direct work to the National Ranges. Otherwise, I believe the program could have become stodgy and limited and the effective support to ESD in knowledge and technical consultation would have been greatly reduced from what it has been.

## 3.0 DESCRIPTION OF THE AIRCRAFT INSTRUMENTATION

The following table provides a brief description of the types of instruments which are presently in the aircraft, together with their measurement accuracy and time constants.

In addition to the above instrumentation, serious consideration is being given towards mounting an infrared radiometer to measure sea surface temperature and a weather radar to measure precipitation characteristics. The engineering aspects of this program have not been discussed in any detail with the Airborne Engineering Laboratories at Hanscom Field.

Figure 2 shows, from the top, the AMQ-8 vortex thermometer, the KS4 aerograph thermometer and relative humidity probe, the University of Texas refractometer cavity and the Rosemount thermometer at the bottom. In Figure 1, the two-cavity, vertical N gradient, refractometer may be seen under the starboard wing tip.


FIGURE 2

TABLE I

| Instrument | Range | Accuracy | Time Constant |
|---|---|---|---|
| 1. Vortex Thermometer | -40° to +40° C | ±1/2° C | 0.5 seconds |
| 2. KS4 Aerograph Thermometer | -40° to +40° C | ±1/2° C | 0.5 seconds |
| 3. Rosemount Platinum Wire Thermometer | -40° to +40° C | ±0.1° C | 0.01 seconds |
| 4. MKS-Pressure Transducer | 1015 to 500 mb | ±0.3 mb | 1 second |
| 5. Giannini Air Speed Transducer | 0 to 300 kts | ±0.5 kts | 1 second |
| 6. KS4-Aerograph Relative Humidity | 0 to 100% | 5% | 1 second |
| 7. University of Texas Refractometer-N | 0 to 400 N | ±0.5 N | 0.1 second (-3 db) |
| 8. Radar Altimeter | 0 to 20,000 ft. | ±20 feet | 0.1 second |
| 9. Master Time-HP Clock | | 1 in $10^8$ | 0.1 second (as normally set) |
| 10. Vertical Acceleration - Strathan | ±1.5 g | ±0.1 g | 0.05 second |
| 11. Flight Research 35 mm Camera on A28 Gyro Mount | 0-20,000 ft. | ±50 feet | 1/16 second |
| EQUIPMENT ENGINEERED BUT NOT INSTALLED | | | |
| 12. CEC Dew-Point Hygrometer | (Not Tested in Aircraft System.) | | |
| 13. University of Texas Refractometers - Pod Mounted | Designed to measure N gradient over 1 meter in vertical. Test flown but further modifications required. | | |

## 4.0 RECORDING SYSTEMS AND DATA OUTPUTS

Three recording systems are used on the aircraft:

1. A 36-channel CEC galvanometer, paper chart, recorder.
2. A 16-channel Ampex, FM-analog tape recorder.
3. A special purpose punched-paper tape digital recorder.

The prime data channels, 1 through 9, Section 3.0, are recorded on all systems. The CEC chart recorder has a real-time developing unit which permits the in-flight operation of these instruments to be monitored.

The magnetic tape records of the raw analog data are extremely useful to obtain fine-structure and to plot strip chart or X-Y plots for later playback analysis. Spectrum analysis has been carried out to a limited degree.

The digital recorder can accept up to 14 channels of information every two seconds or can be used on decreased sampling rates. The data are recorded in standard BCD code, making it very compatible for computer processing.

Figure 3 shows an example of the X-Y magnetic tape records of the variation of radio refractivity, N, with height. The aircraft is generally moving in upward or downward spirals at a 500 foot/minute rate. The horizontal thickness on parts of the record is produced by the horizontal variations of N as the aircraft orbits about the vertical axis.

The raw digital data obtained in punched paper tape are packed on magnetic tape for direct input to special purpose computer programs. Table II shows a sample printout from the computer. The first four sets of data are shown, the first group representing the uncorrected free air variables. Looking at the second to last column it is apparent that data were recorded every two seconds.

In this particular test the platinum wire thermometer was not required and was not calibrated or used directly during the flight. The aerograph and vortex thermometer were used and, due to the effect of air speed, the aerograph readings are greater than the vortex thermometer which is relatively unaffected by speed. The relative humidity was high and in such a case the carbon element in the KS4 aerograph probe can indicate 100% even though the relative humidity may be several percentages less. The radio refractivity, N, together with its variation from a calibration level

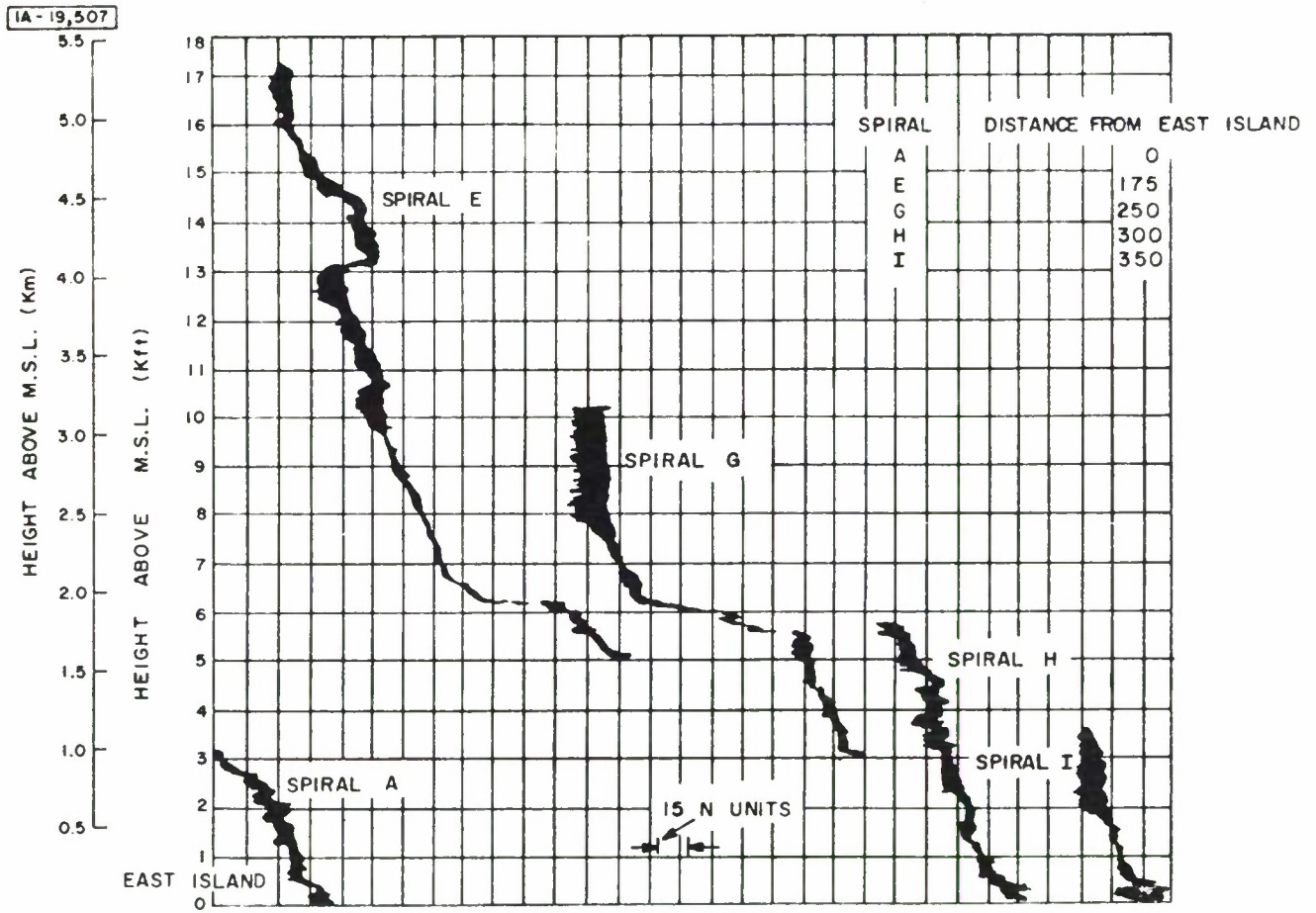


Figure 3. .RELATIVE RADIO REFRACTIVITY PROFILE
9, DECEMBER, 1965 11:00 – 13:45 SAN JUAN LOCAL TIME

TABLE II

SAMPLES OF COMPUTER PRINTOUTS OF PROCESSED AIRCRAFT DIGITAL DATA

INPUT DATA FOR THE COMPUTATION OF FREE AIR VARIABLES
FOR AIRCRAFT FLIGHT - SAN JUAN MISSION NO. 401, 7 DECEMBER 1965

| Reading | Indicated Airspeed Knots | Pressure MB | Aerograph Deg. C | Temperature Plat. Wire Deg. C | Vortex Deg.C | Humidity Carbon S Percent | Refractometer Delta N | N | Altimeter Meters | Time | Event |
|---|---|---|---|---|---|---|---|---|---|---|---|
| 1 | 156.3 | 916.6 | 21.2 | -17.7 | 19.2 | 100 | 56.3 | 321.7 | 870.9 | 70440 | 3 |
| 2 | 155.3 | 915.1 | 21.6 | -17.6 | 19.4 | 100 | 60.0 | 318.0 | 861.9 | 70442 | 3 |
| 3 | 154.7 | 916.1 | 21.4 | -17.6 | 19.5 | 100 | 57.1 | 320.9 | 861.9 | 70444 | 3 |
| 4 | 153.7 | 916.6 | 20.8 | -17.7 | 20.2 | 100 | 53.9 | 324.1 | 858.9 | 70446 | 0 |

FREE AIR VARIABLES COMPUTED FOR AIRCRAFT FLIGHT
SAN JUAN MISSION NO. 401, 7 DECEMBER 1965

| Reading | Pressure MB | Aerograph Deg. C | Temperature Plat. Wire Deg. C | Vortex Deg.C | Aerograph Pot. Temp Deg. C | N Dry | Aerograph Pot. Temp Deg. C | N Dry | Aerograph Mixing R G/KG | N Wet | N | Refractometer + Aerograph Mixing R G/KG | N Wet | N |
|---|---|---|---|---|---|---|---|---|---|---|---|---|---|---|
| 1 | 917.6 | 19.2 | -16.3 | 19.7 | 26.5 | 243.6 | 26.5 | 243.6 | 17.11 | 107.2 | 350.8 | 12.16 | 76.8 | 320.4 |
| 2 | 916.1 | 19.6 | -16.2 | 19.9 | 27.0 | 242.9 | 27.0 | 242.9 | 17.58 | 109.6 | 352.5 | 11.74 | 73.9 | 316.8 |
| 3 | 917.1 | 19.4 | -16.2 | 20.0 | 26.7 | 243.3 | 26.7 | 243.3 | 17.34 | 108.4 | 351.7 | 12.11 | 76.8 | 319.8 |
| 4 | 917.6 | 18.8 | -16.3 | 20.7 | 26.2 | 243.9 | 26.2 | 243.9 | 16.70 | 105.0 | 348.8 | 12.49 | 79.0 | 322.9 |

REFRACTIVE INDEX PROFILE FOR AIRCRAFT SPIRAL
SAN JUAN MISSION NO. 401, 7 DECEMBER 1965

| Reading | N | Height Meters | M | Potential Temp. Deg. C | Refractometer + Aerograph Mixing Ratio G/KG | Pressure MB | Vapor Pressure |
|---|---|---|---|---|---|---|---|
| 1 | 320.4 | 914.0 | 43829.0 | 26.5 | 12.16 | 917.6 | 17.60 |
| 2 | 316.8 | 927.8 | 45992.7 | 27.0 | 11.74 | 916.1 | 16.98 |
| 3 | 319.6 | 918.6 | 44549.7 | 26.7 | 12.11 | 917.1 | 17.52 |
| 4 | 322.9 | 914.0 | 43831.7 | 26.2 | 12.49 | 917.6 | 18.06 |

(delta N) also shows that the relative humidity was very high. The last column is showing a manually induced event, number 3. A variety of event numbers can be indicated, each of which has some particular significance to the mission. In this case, event 3 means "beginning downward spiral" obviously from an altitude of 870 meters above mean sea level.

The second group again shows some of the initial free-air variables but which have now been corrected in the computer program to take account of aircraft speed and altitude. The agreement between the aerograph and vortex readings is now much better. The air pressure reading has also been adjusted by 1 millibar from its original uncorrected value.

The computer next calculates the potential air temperature $\theta$,[10] the dry term of the index of refraction, $N_d$, based on the corrected air temperature and pressure readings. The fact that these data are repeated twice, under the heading aerograph, indicates that these calculations were based on the aerograph thermometer measurements. Of course, any one of the three thermometers may be selected.

The next column shows the mixing ratio[10], wet term of the radio refractivity, $N_w$, and the total, N, calculated from the aerograph thermometer, the aerograph relative humidity probe (carbon strip) and the air pressure records. Using the Smith-Weintraub equation[3] for the radio refractivity, N, the water vapor pressure, e[10], and therefore, the mixing ratio, r, can be calculated since the air temperature, air pressure and refractometer-measured value for N are known.

The aerograph calculations show a greater value for the mixing ratio and the N term due to the fact the carbon strip indicated saturation, whereas the refractometer indicated below saturation conditions.

The last column shows the corrected total value for N using the refractometer but where aerograph thermometer readings were used to correct for thermal expansion of the refractometer cavity. Calibration of the flight facility shows that water vapor calculations are much more accurate using the refractometer data than with the aerograph, providing precipitable water is not present within the refractometer cavity.

The final printout provides a selection of parameters which have been used to the greatest extent in radio propagation studies. The first is, of course, the corrected radio refractivity, N, and the geopotential aircraft altitude, h[10]. A subsequent modification in the program permits the radar altimeter measurement to be printed out adjacent to the geopotential height

column. Over water, these radar measurements are extremely useful. The modified index, $M$[11], is derived from N, the aircraft height, h, and an earth radius factor. It is of special interest in ray tracing analyses[11]. The remaining columns show the potential air temperature, $\theta$, mixing ratio, r, (using corrected refractometer data), the air pressure, P, and the water vapor pressure, $e$[10] (obtained directly from the Smith-Weintraub equation).

## 5.0 FURTHER ANALYSES USING THE RADIO-METEOROLOGICAL DATA

There are, of course, many ways in which the processed data may be used. For radio wave propagation, the most important information is the behavior of the radio refractivity, N, in both its vertical and horizontal dimension.

The preceding N data, together with height, can first of all be used to define the vertical variation of N and its effect on radar tracking errors. For example, the following tables show a comparison of errors using two N profiles, the first obtained with the aircraft and the second obtained from a radiosonde.

In Table III, a typical set of results are determined for a radio ray initiated at a point 60.4 feet above the earth's surface, at an initial elevation angle of 18 mr, and terminating at four different stop heights. The profile N(h) was derived from a particular aircraft sounding in the local area beginning at 2018 hours.

From the results of the ray tracing analyses the electrical ranges are first calculated and then the range error produced by retardation of the velocity of propagation along the path (and, of course, due to the N values) relative to the true geometric path. See Figure 4 for an illustration of the parameters under consideration.

The next column shows the total amount of ray bending which took place and the resulting elevation angle error, E. The next column shows a k value which, when multiplied by the true earth's radius, gives an effective earth's radius, $A_e$. This effective radius represents an enlarged earth over which one may consider the radio waves to travel in straight lines[11].

In Table IV the preceding results obtained with the aircraft measurements are compared with a particular radiosonde sounding. The differences may appear to be small but in many applications where very accurate tracking accuracy is required the results can indicate that radiosonde data are not sufficiently detailed to describe the propagation conditions.

Similarly, with greater difficulty, analyses can be carried out using both the vertical and horizontal characteristics of radio refractivity. In this case aircraft measurements would be required in both the vertical and horizontal directions[12].

TABLE III

CALCULATION OF REFRACTION EFFECTS

| $h_2$ | Range R (nm) | Range Error $(R-R_0)$ ft. | Total Bending $\tau$ (mr) | Elevation Angle Error $\epsilon$ (mr) | k | Effective Earth's Radius $A_e$ (nm) |
|---|---|---|---|---|---|---|
| 8750.0 | 58.135 | 98.84984 | 3.8869643 | 1.8508379 | 1.282458 | 4406.11 |
| 8800.0 | 58.400 | 99.21361 | 3.9110985 | 1.8601380 | 1.282619 | 4406.69 |
| 8850.0 | 58.665 | 99.57561 | 3.9351915 | 1.8694472 | 1.282783 | 4407.27 |
| 8950.0 | 58.901 | 100.29431 | 3.9832550 | 1.8880917 | 1.283120 | 4408.47 |

N(h) = Profile I (A/C Sounding Primrose 2018 hours)

$h_1$ = 60.4 feet

$\theta_0$ = 18.0 mr

$h_2$ = Nominal A/C Pressure Altitude, 8850 feet (Cold Lake)

A3304

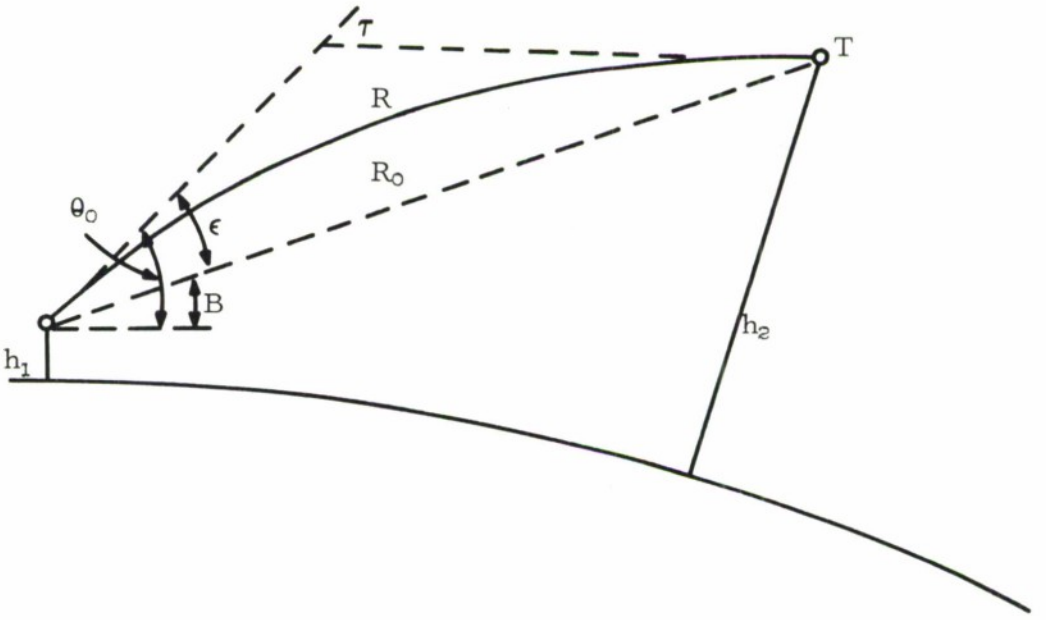


FIGURE 4. RAY-TRACING GEOMETRY

TABLE IV

COMPARISON OF REFRACTION VARIABLES FOR TWO PROFILES

| $h_2$ | Range Difference (nm) | Range Error Difference ft. | $\tau$ Difference | $\epsilon$ Difference | k Difference | (kft) $A_e$ Difference |
|---|---|---|---|---|---|---|
| 8750.0 | -3.194377 | 1.510333 | -0.424719 | -0.296876 | -0.056308 | 177.816468 |
| 8800.0 | -3.208281 | 1.519930 | -0.412768 | -0.297425 | -0.056154 | 174.597458 |
| 8850.0 | -3.221475 | 1.529104 | -0.400832 | -0.297911 | -0.055990 | 171.164189 |
| 8900.0 | -3.233967 | 1.537854 | -0.388911 | -0.298333 | -0.055816 | 167.524125 |
| 8950.0 | -3.245766 | 1.546188 | -0.377005 | -0.298695 | -0.055633 | 163.684481 |

Profile I = A/C Sounding - Primrose 2018 hours.

Profile II = Radiosonde Sounding - Primrose 2018 hours.

$h_1$ = 60.4 feet.

$\theta_o$ = 18.0 mr.

$h_2$ = Nominal A/C Pressure Altitude, 8850 feet (Cold Lake).

In the evaluation of radiometer systems, the line integral of water vapor and temperature are of most direct interest but the ray tracing data are still required to determine the path of the signal. For examination of anomalous propagation conditions the vertical gradient of the radio refractivity is of greatest interest and potential air temperature correspondingly of greatest interest in atmospheric stability analyses[11].

It is apparent that the basic aircraft data can be used in a wide range of interconnected subjects. Also, the addition of a few pieces of selected equipment could greatly enhance the potential of the facility in the areas of sea-air interaction, air pollution and aerosol characteristics, rainfall distributions (water reclamation), and weather modification programs.

## 6.0 SUMMARY

References to the detailed data reduction and ray tracing programs have not been given since these are of little general interest. The essential intention was to indicate the direct airborne measurement capability of this aircraft and to suggest the potential it could have for other expanded areas of investigation in the lower troposphere.

The ray tracing and data reduction analysis were discussed in considerable detail mainly because they are interrelated and represent the important output in most radio propagation experiments.

Finally, the problem of obtaining accurate data with a fast-moving airborne platform is formidable and possibly was not given sufficient attention. This subject was again considered to be of little general interest in spite of the fact that it is an extremely important and difficult area.

The development of the two sensing cavity refractometers to measure the vertical N gradient has been frustrated due to the aircraft's electrical noise generated on long lines passing through the wing and to microphonics associated with the active RF elements. However, recent measurements indicate that it appears possible to measure 0.1 N units variation between the 1 meter vertically separated cavities. New, open cavities are being developed in order to improve the frequency response of the whole system[13].

## REFERENCES


1. Saxton, J. A., September 1951, "Propagation of Metre Radio Waves Beyond the Normal Horizon," Proc. IEEE 98, 360-369.

2. Debye, P., 1957, Polar Molecules, pp 89-90, Dover Publishing Company, New York.

3. Smith, E. K., and S. Weintraub, August 1953, "The Constants in the Equation for Atmospheric Refractive Index at Radio Frequencies," Proc. IRE 41, 1035-1037.

4. Rowlandson, L. G., March 1966, "Measurements of Refractive Index Variations Associated With Clear Air Radio Echoes," The Mitre Corporation, Bedford, Massachusetts, MTR 115.

5. Rowlandson, L. G., March 1967, "Measurements on the Trade Wind Inversion at Aruba, N.A., February-March 1965," The Mitre Corporation, Bedford, Massachusetts, MTR 116.

6. Rowlandson, L. G., June 1966, "Radio Ray Bending in the Lower Troposphere Measured With a Reflection Interferometer," The Mitre Corporation, Bedford, Massachusetts, MTR 114.

7. Starkey, B. J., L. G. Rowlandson, and G. A. Fatum F/L, June 1967, "Cold Lake Radio Propagation and Meteorological Experiment - Description of a Radio Meteorological Experiment to Measure Ray Path Bending in the Troposphere With a Vertical Interferometer," The Mitre Corporation, Bedford, Massachusetts, MTR 118, Volume I.

8. Rowlandson, L. G., June 1967, "Cold Lake Radio Propagation and Meteorological Experiment - Determination of Radio Propagation Conditions From Interferometer and Lake Surface Measurements," The Mitre Corporation, Bedford, Massachusetts, MTR 118, Volume II.

9. Tagliaferri, O. A., and The Radio Meteorological Test Committee, October 1966, "Support to DCA Tropospheric Scatter Tests," Rome Air Development Center, Rome, New York, RADC, TR-66-609, Final Report.

10. List, R. J., 1958, "Smithsonian Meteorological Tables," Publication 4014, The Smithsonian Institute.

11. Bean, B. R., and E. J. Dutton, March 1966, "Radio Meteorology," National Bureau of Standards Monograph 92.

12. Crane, R. K., November 1964, "Ray Tracings in Cloud Cross-Sections for a Long Baseline Interferometer," Proceedings of the Third Tropospheric Refraction Effects Meeting, Electronics Systems Division, USAF, L. G. Hanscom Field, Bedford, Massachusetts, ESD-TDR-64-148, Volume I.

13. Gilmer, R. O., and D. C. Thorn, June 1962, "Some Design Criteria for Open-Ended Microwave Circuits," University of New Mexico, Albuquerque, Engineering Experiment Station, Technical Report EE-65.

Unclassified
Security Classification

## DOCUMENT CONTROL DATA - R & D

*(Security classification of title, body of abstract and indexing annotation must be entered when the overall report is classified)*

| | |
|---|---|
| 1. ORIGINATING ACTIVITY *(Corporate author)*<br>Syracuse University Research Corporation<br>Merrill Lane, University Heights<br>Syracuse, New York | 2a. REPORT SECURITY CLASSIFICATION<br>UNCLASSIFIED<br>2b. GROUP<br>N/A |

3. REPORT TITLE
REFRACTION-INDUCED TRACKING ERRORS AND CORRECTION METHODS FOR THE AIR FORCE WESTERN TEST RANGE

4. DESCRIPTIVE NOTES *(Type of report and inclusive dates)*
None

5. AUTHOR(S) *(First name, middle initial, last name)*
L. G. Rowlandson
J. R. Herlihy

| 6. REPORT DATE | 7a. TOTAL NO. OF PAGES | 7b. NO. OF REFS |
|---|---|---|
| December 1968 | 114 | 47 |

| 8a. CONTRACT OR GRANT NO. | 9a. ORIGINATOR'S REPORT NUMBER(S) |
|---|---|
| F19628-68-C-0209<br>b. PROJECT NO. | ESD-TR-69-52 |
| c.<br>d. | 9b. OTHER REPORT NO(S) *(Any other numbers that may be assigned this report)* |

10. DISTRIBUTION STATEMENT
This document has been approved for public release and sale; its distribution is unlimited.

| 11. SUPPLEMENTARY NOTES | 12. SPONSORING MILITARY ACTIVITY |
|---|---|
| | Aerospace Instrumentation Program Office, Electronic Systems Division, AFSC, USAF, L. G. Hanscom Field, Bedford, Massachusetts 01730 |

13. ABSTRACT

The effect of refraction on radar and ballistic camera tracking accuracy is presented against a background of operational requirements and limitations. A method to compute refraction-induced errors using closed form expressions is presented together with a comparison of these errors against ray tracing results. For a hypothetical missile trajectory it is shown that the closed form solutions using an exponential model atmosphere are in good agreement with the ray tracing results using radiosonde data. The analysis also shows that the closed form expressions can be used to correct ballistic camera tracking errors. In this case a modified form of the exponential model is used to describe the optical refraction profile. Variations in refractivity in time and space are examined for their effect on tracking accuracy. The analysis shows that time variations of the refractivity profile near the radar can produce significant variations in the elevation angle error. Spatial variations far from the radar are restricted in their effect and because of earth curvature only variations near the radar are significant. For tracking below five degrees elevation angle the tracking errors can best be determined from ray tracing analysis with real-time, corrected, radiosonde data. However, the ability to track much below five degrees is shown to be impaired by multipath propagation effects. Recommendations are given for real-time evaluations of the ray tracing and closed form calculations of tracking errors. The advantages of the simplicity of application of the closed form equations for real-time corrections is stressed in the report.

| 14. KEY WORDS | LINK A | | LINK B | | LINK C | |
|---|---|---|---|---|---|---|
| | ROLE | WT | ROLE | WT | ROLE | WT |
| Refraction<br>Radar Errors<br>Missile Trajectory | | | | | | |